A NOVEL VIRTUAL TASK TO PROBE MECHANICAL STOPPING OF PROJECTILES

by

ANA MARIA GOMEZ GRANADOS

(Under the Direction of Deborah A. Barany)

ABSTRACT

An important window into sensorimotor function is how humans interact with and stop moving projectiles, such as catching a ball. Previous studies have primarily investigated stopping of moving projectiles using either real-world experiments, which are constrained by laws of mechanics, or augmented-reality interception paradigms with massless objects, which do not engage postural responses. The purpose of this dissertation was to develop a virtual paradigm that allows for the decoupling of the mechanical interaction between a projectile and the to systematically probe the relationship between object dynamics and limb motor control. In a series of experiments, we used the Mechanical STopping Of Projectiles (MSTOP) task to simulate the physics of mechanical interactions with projectiles, but not the movement of the hands that are required to stop projectiles in the real-world. We aimed to explore how varying the momentum of the projectile, via changes in speed, acceleration, and virtual mass, affected anticipatory and compensatory motor responses. Our results showed that the amplitude of force and arm muscle activation, both in anticipatory (before the collision) and compensatory (during the collision) phases, are similar to results observed in real-life catching studies: response amplitude increased with the

increase in object momentum, regardless of whether the momentum increase was due to object speed, acceleration, or mass. In contrast, the timing of these motor responses in the anticipatory phase, were different to the results observed when interacting with objects in the real-world that experience acceleration due to gravity. Our results showed that participants increased their hand force above baseline levels closer to the time of contact between the hand and the object in anticipation of higher momentum collisions. Finally, our experiments showed, in agreement with previous findings, that the ability to match an objects' velocity with smooth pursuit eye movements decreased with objects moving at higher speeds, for both objects moving at constant speeds and with acceleration. Together, our experiments present a viable framework for using virtual paradigms to mimic the physics of mechanical interactions needed for stopping a projectile, opening new possibilities for understanding how we prepare and update our visuomotor responses in dynamic environments.

INDEX WORDS: Projectile, collision, impulse, momentum, visuomotor, virtual task

A NOVEL VIRTUAL TASK TO PROBE MECHANICAL STOPPING OF PROJECTILES

by

ANA MARIA GOMEZ GRANADOS

B.S., Universidad de Costa Rica, Costa Rica, 2014

M.S., East Carolina University, 2018

A Dissertation Submitted to the Graduate Faculty of The University of Georgia in Partial Fulfillment of the Requirements for the Degree

DOCTOR OF PHILOSOPHY

ATHENS, GEORGIA

2022

A NOVEL VIRTUAL TASK TO PROBE MECHANICAL STOPPING OF PROJECTILES

by

ANA MARIA GOMEZ GRANADOS

Major Professor:	Deborah A. Barany
Committee:	Tarkeshwar Singh
	Jennifer E. McDowell

Electronic Version Approved:

Ron Walcott
Vice Provost for Graduate Education and Dean of the Graduate School
The University of Georgia
December 2022

DEDICATION

This dissertation is dedicated to my parents Carmen and Tobias, my brother and sister-in-law Jose and Gaby, and my nephew and niece Felipe and Maria Isabel. Thank you for your love and always believing in me. I would not have been able to get here without your unconditional support. You all inspire me to be better every day.

ACKNOWLEDGEMENTS

I would like to acknowledge my mentors Dr. Deborah Barany and Dr. Tarkesh Singh. Thank you for your continued guidance and support during my doctoral journey. Working with you has helped me grow as a researcher and person.

I would also like to thank Dr. Jennifer McDowell, Dr. Ellen Evans and Dr. Jing Xu, professors at UGA who played a role in my development as a teacher, researcher, and person during this time. Thank you for your support.

There are many people that have helped make Athens feel like home for the last 4 years. However, I would like to specifically thank Ginny Fredereick, Ewan Williams, Isaura Castillo, Kate White and Kendall Johnson. You have been by my side on the good days and have helped me get by on the hard days. I will cherish your friendship forever.

I would also like to thank the UGA students who participated in my research projects. As well as the students in the lab who helped me with the data collection process.

Finally, I would like to thank the Universidad de Costa Rica for the financial support received during my doctoral program. This support made the pursuit of my degree possible.

TABLE OF CONTENTS

Page

LIST OF TABLES

Page

LIST OF FIGURES

Page

CHAPTER 1

INTRODUCTION

Imagine trying to catch an egg that has been knocked off the counter. To accomplish this time-sensitive task, we need to detect a change in the stimulus (i.e., that it is falling), select an appropriate motor action (i.e., reach toward object), specify the motor plan (i.e., where to move), and execute the movement (i.e., activate appropriate muscles). Each aspect of the motor response is shaped by our perception and changing environmental cues, for example visual perception of the object's mass and shape to scale our grip forces, or perception of the object's speed to time the movement. Understanding the behavioral and neural mechanisms underlying these types of perception-action or sensorimotor tasks will provide an important window into how human's successfully (or unsuccessfully) interact with moving objects that require simultaneous force control and posture stabilization.

Catching a falling object is an example of a class of actions that involve stopping a projectile. Stopping a projectile is a complex sensorimotor task that requires consideration of the properties of the projectile to create and execute an appropriate motor plan. Other real-life examples of stopping a projectile are: stopping a car door pushed by the wind from closing, stopping a child on a swing, stopping an object sliding across a surface, stopping a ball thrown at you with a tool (racket, bat, paddle), and catching an object thrown at you with your hand. We might not always consider these types of tasks as "complex" given their prevalence, however, studying them allows us to

gain insight into how we process kinematic information from projectiles and ultimately how we shape our motor responses depending on this information. In this chapter, we focus mainly on catching literature since it is the most extensively studied stopping task and mostly resembles the mechanics of the virtual task introduced in this dissertation.

Catching a ball or an object following a projectile motion is widely used in many sports and in some situations of our daily living. The eye-hand coordination required to catch a ball with one hand is typically acquired at around 4 years of age and refined for the following 6+ years (Williams, 1992). One-handed catching relies on integrating perceptual information about the object, such as its size, texture, speed, and location, with previous experience to make decisions that allow us to specify the appropriate motor command.

In a catching task, early visual information provides information about an object's location in space of the object and the timing at which the impact will occur (Panchuk et al., 2013). Accurate perception of this information is facilitated through eye movements, Typically, our oculomotor system engages in three main types of eye movements during catching: fixations, saccades, and smooth pursuit. Fixations occur when observers keep their gaze at a stationary location, holding the image of an object stable on the fovea (Fooken et al., 2021). Saccades are discrete, step-like, ballistic movements that direct the eyes toward a visual target within tens of milliseconds (Collewijn & Tamminga, 1984; Krauzlis, 2005). Smooth pursuit eye movements (SPEM) are defined as slow eye movements used to track moving objects, that aim to closely match the velocity of the eye with the velocity of moving objects, to maintain a high spatial resolution of the fovea (Ilg, 1997). SPEM is of particular importance for catching. The primary goal of SPEM is

to stabilize the retinal image of the moving object of interest (Souto & Kerzel, 2021). Catch-up saccades are saccades that take place during SPEM. These catch-up saccades are necessary during the tracking process when the eye starts lagging behind the target, due to a high velocity or to an unexpected trajectory change (Orban de Xivry & Lefevre, 2007). However, even if they help the eye catch-up to the moving target quickly, during the time of its execution the visual system is not able to detect displacement in the visual world (Bridgeman et al., 1975). Therefore, the ability to match the velocity of the moving object with the eyes (referred to as SPEM gain), and to therefore minimize catch-up saccades, is useful for successful interceptive tasks such as catching (reviewed in Fooken et al., 2021).

The motor responses required to catch a ball or more generally stop a projectile can be grouped into two main phases: *before* and *after* impact with the projectile. The time before the contact of the object with the hand will be referred to as the *anticipatory phase*. In ball-drop tasks, this phase is sometimes referred to as anticipatory muscle activation or anticipatory postural adjustments (Berg & Hughes, 2017; Lacquaniti & Maioli, 1989b; Lang & Bastian, 1999; Shiratori & Latash, 2001). In this phase, the motor responses are guided based on the perception of the characteristics of the object (e.g., baseball or tennis ball) (Ilg, 2008) and its trajectory (e.g., straight-line or curved path) (Fink et al., 2009), as well as prior exceptions about the object's flight path (e.g., playing catch with our little brother vs. a professional baseball player) (Kazennikov & Lipshits, 2010a). In essence, any movement or preparatory activity (of the muscles, eyes, etc.) occurs in *anticipation* to what we think the impact between the object and the hand will be like. The anticipatory phase is related to feedforward control, which is the predictive

component needed in fast and coordinated movements when sensory information is limited and delayed. Feedforward responses are planned in advance based on the efference copy of the motor command (Kawato, 1999; Pisotta & Molinari, 2014). This type of control has the advantage that it allows for quick reactions, given that the errors can be anticipated instead of detected (Ohyama et al., 2003).

As soon as the initial contact happens, there is additional sensory information available about the actual impact and the accuracy of the anticipation of the impact. This additional sensory information will produce compensatory movements. Thus, motor responses recorded after the impact will be categorized as the *compensatory phase*. The compensatory phase is related to feedback control, which involves modifying ongoing movements based on information from the sensory receptors (Seidler et al., 2004). This type of control allows for modulation of the initial motor command when it is found to be inaccurate (Desmurget & Grafton, 2000). In ball-drop tasks, the time after contact is typically referred to as the “reflexive response”. However, here we prefer the term compensatory, which encompasses both the reflexive and voluntary feedback-based mechanisms likely to occur after contact (Berg & Hughes, 2017).

Consider the example of stopping a tennis ball with a racket, which will elicit both anticipatory and compensatory control mechanisms (Fig. 1.1). The anticipatory phase, mainly involving feedforward control, will occur before the contact of the ball with the racket. The feedforward control will take into consideration the initial hand/racket location, and the initial target/ball location. Based on the desired outcome, which is to stop the ball, a motor plan will be calculated using an internal model, anticipating the force that needs to be applied to stop the ball. Finally, the motor command will be

executed. As soon as the ball touches the racket, information from the sensory and proprioceptive receptors can be compared to the ongoing motor command to guide compensatory responses, making corrections as needed to achieve the desired outcome. Both anticipatory and compensatory responses are shaped by a “forward model” of limb dynamics, which generates and updates an estimate of motor plan based on continuous motor (i.e., current position and forces of the arm) and sensory (i.e., current position and momentum of the target) information.

In the sections below, we detail the known neural mechanisms thought to underlie responses in both the anticipatory and compensatory phases (Fig. 1.2). The central nervous system will be divided in 3 of its main areas: the cerebellum, the cortex, and subcortical regions. The involvement of each area will be described for both anticipatory and compensatory phases.

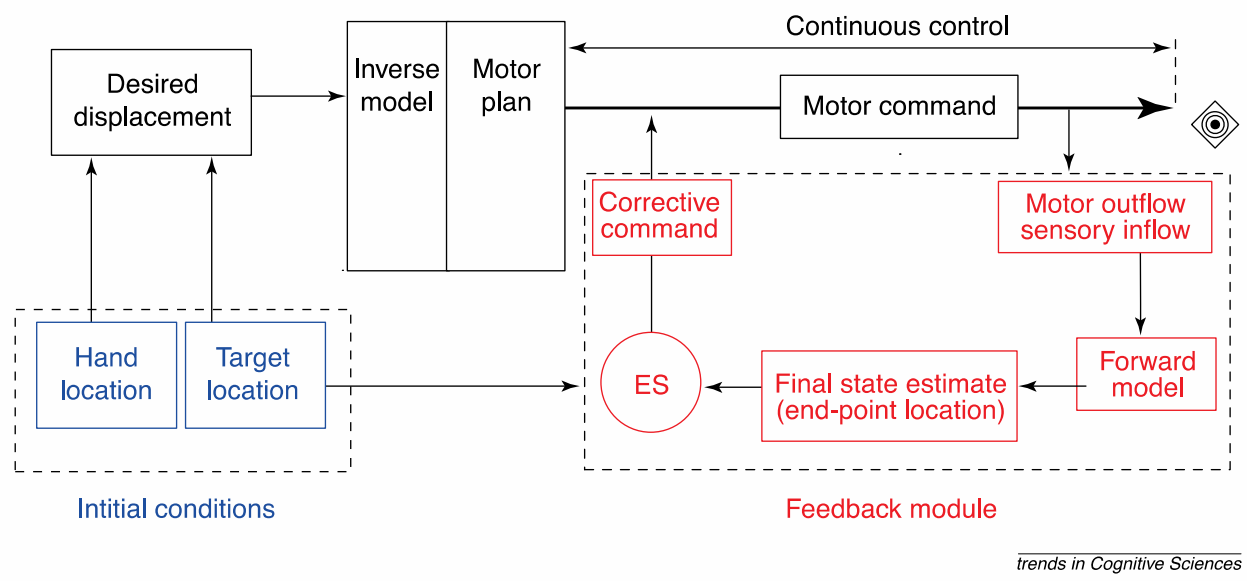

Figure 1.1. Feedforward and feedback control diagram. Forward model of arm dynamics to control hand movements. In the example of stopping a tennis ball with a racket, the anticipatory phase starts with the hand location and the moving target location, which is constantly being updated by the visual system. Based on the desired outcome of stopping the ball, a forward model is used to estimate the needed motor plan. In the anticipatory phase, the motor command is executed without any additional information from the collision. The compensatory phase happens after the collision between the racket and the ball. When the collision happens the feedback controller uses additional sensory information from the collision to identify any error signals (ES) based on the predicted and the actual outcome to estimate the corrective command and execute compensatory movements as needed. Figure from Desmurget & Grafton (2000).

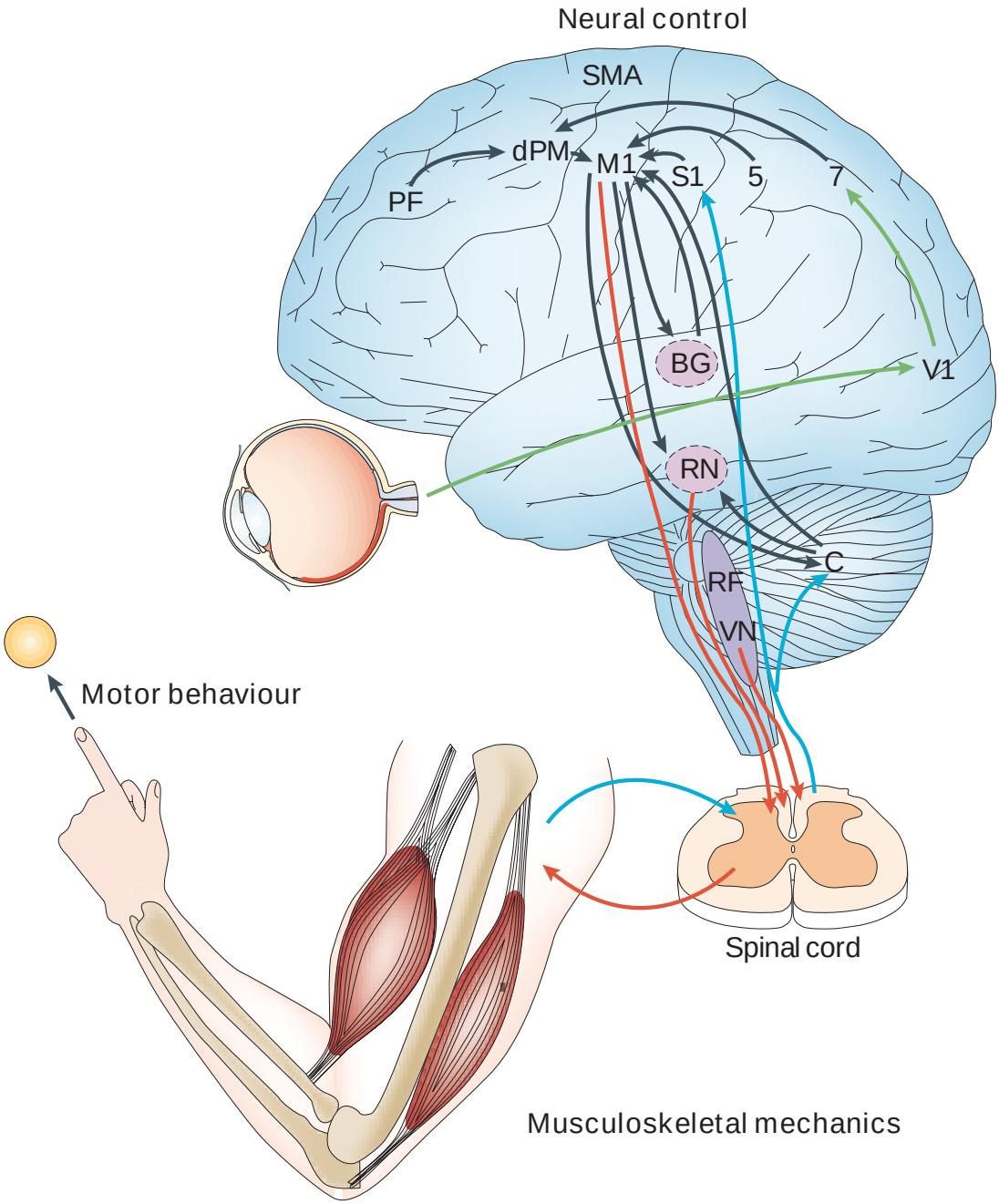

Figure 1.2. Neural control involved in anticipatory and compensatory phases of motor control. The main cortical areas involved in anticipatory control are: primary motor (M1), medial frontal (PF), and posterior parietal cortices. The main cortical areas involved in compensatory control are: primary somatosensory (S1), primary motor, posterior parietal areas 5 (5) and 7 (7), and premotor cortices (dorsal premotor, dPM;

supplementary motor area, SMA). Cortical areas send direct projections to motor neurons in the spinal cord and indirect projections via the brainstem to influence muscle activity. The cerebellum (C) and basal ganglia (BG) each play distinct roles in both the anticipatory and compensatory phases. Together, there are multiple circuits involving connections between the cortex, basal ganglia, thalamus, cerebellum, and brainstem that continually integrate sensory information with motor output during anticipatory and compensatory control. V1: visual cortex; RN: red nucleus; RF: reticular formation; VN: vestibular nuclei. Figure from Scott, 2004.

Neural Mechanisms of the Anticipatory Phase

Anticipatory (or feedforward) control is mediated by a highly interconnected network between the cerebellum, cortex, and subcortical regions. In this section, we will review the known functions of these regions and describe how they are hypothesized to contribute to anticipatory control.

Cerebellum

The cerebellum is involved in temporally-specific learning, playing an important role as a sensorimotor predictor (Bastian, 2006; Ohyama et al., 2003; Pisotta & Molinari, 2014) to modulate the feedforward response. There is also evidence that it might be involved in a network that processes cognitive prediction, with its output being projected to the prefrontal cortex through the thalamus (Fautrelle et al., 2011).

Several internal models have been proposed to explain the cerebellum's role in motor learning and control (Ebner & Pasalar, 2008; Miall et al., 1993). The internal model hypothesis proposes the need of an inverse dynamics model to explain the

execution of fast and coordinated movements that could not be executed by biological feedback loops alone (Kawato, 1999; Tanaka et al., 2020). There are two different types of internal models—forward and inverse models. There are advantages to each type of internal models when considered individually, and there is also evidence on the advantages of a computational model that has multiple paired forward and inverse models (as reviewed in Wolpert et al., 1998).

Forward internal models take the efference copy of the motor command to predict the sensory consequences; meaning that given the current state of the system and the motor command, it predicts the next state, allowing preparation of the musculoskeletal system for successful movement execution (Kawato, 1999; Pisotta & Molinari, 2014; Wolpert et al., 1998). An experiment of eye-hand coordination provides evidence of cerebellar areas, including the paramedian and biventer lobules (VIII), and the vermis (VII), playing a role in learned eye-hand tracking tasks (Miall & Jenkinson, 2005). This learning is suggested to be achieved with a forward model based on a predictive signal originated in the cerebellar area controlling the leading effector (eye or hand).

Inverse internal models calculate and provide the necessary motor command to achieve a desired change in state (Kawato, 1999; Wolpert et al., 1998). In a study with predictable perturbations while holding an object with precision grip, Monzée & Smith (2004) observed that the interpositus nucleus in the cerebellar white matter and the intermediate zone of the cerebellar cortex are involved in the generation of an internal inverse dynamics model that compensates for predictable perturbations in grasping and object manipulation (Monzée & Smith, 2004). In this case, the necessary motor

command to resist the perturbation would be calculated from an inverse model of the arm, hand, and object.

Experiments with patients with cerebellar deficits performing goal-directed arm movements such as reaching have been instrumental in determining the role of the cerebellum in motor control and learning. Studies that exposed participants to force fields while reaching showed that motor adaptation to external forces is impaired in patients with cerebellar degeneration. In contrast to healthy adults, who implicitly adapt to the force field after a few trials, in cerebellar patients changes in motor commands from trial to trial were random and unrelated to the previous trial error (Maschke et al., 2004; Smith & Shadmehr, 2005). Also, this impairment is highly correlated with the progression of the cerebellar degeneration (Maschke et al., 2004). Movement planning has also shown to be impaired in both predictable and unpredictable aiming movements with the contralateral arm of patients with unilateral cerebellar hemisphere stroke (Fisher et al., 2006).

In a series of experiments, Lang and Bastian (1999, 2001) tested catching performance in healthy individuals and individuals with lesions to cerebellar regions. In one experiment, participants were instructed to catch a ball that would eventually change in weight but not in appearance. Patients with cerebellar damage presented a specific impairment in the generation of appropriate anticipatory muscle activity, which was not the case for participants without the lesion (Lang & Bastian, 1999). In a follow-up experiment, participants received preparatory information about the ball by having them hold and release the ball with their non-catching hand, thus providing information about the weight and height of the ball, as well as release time. Despite this advanced

information about the object's properties, patients with cerebellar lesions showed the same impairment in adjusting the muscle activity in preparation for the impact (Lang & Bastian, 2001), suggesting an inability to appropriately modulate feedforward control based on previous experience.

Cortical areas

In eye-hand coordination tasks, before the hand movement even begins there is cortical activity along frontoparietal networks corresponding to the processing of sensory stimuli and motor planning (Gallivan & Culham, 2015). During the execution of the task, parietal, premotor, and primary motor cortical areas will show additional activity related to the sensorimotor integration and motor execution. Cortical representations of both eye and hand movements in parieto-frontal circuits are widespread and overlapping, enabling coordination (Filimon, 2010). In this section we will describe which cortical areas are involved in the anticipatory phase, including the preparation time before motor execution (before the object release in a catching task) up to the contact of the object with the hand (time between object release and catch).

In the anticipatory phase of a free-falling catching task, a study with middle-aged adults showed there was cortical activity integration seen in the contralateral left hemisphere (for right hand catches) in three main areas: primary motor, medial frontal cortex, and posterior parietal cortices. The activity in these areas, measured with electroencephalography, increased during the period of expectancy before the release of the ball, and significantly decreased after the drop of the ball (but before the catch) (Machado et al., 2008).

The primary motor cortex has reciprocal connections with other cortical regions, such as the supplementary motor cortex and the premotor cortex, as well as connections with thalamic nuclei (Brunia, 1999). These cortico-cortical and thalamo-cortical loops not only explain the well-known function of the primary motor cortex in motor execution, but they also result in anticipatory activity related to sensory facilitation and implicit memory processes in preparation for motor actions (Brunia, 1999; Machado et al., 2008; Zang et al., 2003). For example, when preparing a hand motor action, there is evidence of distinct hand representations in dorsal and ventral premotor areas, that provide the major sources of input from the frontal lobe to the primary motor cortex (Dum & Strick, 2005; Hoshi & Tanji, 2007). In a repetitive transcranial magnetic stimulation study, premotor cortex was shown to play a causal role in using prior expectations to aid in preparation for interception (de Azevedo Neto & Bartels, 2021). The left supplementary motor cortex has also been shown to be involved during the preparation period in a 2D manual catching task that involved feedforward control (Tombini et al., 2009).

Primary motor cortex receives top-down influence from prefrontal areas via dense connections with premotor cortices. Activity in contralateral medial frontal cortex is related to planning and preparation of a motor action, especially for self-generated movements and timing (Machado et al., 2008). Thus, this region may interact with more lateral premotor areas involved in attentional orienting and anticipation (Coull & Nobre, 1998; Szurhaj et al., 2003) to control the timing and anticipatory postural adjustments for catching.

Lastly, during the expectancy period in a catching task, there is activity seen in the posterior parietal cortex in the contralateral left hemisphere (Machado et al., 2008). In accordance with Machado et al. (2008), activation localized to the left hemisphere has been seen in preparation of praxis movements (tool use pantomime and communicative gestures) (Wheaton et al., 2005). Activation in both hemispheres in the posterior parietal cortex has demonstrated to play a role specifying the spatial location of the target as well as the location of the hand in the planning of a reaching movement requiring arm-finger coordination in eye-centered coordinate frames (Beurze et al., 2007; Ramnani et al., 2001). Evidence from functional MRI in human subjects suggests that ipsilateral posterior parietal activation contributes to grip and load force coordination to provide grasp stability, which is essential in dynamic object manipulation (Ehrsson et al., 2003). Finally, along with the cerebellum, the posterior parietal cortex has been proposed as representing a forward model for rapid online motor control, predicting the current state of the moving limb as well as the sensory consequences of the movement (Desmurget et al., 1999; Mulliken et al., 2008).

Subcortical areas

The previously mentioned cortical and cerebellar areas involved in anticipatory responses have connections with several subcortical areas that aid in the preparation of these responses. The main subcortical areas that we will discuss in this section will be the thalamus and the basal ganglia.

Structurally there is evidence of many basal ganglia-thalamocortical circuits. In general, these circuits have the following organization in common: specific areas in the cortex send excitatory projections to the striatum, including the putamen, the caudate

nucleus, and the ventral part of the striatum (Spencer, 1976). The striatum discharges and sends inhibitory projections through the other nuclei in the basal ganglia, such as the globus pallidus, the substantia nigra pars reticulata and the ventral pallidum, which in turn projects to the nuclei in the thalamus. Finally, the thalamus sends excitatory projections back to the cortex (Alexander & Crutcher, 1990a; Brunia, 1999). However, there is also evidence of some of these circuits act as loops, where the path back to the cortex has not only the thalamocortical circuit described above, but also a nonreciprocal corticothalamic pathway (McFarland & Haber, 2002).

The basal ganglia motor circuit, specifically, has projections from the primary motor cortex, premotor cortex, supplementary motor area, and somatosensory cortex to the putamen. These projections have a somatotopic organization in the putamen (Alexander & Crutcher, 1990a; Brunia, 1999). Then the putamen sends projections to four nuclei of the thalamus via the globus pallidus and the substantia nigra pars reticulata, which then project back to the cortex. Specifically, the ventral anterior mangnocellular nucleus of the thalamus projects to the supplementary motor area, the ventral anterior parvocellular nucleus projects to the premotor cortex, the centromedian nucleus projects to the motor cortex, and the pars oralis of the ventral posterolateral nucleus projects to all three cortical areas (Schell & Strick, 1984; Strick, 1976).

In behavioral studies, there is evidence of activation in the putamen not only when executing movements, but also during preparation. The preparatory activity for visually-guided arm movements in this area has shown selective directionality—both limb-dependent, where the activity encodes specific limb movements irrespective of target location, and target-dependent, where the location of the target is encoded

irrespective of the limb movement needed to reach it (Alexander & Crutcher, 1990b). This same preparatory activity seen in the putamen was simultaneously seen in the supplementary motor area and primary motor cortex, indicating parallel processing (Alexander & Crutcher, 1990b). This parallel processing is supported by the structural organization and functional specificity seen in the basal ganglia (Alexander et al., 1986; Haber, 2010).

The thalamus has different nuclei that send excitatory projections to the cortex. The reticular nucleus, however, does not have projections to the cortex, instead it plays an inhibitory role within the thalamic relay nuclei. This inhibitory control is believed to aid with selective attention and motor preparation by inhibiting irrelevant information and enhancing relevant information (Brunia, 1999). The involvement of the thalamus in movement preparation has been shown in a study with patients with deep brain stimulation electrodes in the thalamus. There is activation seen in the movement preparation phase in this area before performing a self-paced wrist extension movement (Paradiso et al., 2004).

Muscle Activity During the Anticipatory Phase

Muscle activity prior to a catch is typically measured with surface EMG to define both the amplitude and timing of the anticipatory response. Amplitude refers to quantifying the strength of the response before the impact, whereas timing typically refers to quantifying when the muscle activity increases above baseline in relation to the contact of the ball with the hand. Both parameters are important to understand what variables are taken into consideration when preparing an anticipatory response. The

muscle activity anticipatory response will also vary depending on the muscle that is being measured and the role it plays, i.e., whether it is an agonist or an antagonist.

In previous studies with free-falling balls, the amplitude of the EMG responses in muscles involved in this type of catching, such as the wrist flexors, has constantly been shown to increase with higher ball weights. This amplitude-dependent response is observed when participants are given prior information on the weight of the ball or perform the task in a block design (Berg & Hughes, 2017, 2019; Eckerle et al., 2012; Kazennikov & Lipshits, 2010b). In contrast, there are inconsistencies in the findings when catching balls of unknown weights. Some studies showed an intermediate EMG activation relative to the maximum EMG needed for the task (i.e., EMG was 92.8% of the activation used to catch the heaviest ball) (Berg & Hughes, 2017; Eckerle et al., 2012), whereas others showed an EMG amplitude activation as if anticipating to catch the heaviest load (i.,e EMG was 99.7% of the activation used with the heaviest ball) (Berg & Hughes, 2019; Kazennikov & Lipshits, 2010b). These findings suggest that participants use prior expectations about the mass of the object to-be-caught to scale the amplitude of the anticipatory EMG response.

In a series of experiments, Lacquaniti & Maioli (1989b) not only manipulated the mass of the ball, but also the height of the ball drop. With these experiments they were able to create similar values of ball momenta (*mv*: mass x velocity at impact) at impact, by using different combinations of ball masses and drop heights. They found a linear relation between ball momentum and mean amplitude of late EMG anticipatory responses (computed during the 50 ms interval before impact) from the biceps, triceps,

and flexor and extensor carpi radialis. This suggests that the momentum of the ball modulates the amplitude of the EMG anticipatory response.

Shiratori & Latash (2001) conducted a similar study that manipulated both the mass and height of the load. In this study, however, they also estimated the kinetic energy (*mgh*: mass x gravity constant x release height), which is not dependent on the velocity of the object during the fall but can be estimated in advance with the available information of the mass and distance between the object and the hand. When correlating the anticipatory EMG magnitude with both the momentum and the kinetic energy, the kinetic energy showed a higher correlation than the momentum under the condition where the experimenter released the load. This condition provided some uncertainty on the exact load release time since it happened randomly between 1-3 s after a warning tone. However, there were no differences in the correlations under the self-release condition, where the participant released the load with their other hand. This suggests that under time constraints, like in the experimenter-release condition (the exact release time was unknown and the release height was smaller than that in the Lacquaniti & Maioli (1989b) experiments), the anticipatory response might have been planned based on the available information prior to the release, suggesting predictive processes. In contrast, in the self-release condition, the release time is known, allowing the participant to use the flight information to estimate the momentum at the time of contact, suggesting more reactive processes.

To estimate the timing of the anticipatory EMG activation during catching, some studies calculate the total amount of muscle activity (EMG integral) for different intervals of time preceding the drop and the catch, and in other studies the onset of muscle

activity (increase above baseline values) is analyzed in relation to the object drop or to the contact between the object and the hand. Each type of analysis provides complementary information about response timing and its underlying mechanisms.

The first approach was used in a study by Berg & Hughes (2017), where they analyzed total muscle activity in three separate fixed time intervals: 500 - 100 ms (far) and 100 ms (near) prior to the ball drop, and ~400 ms after the drop but before the catch. By looking at different muscles involved in catching and stabilizing, they were able to identify the earliest time period in which modulation related to the characteristics of the catch occurs. They found that in both the far and near pre-drop intervals, the biceps, triceps, and anterior deltoid (arm stabilizing muscles), and the lumbar erector spinae (posture stabilizing muscles) did not modulate their response based on the weight of the ball, whereas the wrist flexors (main catching muscles) did. In the interval after the drop and before the catch, in addition to the wrist flexors, the biceps, triceps, and the anterior deltoid also showed modulation based on the weight of the ball. Together, the results of this study suggest that with a short yet constant flight time, the only muscles preparing for the expected impact in a predictive way are the main catching muscles, whereas once the ball is released the arm stabilizing muscles are also engaged.

Similar to the above mentioned study, D'Andola et al. (2013) showed that when catching balls with short flight times, the anticipatory EMG activation reflected a combination of both reactive and predictive processes. In this case, participants had to catch flying balls projected frontally with different flight times. Their results showed that arm and shoulder muscles were activated mainly in two phases: an early phase of

activation was generated in response to the detection of the ball launch and involved muscles used to raise the hand from the resting position to the region of interception. The late phase was timed with the hand-ball impact and involved muscles that guided the hand to the interception point.

In accordance to these results, Lacquaniti & Maioli (1989b) ball-drop experiments showed that the latency of EMG anticipatory responses had two phases with time fixed components relative ball release and impact. The early phase was fixed at about 130 ms after the release of the ball independently of release height. The late phase however, did show an increase in mean latency values with height. This result was replicated by Shiratori & Latash (2001) in a paradigm in which the same load was dropped from different heights. The height of the drop showed to influence the timing of the EMG activation prior to the catch, with the muscle activation starting earlier for the largest release height.

Force Responses During the Anticipatory Phase

Measuring arm and hand forces during real-life catching tasks is not as straight forward as measuring muscle activation. Because of this, to get an idea of the anticipatory force response when interacting with moving objects with momentum, experimenters have come up with different experimental set-ups to simplify the movement and isolate groups of muscles.

Finger grip force is one of the most commonly studied measures for investigating anticipatory control. Catching grip force studies typically use a protocol where participants hold a receptacle with their fingers, and a load is dropped into it. In this case, the force applied against the receptacle is measured when holding the receptacle

alone in preparation for the load perturbation. With this type of setup Johansson & Westling (1988) and Kazennikov & Lipshits (2010b) showed similar results in anticipatory force latency and amplitude. For the latency, the increase in grip force was recorded about 150-200 ms prior to the impact of the load with the receptacle, and this latency was not affected by the mass of the load, even when the participants were not aware of the load. Both studies showed amplitude modulation according to the weight of the ball, with greater anticipatory force seen with the heavier loads. Johansson & Westling (1988) included in their study different drop heights, finding that the height of the drop influenced grip force, with longer anticipatory periods of grip force increase seen in higher drops. On the other hand, Kazennikov & Lipshits (2010b) included different load knowledge conditions, where verbal information about the mass of the load was provided prior to the drop in some trials. They found that in the absence of mass information, the grip force amplitude was adjusted to receive the impact of the heavier load.

Kazennikov (2011) performed different variants of the finger grip force protocol to vary the release height, availability of visual information, and the load release time. In the first variant, the setup was the same as the described in the two previous studies, but a wide range of drop heights were tested. For the greater heights (>70 cm), the grip force latency was associated with the time of the impact and varied with height, with grip force increase starting closer to the impact with increasing heights. However, for the smaller heights, the latency was associated with the time of the drop and did not vary with height. In the second variant, participants released the load but were deprived of visual information during the fall. In this case, the latency of the grip force was

associated with the time of the impact, based on previous experience. In both variants, the amplitude of the grip force showed modulation based on the height of the drop, with greater amplitude seen at the moment of the impact in the trials with greater heights.

Smooth Pursuit Eye Movements (SPEM) During the Anticipatory Phase

SPEM is used for accurate perception of object characteristics during a sensorimotor task involving a moving target. In tasks involving stopping projectiles, SPEM primarily contributes to the anticipatory response, though few studies have measured eye movements during free-falling catching. In this section we will define the main features of SPEM, describe the neural pathways that process visual information gathered with SPEM, and discuss the role of SPEM in perception-action paradigms.

The main goal of SPEM is to avoid retinal motion when tracking moving targets (Souto & Kerzel, 2021). For the initiation of SPEM, if the moving target cannot be anticipated, or its trajectory cannot be predicted, the onset of SPEM will lag about 100 ms, because of delays in the visual system (Thier & Ilg, 2005). SPEM will often utilize on-line gain (eye velocity over target velocity) adjustments when tracking moving targets that experience perturbations or sudden changes in the motions (Ono, 2015). There are two recognized different phases in SPEM: the initiation or open-loop phase, and the steady state or closed-loop phase. The open-loop and closed-loop phases are driven by retinal versus extraretinal control signals, respectively (Lisberger, 2010).

The initiation or open-loop phase happens at the beginning of the movement, typically defined as first 100 ms. This phase consists of constant acceleration to be able to match the target's velocity and foveate it, and then usually ends or is followed by a catch-up saccade. Importantly, during this phase the eye movements are not affected

by visual feedback or compensatory eye movements. In relation to the stages in motion integration, the initiation phase is driven by first-order motion signals (i.e., a pattern defined by luminance) (Souto & Kerzel, 2021; Thier & Ilg, 2005).

In the following phase, the closed-loop or steady state, the velocity of SPEM is closer to the velocity of the object, thereby decreasing the retinal position error; however, this error is not kept constant or eliminated. Usually the SPEM gain is kept around 0.95 at its highest (Collewijn & Tamminga, 1984), with the eye lagging in relation to the target. This phase can be driven by second-order motion signals, suggesting it is sensitive to top-down attention, unlike the open-loop phase (Souto & Kerzel, 2021).

Neural pathways for SPEM

Many brain structures contain anatomically differentiated regions specialized for either saccades or SPEM. Saccades and SPEM are driven by shared retinal inputs and controlled by distinct yet overlapping brain regions, pointing to an integrated system that combines both pathways to achieve a main goal when tracking a moving object (Orban de Xivry & Lefevre, 2007). In this section we will describe specifically the cortical and subcortical pathways specialized in SPEM, since this eye movement is of the most interest to us.

Sensory information from moving targets is identified through retinal motion. Neuroreceptors in the retina transmit this information via the optic nerve to the lateral geniculate nucleus (LGN), where the information is divided in six different layers. The inputs from these layers arrive in the primary visual area (V1) in the cortex. Two of these LGN layers correspond to magnocellular pathways, which have motion-

processing information as their input (Bassi & Lehmkuhle, 1990; Merigan & Maunsell, 1993).

The middle temporal visual area (MT), also known as area V5, in the cortex receives direct projections from V1. MT specializes in the processing of visual motion and contains neurons that have a high degree of direction and speed selectivity (Maunsell & Van Essen, 1983). In this area, the representation of object motion occurs relative to the retina (retina-centered coordinates). In contrast, the neighboring middle superior temporal area (MST), which receives input from MT, represents object motion in relation to the world (world-centered coordinates) (Ilg et al., 2004; Thier & Ilg, 2005). MST is divided in two main areas that have different functions—the lateral-anterior part of MST (MSTl) and the dorsal-medial part of MST (MSTd).

Neurons in MSTl have small receptive fields and respond at short latencies (~50-80 ms) from target motion onset (Ono & Mustari, 2011). Neurons in this area are responsible for the integration of visual signals with ocular and head motion, allowing to represent targets in world-centered coordinates (Thier & Erickson, 1992). On the other hand, MSTd contains neurons that have large visual receptive fields and have directional selectivity (Ono, 2015). Activation in this area is often present 50 to 100 ms after eye movement onset, suggesting no involvement in the initiation, but rather in the maintenance of SPEM (Newsome et al., 1988; Ono & Mustari, 2011). Neurons in this area have shown sensitivity to nonretinal information such as pursuit of imaginary targets or pursuit of targets that briefly disappear (Ilg & Thier, 2003; Newsome et al., 1988).

After visual motion signals are processed in MST, these are transformed into eye movement commands, initiating and controlling SPEM through different descending pathways (Krauzlis, 2005; Thier & Ilg, 2005). One of the pathways has projections from MST to the frontal lobe, specifically to the frontal eye field (FEF) and supplementary eye field (SEF).

SPEM in the FEF has been shown to be represented in the arcuate fundus and posterior bank, approximately at the level of the principal sulcus (Gottlieb et al., 1994). Neurons in this area contribute to SPEM initiation and maintenance, as well as the modulation of gain signals at different stages of processing (Gottlieb et al., 1994; Tanaka & Lisberger, 2002a, 2002b). FEF neurons also aid in the prediction of target trajectories, as compensation for long delays in visual motion processing (Fukushima, Yamanobe, Shinmei, & Fukushima, 2002). Furthermore, an area of FEF encodes eye movements in three-dimensional cartesian representations, in addition to the separate encoding of frontal pursuit (both eyes moving in the same direction) and vergence tracking (eyes moving in opposite direction for depth) common in other cerebral cortex and brainstem areas (Fukushima, Yamanobe, Shinmei, Fukushima, et al., 2002; Gamlin & Yoon, 2000).

SEF is located in the most anterior dorsal aspect of the supplementary motor area (Shook et al., 1990). Neurons in SEF have been shown to facilitate anticipatory SPEM by increasing eye velocity and decreasing the eye movement latency only when target motion is predictable; however it is not able to trigger SPEM initiation if the target motion is not expected (Missal & Heinen, 2004). Both FEF and SEF have known direct

and indirect connections to pre- and paraoculomotor areas of the brain stem (Shook et al., 1990).

The main subcortical structures known to be involved in SPEM control include the superior colliculus, basal ganglia, pontine nuclei, and some other premotor nuclei (Krauzlis, 2005; Thier & Ilg, 2005). A direct projection from the cortex to the brain stem is through the superior colliculus. The rostral area of the superior colliculus seems to coordinate the initiation of SPEM through buildup activity (Krauzlis, 2003) determined by a position signal through a real-time estimation of the retinal location (Basso et al., 2000; Krauzlis, 2001, 2005).

Nuclei within the basal ganglia, such as the substantia nigra pars reticulata (SNr) and the caudate nucleus, are not only involved in the production of saccades, but also play a role in SPEM. The FEF subregion encoding SPEM has efferent connections to the caudate nucleus in the basal ganglia, with only limited overlap with the terminal fields from the FEF subregion encoding saccades (Cui et al., 2003). SNr has been shown to receive input from both the SPEM subregion of the FEF (Basso et al., 2005) as well as the caudate nucleus (Lynd-Balta & Haber, 1994). The SNr provides a permissive disinhibition, with neurons showing a reduced discharge rate during the initiation and maintenance of SPEM (Basso et al., 2005).

The two main pontine nuclei that play an important role in SPEM are the dorsolateral pontine nucleus (DLPN) and the nucleus reticularis tegmenti pontis (NRTP). The DLPN receives input related to metrics of SPEM, such as position, velocity, acceleration, and gain control, from cortical areas MT and MST, and projects as mossy fibers to the flocculus of the cerebellum (Glickstein et al., 1994; Mustari et al.,

1988; Ono & Mustari, 2007; Ono & Mustari, 2011). Lesions in the DLPN produce deficits in the initiation, maintenance, and adaptation of SPEM (May et al., 1988; Ono & Mustari, 2007). The NRTP receives input from the FEF and the superior colliculus, and projects to the cerebellar vermis. Lesions in the NRTP has been shown to be involved in the initiation and maintenance of SPEM (Suzuki et al., 1999; Thielert & Thier, 1993).

The cerebellar flocculus plays a role in the transmission of visual motion information used for the initiation of SPEM, and it also provides gaze velocity feedback during the steady state phase of SPEM aiding in the process of maintaining eye velocity (Stone & Lisberger, 1990). Cerebellar vermal lobules VI and VII (oculomotor vermis) integrate eye movement and spatial orientation information from all major precerebellar nuclei, allowing it to coordinate saccades and SPEM, contributing to the tracking of moving objects (Shinmei et al., 2002; Takagi et al., 2000; Thielert & Thier, 1993).

After all this information is integrated in the cerebellum, it is relayed through connections with brainstem pre-motor circuits, mainly with the vestibular nuclei, which is involved in the programming of eye movements (Keller & Heinen, 1991; Miles, 1974). Vestibular nuclei neurons are essential for SPEM generation both during eye-only tracking (head-restrained) and eye-head tracking (unrestrained), supporting the hypothesis that these nuclei are the final neural integrators used by the oculomotor system to communicate the motor plan to the motoneurons (Cannon & Robinson, 1987; Cullen et al., 1993; Lisberger et al., 1994; Roy & Cullen, 2003).

SPEM in perception-action

The effect of SPEM on motion perception is still under debate. Some evidence show that SPEM impairs motion perception, whereas others suggest SPEM enhances

perception, and some evidence showing no effect (Spering & Montagnini, 2011). In this section we will share some evidence for each of those different findings.

An example of the impairment of motion perception with SPEM is the Aubert-Fleischl phenomenon identified decades ago, where an object is perceived to move more slowly when it is tracked with SPEM compared to when it is viewed during fixation (Gibson et al., 1957). Similarly, there is evidence of eye movements affecting the perceived speed of a distal stimuli. A distal stimulus is perceived as slower when the eyes are moving in the same direction as the stimulus, compared to when the eyes are still. When the eyes move in the opposite direction as the stimulus, the perception of speed depends on the on the size of the stimuli, with small stimuli increasing the perception of speed and large stimuli decreasing the perception of speed (Turano & Heidenreich, 1999).

In other contexts, perception can be enhanced with SPEM. For example, a virtual paradigm (“eye soccer”) in which participants had to judge whether a target would hit or miss a vertical line showed that motion direction prediction was significantly different depending on eye movements. Specifically, motion prediction was significantly better when tracking the target than when fixating on it (Spering et al., 2011). Estimation of time to contact in a prediction motion task is enhanced when pursuing the object rather than fixating at the arrival location, showing the importance of extra-retinal and retinal input for this task (Bennett et al., 2010). Another aspect of perception being enhanced with pursuit over fixation is for perceptual coherence (integration of local features into global constructs), shown in a task where participants were presented with a chevron symbol moving behind an occluder with two apertures (Hafed & Krauzlis, 2006).

In a prediction motion paradigm where the time to contact of an accelerating object had to be estimated with a motor response by pressing a button, SPEM does not seem to benefit this temporal prediction, but it does not impair it either (Benguigui & Bennett, 2010). In the same way, perceptual direction discrimination did not differ with SPEM or fixation, with similar direction thresholds and perceptual performance for both eye movements (Krukowski et al., 2003).

Neural Mechanisms of the Compensatory Phase

Cerebellum

As previously discussed, the cerebellum plays an important role as a predictor using internal forward models. In this section, we will consider the cerebellum's role in the correction of motor errors in response to the difference between the sensory feedback information and the desired planned outcome from the forward model.

In a study with patients with cerebellar ataxia and control subjects, participants were asked to perform a hand pursuit task where the movement in their wrist determined the direction of the cursor (Kakei et al., 2019). They had to maintain the cursor position inside the moving target as much as possible while the target moved at a constant speed in a determined pattern that they had practiced. Using this task, both a predictive and feedback component of the pursuit movement could be extracted. The results showed that as expected, the predictive control component was missing in the patients with cerebellar ataxia as expected. In contrast, a corrective control based on sensory feedback was similar for both patients and control subjects, suggesting no impairment in feedback control.

Therefore, the cerebellum may not play a role in sensory feedback control directly, which is why even when cerebellar damage is present, in tasks that don't require a predictive component, we are still able to identify motor errors when sufficient sensory information (e.g., visual errors in visuomotor adaptation tasks) is available to see the discrepancy between our end goal and current state. However, the inability to use sensory prediction for our motor plans does have consequences in the characteristics of our movements (ataxia) and ultimately our sensory prediction error learning is impaired (Therrien & Bastian, 2019). This suggests that the cerebellum does play a role reducing future prediction errors by adapting to the difference between the actual sensory information and the one predicted from the forward model (Desmurget & Grafton, 2000).

Cortical areas

The cortex is the main structure involved in feedback control. Feedback control in sensorimotor tasks require processing of somatosensory and visual information to influence our ongoing motor actions. The main cortical areas that we will discuss in this section are the primary somatosensory cortex and the primary motor cortex as sensory receptors; and the dorsal premotor, primary motor, and posterior parietal cortices, as effectors of the corrections.

To be able to identify a mismatch between our goal and our current state, we need continuous information of our interaction with the environment through somatosensory and proprioceptive signals. The primary somatosensory cortex constantly receives limb afferent signals like cutaneous information, helping us identify, for example, stretching of the skin in the case of a perturbation (Omrani et al., 2016).

The primary motor cortex, on the other hand, receives proprioceptive afferent signals from the different body parts giving the current status of the musculoskeletal system for fast feedback control (Scott & Kalaska, 1997).

The dorsal premotor cortex has shown to play a role in goal-directed corrections in response to mechanical perturbations, showing perturbation-related activity about 30 ms after the perturbation. In cases when the perturbation was used as the signal to initiate a movement into a target, the dorsal premotor cortex seems to play a role in selecting the appropriate action based on the sensory feedback (Omrani et al., 2016). More evidence of the involvement of this area in feedback control is seen with its deactivation by cooling, where the corrections to perturbations become slower and less accurate (Takei et al., 2021).

The primary motor cortex has shown to be able to integrate afferent information into motor commands that account for the limb's mechanical properties. In the case of a perturbation, these motor commands evidence fast feedback control, appropriately countering the torque within 50 ms (Pruszynski et al., 2011). In unperturbed reaching, the primary motor cortex also shows activity that seems to be modulated by the sensory feedback from the limb (Takei et al., 2018).

Posterior parietal cortex has been shown to be involved in online adjustments of hand trajectory contributing to the estimate of limb kinematics (Archambault et al., 2011). Deactivation of the posterior parietal cortex showed impaired spatial accuracy by increasing the endpoint error when making corrections to unexpected mechanical perturbations (Takei et al., 2021).

Subcortical areas

The current knowledge of the role of the basal ganglia in feedback control is oriented towards the use of offline feedback control in learning. Specifically, the basal ganglia is involved in processing the motor output of a trial to influence future trial performance. Specifically, the subthalamic nucleus shows greater activity with movements that have small motor errors (a positive outcome), influencing the programming of subsequent trials (Brown et al., 2006; Kempf et al., 2007). These findings point to the role of the basal ganglia in using feedback from accurate responses for selecting motor parameters for future movements (Brown et al., 2006).

The thalamus, on the other hand, does seem to have a role in online feedback control through the processing of sensory information. Several nuclei in the dorsal thalamus show topographic representations of skin, muscle, and joint receptors of the contralateral body, with projections to anterior and posterior parietal somatosensory areas in the cortex (Padberg et al., 2009).

Muscle Activity During the Compensatory Phase

Compensatory muscle activity is observed in direct response to the increase in load generated by the impact. Depending on the latency of the muscle activity, the compensatory activity can be categorized as reflexive (20-105 ms after perturbation) or voluntary (120 ms after perturbation). The reflex activity happens in response to the stretching of agonist muscles as a result of the impact. The reflexive responses can be further categorized as short-latency (20 - 45 ms) and long-latency (45 -105) responses (Cluff & Scott, 2013; Pruszynski et al., 2008). The short-latency period engages spinal circuits in response to the lengthening of the muscle, whereas the long-latency period

engages cortical areas, which allows for movement corrections depending on the circumstances (Scott et al., 2015).

Before the muscle activity increases in response to the impact, there is a depression in activation seen right before and after the moment of impact (±10 ms) (Johansson & Westling, 1988; Shiratori & Latash, 2001). This decrease in muscle activity is seen despite the previous increase in EMG activation due to the anticipatory response. The decrease in the activity is thought to indicate that the drive of the involved muscles is accurately timed to the impact (Johansson & Westling, 1988).

Muscle activation in the compensatory stage has been studied in the context of catching free-falling objects. Berg & Hughes (2017) defined the compensatory response by analyzing the overall activity in a 500 ms period after the ball drop under different conditions. They found that there was greater compensatory muscle activity when catching heavier masses. In addition, the uncertainty of the mass modulated the compensatory activity, with greater muscle activity seen in the trials where the mass of the load was not known in advance. Specifically in the short-latency window, the mean amplitude of the compensatory response has seen to be 13 times the activity seen in the baseline amplitude (Lacquaniti & Maioli, 1989b). The baseline values for this analysis were calculated as the average over 20 ms centered on impact time. Compensatory muscle response amplitude has also shown to be sensitive to visual information. In the absence of vision, long-latency compensatory muscle activity was greater compared to when visual information was available (Lacquaniti & Maioli, 1989a).

The latency of the compensatory muscle activity observed tends to vary across the different experiments and the muscles used in the task; however, the majority of the

compensatory activity is generally isolated to the short-latency window. Lacquaniti & Maioli (1989b) found that both flexor and extensor muscles had latencies between 15-20 ms, with a return to baseline values between 40-60 ms after impact. Kazennikov (2011) saw activity in the biceps brachii starting at 20-25 ms, and in the extensor carpi radialis at 25-28 ms after impact. Shiratori & Latash (2001) saw latencies between 35-45 ms for flexor and extensor arm muscles. Finally, Johansson & Westling (1988) found differences in latencies between proximal and distal arm muscles, with shorter latencies between 35-40 ms for the proximal muscles (triceps brachii, brachioradialis), and latencies in the long-latency window between 55-65 ms for the distal hand muscles (abductor pollicis brevis, first dorsal interosseus).

Force Responses During the Compensatory Phase

Depending on where the force sensors are placed, some protocols allow for the recording of both anticipatory and compensatory catching forces. For example, in the protocol described above where participants hold a receptacle in which a load is dropped, compensatory forces in response to the load perturbation can be measured in addition to anticipatory forces applied to the receptacle. Protocols where participants are directly catching a load can also provide compensatory force information. Since in this case, the load has the force sensors itself, more specific information of object manipulation can be extracted, but force information can only be recorded after the contact between the load and the hand (i.e., only the compensatory response is measured).

When holding a receptacle where a load was dropped, grip force reached its maximum value 54 ms after the hit with the receptacle (note that the latency of the grip

force was before the impact), and this value did not depend on the mass of the load or previous knowledge of the load. Instead, the compensatory peak grip force depended on the mass of the load when the load was known, with higher values for the heavier loads. However, this effect was only found when preliminary mass information about the load was provided (Kazennikov & Lipshits, 2010b).

In the absence of visual information during the fall and timing of the drop, success rates were low, resulting in a high number of receptacle slips. In the successful trials no anticipatory activity was present, and grip force latency varied between 70-80 ms (Johansson & Westling, 1988) and 63-71 ms after the onset of the impact, reaching its peak value at about 100 ms (Kazennikov, 2011).

Nowak & Hermsdörfer (2004) looked at compensatory finger grip force when directly catching a free-falling load either released by the participants opposite hand or by an experimenter. In both conditions the load was released within 3 s of a verbal “go” signal provided by the experimenter. This study showed that there was a difference in the maximum rate of grip force increase and maximum grip force between conditions, with greater values seen in the experimenter-release condition. The time to reach maximum grip force (relative to the time point from the first detectable grip force signal) was longer in the experimenter-release condition. These findings indicate a greater insecurity when the load was not manipulated by the participant before the drop, which would provide more accurate information about the mass of the load, and the precise time of release, even with this protocol where the weight did not vary between trials, and visual information about the object and hand of the experimenter were always available.

Experimental Overview

In real-life interactions, we are used to dealing with objects with mass moving at non-constant speeds. For example, when catching an object following a projectile motion, we always have to take into consideration the acceleration and deceleration caused by gravity. Similarly, we need to account for the friction between the object and the surface when intercepting an object rolling toward us, which causes the speed of the object to change. Most catching tasks used to study motor control concern catching falling objects, which by necessity will occur under accelerating conditions (Berg & Hughes, 2017; Lacquaniti & Maioli, 1987; Lang & Bastian, 1999; Shiratori & Latash, 2001). However, previous experiments involving some aspect of catching using virtual environments typically involve interception tasks with massless objects moving at constant speeds, or do not include limb kinetics associated with the projectile kinematics of the target (Bosco et al., 2012; Faisal & Wolpert, 2009).

To better mimic real-world interactions with projectiles in virtual environments, it is necessary to incorporate force conditions and acceleration to the moving objects. To bridge the gap between real-world catching and virtual interception studies, we developed a virtual paradigm that we called Mechanical STopping Of Projectiles (MSTOP) (Fig. 1.3). This paradigm simulates the physics of mechanical interactions between the hand and a projectile moving in a horizontal plane. This paradigm allows us to control object characteristics, such as speed, acceleration, and mass, that affect the impulse experienced by the hand when interacting with a projectile, and to look at motor responses such as force, EMG activity, and eye movements.

The MSTOP task leverages an augmented-reality robotic manipulandum (KINARM End-Point Lab, KINARM, Kingston, ON, Canada) with integrated eye-tracking (Eyelink 1000; SR Research, Ottawa, ON Canada). Figure 1.4 depicts the general set-up used for the MSTOP task. Participants are seated with their forehead resting on the top of the apparatus (to facilitate accurate eye-tracking) while they view virtual targets displayed on horizontal screen. Participants interact with the virtual targets by grasping the robotic handle with their right hand and moving the handle to control the position of a virtual cursor displayed on the screen. The robotic handle both applies and records force data. EMG electrodes are placed on their right arm to capture muscle activity while performing the task.

Our ability to stop moving objects in real-world conditions depends on our estimation of the object properties, and in particular, object acceleration. One appealing hypothesis that humans have an internal model of gravity, stating that the lifelong exposure to this constant acceleration is internalized and learned through experience (Zago & Lacquaniti, 2005a). Our estimation of the time-to-contact with objects accelerating under gravity conditions is good; however previous research has shown that our visual system's ability to identify arbitrary accelerations is not very accurate (reviewed in Zago & Lacquaniti, 2005b). Because of this, in the second experiment we included acceleration conditions, positive and negative, to see if it had any effect on the motor responses, particularly on the timing of the anticipatory responses.

Experiment 1 (Chapters 2 and 3):

The aim of this experiment was to determine how varying the momentum of a projectile by changing its speed or mass affected the anticipatory and compensatory

responses. We hypothesized that the amplitude and timing of force and EMG anticipatory responses would be scaled by the momentum of the object regardless of how the momentum was modified, as well as the compensatory force response. We also hypothesized that participants would use SPEM to better estimate the time of contact with the object, and that its gain would be lower with higher speeds.

Experiment 2 (Chapter 4):

The aim of this experiment was to examine anticipatory and compensatory motor responses when stopping a projectile with different accelerating conditions. We hypothesized that the motor responses would be affected by the type of acceleration of the moving objects. We predicted that the use of early visual information, as well as the poor accuracy in identifying arbitrary accelerations, would cause participants to underestimate the object's momentum when it was accelerating, and to overestimate the momentum when the object was decelerating. We also hypothesized that SPEM responses would be similar for the different acceleration groups because of our visual system's poor ability to identify arbitrary accelerations.

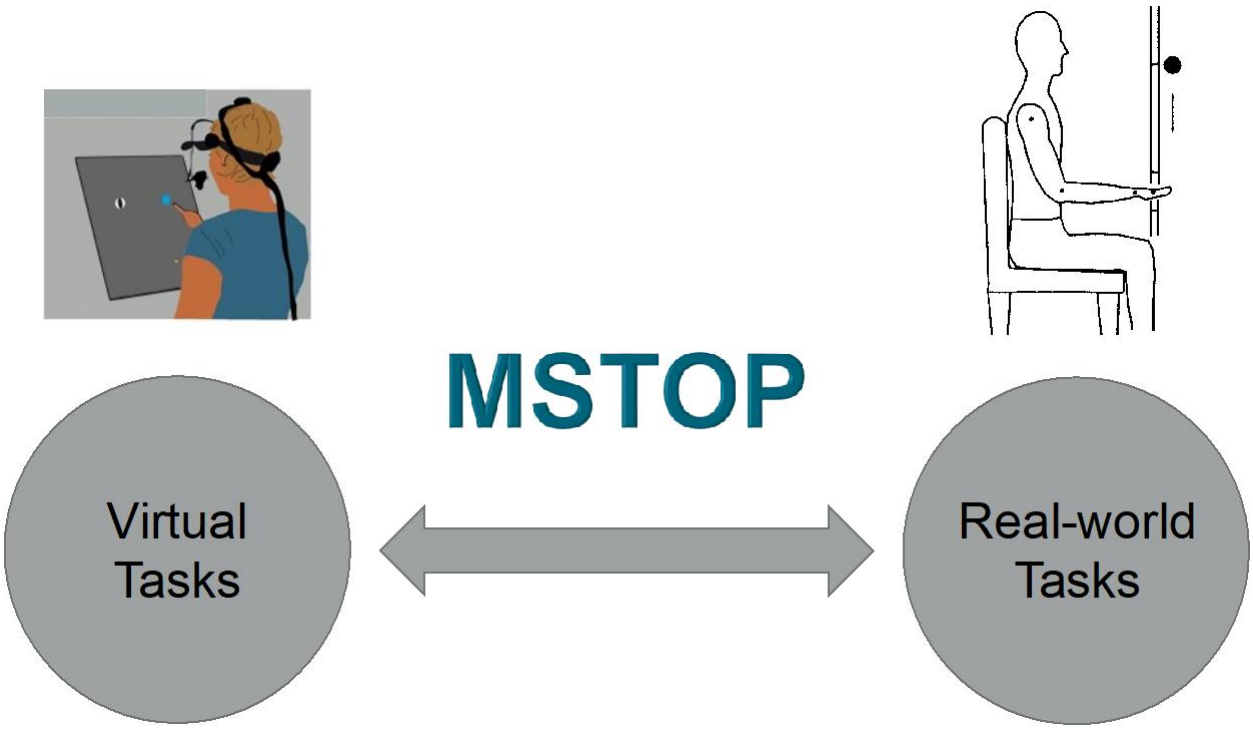

Figure 1.3. Main goal of the Mechanical STopping Of Projectiles (MSTOP) task. The majority of virtual tasks (left) that study timing of motor responses when interacting with moving objects are based on interception of massless objects. These tasks typically do not require postural adjustments or measure limb kinetics. Real-world catching of falling objects tasks (right), have the advantage of a real physical interaction between the ball and the hand. However, the motor responses will always be shaped to objects experiencing gravity-specific acceleration The MSTOP task was created to bridge the gap between current virtual and real-world tasks. It simulates the physics of mechanical interactions with projectiles, but also has the advantage the virtual environment, where objects do not need to conform to the laws of nature. The top left figure was taken and modified from Malla, Smeets & Brenner (2017), and the top right figure from Lang & Bastian (1999).

Figure 1.4. Robotic manipulandum used for the MSTOP task. The KINARM End-Point Lab (KINARM, Kingston, ON, Canada) was used to develop the MSTOP task. The robotic handle applies and records force data, while gaze data is collected with an embedded eye-tracking system (Eyelink 1000; SR Research, Ottawa, ON Canada) and EMG activity is recorded from four muscles of the right arm. Figure from Barany et al., (2020).

CHAPTER 2

OBJECT MOTION INFLUENCES FEEDFORWARD MOTOR RESPONSES DURING MECHANICAL STOPPING OF VIRTUAL PROJECTILES: A PRELIMINARY STUDY

Gómez-Granados, A., Kurtzer, I., Gordon, S., Barany, D., Singh, T.

Submitted to *Experimental Brain Research*

Abstract

An important window into sensorimotor function is how humans interact and stop moving projectiles, such as stopping a door from closing shut or catching a ball. Previous studies have suggested that humans time the initiation and modulate the amplitude of their muscle activity based on the momentum of the approaching object. However, real-world experiments are constrained by laws of mechanics, which cannot be manipulated experimentally to probe the mechanisms of sensorimotor control and learning. An augmented-reality variant of such tasks allows for experimental manipulation of the relationship between motion and force to obtain novel insights into how the nervous system prepares motor responses to interact with moving stimuli. Existing paradigms for studying interactions with moving projectiles use massless object and are primarily focused on quantifying gaze and hand kinematics. Here, we developed a novel collision paradigm using a robotic manipulandum where participants mechanically stopped a virtual object moving in the horizontal plane. On each block of trials, we varied the virtual object's momentum by increasing either its speed or mass. Participants stopped the object by applying a force impulse that matched the object momentum. We observed that arm force increased as a function of object momentum linked to changes in virtual mass or speed, mirroring results from studies involving catching free-falling objects. In addition, increasing object speed resulted in later onset of hand force relative to the impending time-to-contact. These findings show that the present paradigm can be used to determine how humans process projectile motion for hand motor control.

Introduction

An important visuomotor task that humans perform with relative ease is stopping projectiles. For example, in everyday contexts humans may be tasked with stopping a door with a spring from closing shut or catching a saltshaker slid across the table. Similarly, many sports rely on stopping moving objects, such as a hockey goalie stopping a puck with their stick or a soccer player stopping the ball with their foot. These actions require that the activity of antagonist limb muscles be appropriately scaled and precisely timed to absorb the projectile momentum during contact.

In a series of seminal studies, Lacquaniti and colleagues showed that projectile kinematics directly influenced activation of muscles both before and during impact (Lacquaniti et al., 1991, 1992; Lacquaniti et al., 1993; Lacquaniti & Maioli, 1989a, 1989b). They showed two interesting results. First, the anticipatory muscle responses were tuned parametrically to the estimated momentum (mass x speed) of the projectile (reviewed in Fig. 3, Zago and Lacquaniti 2005a) such that the consequent increase in limb impedance stabilized the arm during the large and transient transfer of momentum from the projectile to the arm. Second, projectile speed appeared to have little to no effect on the timing of anticipatory muscle activation prior to contact (reviewed in Zago and Lacquaniti 2005a). However, since these studies primarily used balls falling freely under gravity, they could not manipulate the motion of the projectiles to test how motion-processing of moving projectiles contributes to timing and scaling of limb motor responses.

The goal of the present study is to understand how the visuomotor system transforms motion signals to control interactions between the body and moving objects.

To that end, we developed an augmented-reality based paradigm. We simulated the physics of mechanical interactions between the hand and a projectile moving in the horizontal plane (no acceleration). We call this the *Mechanical STopping Of virtual Projectiles (MSTOP)* paradigm. This paradigm allows us to replicate the mechanical interaction between a projectile and the hand when humans apply limb force to stop moving projectiles. In our paradigm, we programmed a robotic manipulandum to replicate the mechanical interaction between a projectile and the hand during collision. We did that by simulating the physical equivalence between momentum and applied impulse (area under force-time curve) defined by Newton's Second Law. We also adopted an explicit and strict task criterion - to successfully stop the projectile, participants must apply a force impulse within a 5% margin of error to the momentum of the projectile. Our paradigm is different from existing paradigms that use massless virtual objects to quantify how humans prepare and execute interception movements to moving objects (Brenner & Smeets, 2011; Mrotek & Soechting, 2007; Tresilian, 2005). Specifically, our paradigm also allows us to measure how humans control limb force and stabilize posture during interactions with moving projectiles.

In this paper, we introduce this new motor control paradigm with a simple experiment. We tested how systematically varying the momentum of a projectile by changing either its speed or its mass affected limb force. We varied the mass and speed of virtual objects moving towards the participant in different blocks and measured limb forces before and during contact between the hand and the virtual object. Based on previous reports (reviewed in Zago and Lacquaniti 2005a), we predicted that the amplitude of the feedforward limb forces prior to the contact would scale with object

momentum whether the momentum increased due to speed or mass. Our results confirmed this expectation; participants increased limb force prior to impact based on the momentum of the object. In addition, our virtual paradigm allowed us to decouple the mass and speed of the object to test the prediction that motor response timing is based on a continuous estimate of time-to-collision (Lee, 1976; Tresilian, 1991). In contrast to reports on catching free-falling objects that found timing is invariant to object motion characteristics (Lacquaniti & Maioli, 1989b), we observed that participants increased limb force closer to the time of impact at higher momentums, especially when the increase in object momentum was due to an increase in its speed. These proof-of-concept results will allow us to test specific hypotheses in the future to probe how humans control limb forces in anticipation of a mechanical interaction with moving projectiles.

Methods

Participants

Twenty participants (20.6 ± 2.04 years; 10 ♀) completed the study. All participants were right-handed, had no history of neurological disorders, and had no current injuries or pain of the upper limbs. Each participant provided written informed consent prior to participating and were compensated for their time. All procedures were approved by the local Institutional Review Board of the University of Georgia, Athens, GA.

Apparatus

The task was performed on a robotic manipulandum (KINARM End-Point Lab, KINARM, Kingston, ON, Canada) that participants grasped with their right hand. The

robotic arm could be moved in a horizontal plane and a mobile arm support (SaeboMAS, Saebo Inc., Charlotte, NC, USA) was used to support the weight of the participant's arm to avoid fatigue. Visual objects were generated using an online Gabor-patch generator (https://www.cogsci.nl/gabor-generator), with fixed parameters (orientation: 90°, size: 96 pixels, Gaussian envelope, standard deviation: 24 pixels, frequency: 0.1 cycles/pixel, and phase: 0 cycles). The color scheme of the object was used to differentiate the object's assigned virtual mass (see below). Note that unlike true Gabor patches, the object had a clear boundary and was easily detectable in the workspace (see Fig. 2.1).

Task Design

Participants performed a *Mechanical STopping Of Projectiles (MSTOP)* task where the objective was to "stop" a virtual circular object moving in the negative Y direction (towards the body, Fig. 2.1A) by applying a force pulse to bring object momentum to 0. We assigned a virtual mass to an object and then multiplied it with its speed (in the KINARM frame of reference) to obtain a momentum for the virtual object. Since the change in momentum and applied impulse (area under force-time curve) are equivalent (Eq. 1, Newton's Second Law), we converted the momentum of the object into an impulse template (see Fig. 2.1B) that the KINARM robot applied to the participant's hand when the object contacted the hand (right panel, Fig. 2.1A). This allowed us to replicate critical aspects of mechanics of catching.

$$\mathrm{m} \times \Delta \mathrm{V} = \int_{\mathrm{t}=0}^{\mathrm{t}=\Delta \mathrm{t}} \mathrm{F}(\mathrm{t}) \mathrm{dt} \quad (1)$$

Here, the term on the left-hand side is the change in momentum; the term on the right-hand side is the impulse, the integral of force and time. To bring an object approaching the body with a speed V and an assigned mass ‘m’ to a complete stop, the hand will have to apply a time-varying force F(t) over Δt s. We fixed Δt to 90 ms. When the object contacted the hand, the robot applied the impulse on the left-hand side of Eq. 1 over 90 ms with a 10 ms long rise time and fall time and a 70 ms steady state force. Participants experienced that impulse as simulating a contact between the object and the hand. During the contact between the hand and the object, participants were instructed to try to match that impulse applied by the robot as closely as possible (±5% of the impulse applied by the robot) to bring the object to a stop. Exemplar force profiles applied by the robot are shown in Figure 2.1B (left panel) for objects with different speeds and masses.

Object momentum (*Low* or *High*) was varied across experimental blocks via changes to either the object’s speed or mass (right panel of Fig. 2.1B and Table 2.1). The momentum difference between the *Low* (0.41 kg.m/s) and *High* (0.58 kg.m/s) momentum conditions was ~41%. For each condition, there were two sub-conditions: one in which the difference between *Low* and *High* momentum was due to object speed (*Speed Low* vs. *Speed High*) and one in which the momentum difference was due to object ‘mass’ (*Mass Low* vs. *Mass High*). Object mass was visually represented by using different colors for *Mass High* (dark blue with gray lines on the Gabor patch) and *Mass Low* (light blue with gray lines). In the Speed sub-conditions, the object was always red with yellow lines to denote no changes in mass. The purpose of the sub-conditions was to explore whether any differences in limb motor control observed with

increases in momentum depended on specific features of the object dynamics. Importantly, this decoupling of speed and mass can only be achieved in augmented-reality environments.

Table 2.1

Object mass, speed, and momentum/robot impulse values for the experimental sub-conditions.

Sub-condition	Mass (kg)	Speed (m/s)	Momentum (kg.m/s) or Impulse (N.s)
Speed Low	2.32	0.18	0.41
Speed High	2.32	0.25	0.58
Mass Low	1.87	0.22	0.41
Mass High	2.65	0.22	0.58

Procedure

At the beginning of each trial, participants moved the cursor representing their hand location into a designated collision area (5 x 10 cm, rectangle) and maintained a static hold until the end of the trial. If their hand escaped the rectangle, the trial was aborted and repeated. When participants entered their hand in the rectangle, a background load (4 N in the -Y direction, see Fig. 2.1A) was applied and stayed on for the remainder of the trial. Background loads were applied to stabilize the hand prior to

the presentation of the moving object (Barany et al., 2020; Singh et al., 2017) and to minimize unnecessary anticipatory hand movements that would affect the measurement of force onset. After a fixed delay of 1,700 ms, a fixation cross appeared in the middle of the screen (20 cm away from the center of the rectangle). Participants were instructed to fixate on the cross until it disappeared (600 ms). Then the circular object (1 cm radius) appeared on the same position 200 ms after the cross disappeared and immediately started moving in the -Y direction towards the middle of the collision area (Fig. 2.1A).

Participants were asked to stop the object by matching the force impulse applied by the robot. The precise instruction given to the participant was “match the force applied to the hand so that the object stops.” Participants were allowed to move their hand as long as the hand stayed within the rectangle. It is important to note that the mechanical interaction during the contact is primarily determined by feedforward commands to muscles and muscle’s intrinsic viscoelastic properties (Burdet et al., 2013) because the 90 ms contact duration is too short for voluntary feedback correction. Though fast feedback corrections are observed in muscle activity within the first 50-100 ms after mechanical perturbations (reviewed in Scott 2012; Kurtzer 2015), hand force is likely low-pass filtered by the musculoskeletal system (Burkholder, 2016) and consequently may not include effects of feedback responses.

The performance of a participant in three different trials of the Speed Low sub-condition along with the impulse applied by the robot (Robot Force as a function of time) is shown in Figure 2.2A. For ideal task performance, the limb force should mirror the robot force. However, ideal performance is almost never achieved because Newton’s

Third Law does not apply to a free limb, i.e., a limb is not a rigid body. Other groups have also modeled non-rigid mechanical interactions during collision between the hand and a moving projectile using Hooke's Law (Kuling et al., 2019). Thus, because the two reactive forces (object on hand and hand on object) are not equal, we provided a ±5% force error margin for participants to be successful on a trial. Note that the 5% error margin was a fairly strict criteria as the Weber fraction for force production is between 10-20% (Debats et al., 2012; Jones, 1986).

Participants were given two forms of feedback – one with the object and another one with a visual scale (see Fig. 2.2B). Object feedback had three different levels: if the impulse was matched within a ±5% margin of error (see Eq. 2), that would imply that an appropriate impulse was applied to match the momentum of the object and the object would stop after the contact (reflecting a successful stop). If the impulse applied by the participant was higher than the 5% margin of error, that would imply that more than the necessary impulse was applied, and the object would "fly back" and move in the +Y direction (overshoot). Lastly, if the impulse applied by the participant was lower than the margin of error, the object would continue unabated on its original trajectory in the -Y direction towards the participant (undershoot).

$$-5 \leq \sum_{t=1\ ms}^{t=90\ ms} \left(\frac{F_{Hand}\Delta t - F_{Robot}\Delta t}{F_{Robot}\Delta t} \right) \times 100 \leq 5 \quad (2)$$

In addition to discrete object feedback, participants were provided a more continuous measure of performance by adding a visual analog scale that had a green center region surrounded by red region. The scale was set up based on Eq. 2, with the

green region indicating the ±5% margin of error and the red regions indicating how low or high the applied impulse was from the impulse required to bring the object to rest. Feedback was displayed for 1,700 ms, followed by an inter-trial delay of 2,500 ms.

Participants performed two blocks of 35 trials for each of the four sub-conditions (8 blocks, 280 trials total). The block order was counterbalanced across participants such that half of the participants performed the four Mass sub-condition blocks first and the other half performed the four Speed sub-condition blocks first. Within each sub-condition, the block order (e.g., Momentum *High* or *Low*) was randomized for each participant and across participants.

Data recording and analysis

All analyses were performed in MATLAB (Mathworks R2020b, Natick, MA). We treated the first three trials in each block as practice and only performed analyses on the remaining 32 trials. Hand kinetics and kinematics were sampled at 1 kHz and digitally low-pass filtered (second-order, dual-pass Butterworth, 50 Hz effective cutoff). For each sub-condition, we calculated the number of trials in which the hand impulse (1) successfully matched the robot impulse within the 5% margin of error (correct), (2) was above the margin of error of the robot impulse (overshoot), and (3) was below the margin of error of the robot impulse (undershoot). For each trial within a block, we calculated the overall hand impulse applied as well as the percentage difference between the impulse applied by the robot and the participant (see Equation 2), ΔImpulse (%).

Participants typically increased their hand force and moved their hand slightly toward the object (1-3 cm) right before contact. Thus, we quantified when the hand

force and hand speed increased above baseline values in anticipation of the contact with the object during the static hold. Since analyses based on hand speed produced similar results to analyses of hand force, we used the force data for all subsequent analyses.

We first calculated the mean force applied against the background load in an interval (t = [-500, -400 ms]) prior to the contact and then subtracted it from the peak force recorded from the force sensor during contact. Then starting from the point of contact (t = 0), we went backward in time and defined hand force onset as the first time point when the hand force dropped below 5% of the peak force value (Fig. 2.3).

We then calculated two parameters for the feedforward control of hand force. First, we calculated the peak hand force at contact (t = 0) and called it the *anticipatory peak force* (APF). We then fit a first order polynomial to the force data between the hand force at the time of hand force onset and APF and computed the slope of the fitted line. This slope provided a measure of rate of force development (RFD) between hand force onset and APF.

Finally, we calculated the distance along the Y-axis between the hand and the object at hand force onset. We then computed the *time of hand force onset*, TOFO, by dividing this variable by object speed (see Equation 3) (Lee, 1998; Tresilian, 1999).

$$\mathrm{TOFO} = \frac{y_{\mathrm{object}} - y_{\mathrm{hand}}}{\text{object speed}} \qquad (3)$$

Statistics

We conducted two-way repeated measures ANOVAs using object momentum (*Low* or *High*) and sub-condition (*Mass* or *Speed*) as within-subject factors to compare

collision performance, hand impulse, ΔImpulse, RFD, APF, and TOFO across conditions. The level of significance was set at a = 0.05 and effect sizes are reported using generalized η^2. Post-hoc comparisons were performed using paired *t*-tests, with adjusted *p* values using the Bonferroni method. All values are reported as mean ± SE. All statistical analyses were performed in R (version 4.0.4).

Results

Limb force during collision depends on object momentum

Participants applied impulses within the acceptable range of 95-105% of the impulse applied by the robot in 48.07 ± 1.40% across all conditions. There was a small main effect of object momentum on the percentage of correct trials ($F(1,19) = 5.35$, $p = 0.03$, $\eta^2 = 0.01$). Post-hoc comparisons showed participants performed better in the *Mass High* (51.3 ± 2.6%) than in the *Mass Low* (46.4 ± 2.96%) sub-condition ($p = 0.01$), and no difference between the *Speed High* (47.7 ± 2.88%) and *Speed Low* (46.9 ± 2.83%) sub-conditions ($p = 1.00$). On trials that participants did not match the robot impulse correctly, they were more likely to apply too much force (overshoot) at the *Low* momentum conditions (main effect of momentum: $F(1,19) = 48.91$, $p < 0.001$, $\eta^2 = 0.16$) and to not apply enough force (undershoot) in the *High* momentum conditions (main effect of momentum: $F(1,19) = 24.03$, $p < 0.001$, $\eta^2 = 0.08$). Post-hoc comparisons showed that this pattern of overshooting and undershooting the ideal impulse was consistent for both *Mass* and *Speed* sub-conditions (all p's < 0.05) (Fig. 2.4A).

On average, participants were able to match the applied robot impulses of 0.41 N.s (*Low*) and 0.58 N.s (*High*) almost exactly: there was a large main effect of object momentum on the limb impulse ($F(1,19) = 2980.05$, $p < 0.001$, $\eta^2 = 0.96$), with larger

hand impulses for *Mass High* (0.58 ± 0.004 N.s) and *Speed High* (0.57 ± 0.004 N.s) than *Mass Low* (0.42 ± 0.005 N.s) and *Speed Low* (0.41 ± 0.003 N.s) ***p's*** < 0.001). This confirms that the task was doable in that participants proportionately increased their hand impulse with an increase in object momentum due to increases in either speed or mass (Fig. 2.4B).

There was a significant main effect of object momentum on ΔImpulse ($F(1,19) = 23.65$, $p < 0.001$, $\eta^2 = 0.08$). The average ΔImpulse was slightly positive in the *Mass Low* sub-condition (0.66 ± 0.68%), whereas it was significantly smaller and negative in the *Mass High* sub-condition (-0.92 ± 0.57%) ($p = 0.03$). Similarly, there was a significant difference in the average Δ Impulse between the *Speed Low* (0.09 ± 0.70%) and *Speed High* (-1.78 ± 0.70%) sub-conditions ($p = 0.004$), reflecting the tendency to overshoot the ideal force at lower momentum and undershoot the ideal force at higher momentum (Fig. 2.4C).

Motor response amplitude and timing scales with object momentum

The rate of force increase between hand force onset and anticipatory peak force (APF) at collision, RFD, was higher in the *High* momentum conditions (main effect of momentum: $F(1,19) = 82.58$, $p < 0.001$, $\eta^2 = 0.12$) for both mass (*Mass Low*: 27.4 ± 3.02 N/s; *Mass High*: 36.2 ± 3.54 N/s, $p < 0.001$) and speed (*Speed Low*: 26.3 ± 2.87 N/s; *Speed High*: 39.1 ± 3.87 N/s, $p < 0.001$) (Fig. 2.5A). There was a small but significant interaction such that the increase in RFD was larger when the increase in momentum was due to changes in speed than due to changes in mass (interaction: $F(1,19) = 10.50$, $p = 0.004$, $\eta^2 = 0.005$). APF was also significantly higher in the *High* momentum conditions (main effect of momentum: $F(1,19) = 247.45$, $p < 0.001$, $\eta^2 =$

0.15), for both changes due to mass (*Mass Low*: 6.15 ± 0.16 N; *Mass High*: 6.69 ± 0.16 N, $p < 0.001$) and speed (*Speed Low*: 6.16 ± 0.17 N; *Speed High*: 6.84 ± 0.19 N, $p < 0.001$) (Fig. 2.5B). However, in terms of absolute magnitude, this difference was rather small (9-11%) compared to the 41% increase in object momentum from the *Low* to the *High* momentum conditions (see Table 2.1).

There was a significant interaction between momentum and mass/speed sub-condition on the time of limb force onset, TOFO, ($F(1,19) = 71.69$, $p < 0.001$, $\eta^2 = 0.04$). While TOFO decreased from *Low* to *High* momentum for both mass (*Mass Low*: 0.25 ± 0.02 s; *Mass High:* 0.24 ± 0.02 s, $p = 0.004$) and speed (*Speed Low*: 0.29 ± 0.02 s; *Speed High* 0.22 ± 0.02 s, $p < 0.001$), this decrease was much larger for the speed sub-conditions (Fig. 2.5C). Note that the average TOFO for both of the Mass sub-conditions was between the *Speed Low* and *Speed High* conditions, reflecting that the selected object speed for the Mass sub-conditions was an intermediate value (0.22 m/s) between *Speed Low* (0.18 m/s) and *Speed High* (0.25 m/s) (see Table 2.1). Together, this suggests that in preparation for contact between the object and the hand, participants increased hand force above baseline levels much closer to the time of contact when anticipating a higher momentum collision, especially when the higher momentum was due to the object traveling at faster speeds. The distance of the target from the hand at which the hand force increased above baseline levels was similar across the different sub-conditions *(Mass Low*: 55 ± 4 mm; *Mass High:* 53 ± 4 mm; *Speed Low*: 53 ± 4 mm; *Speed High*: 53 ± 4 mm)*,* suggesting that participants may have increased hand force when the target was at a certain distance from the hand. There was no main effect of momentum or any effect of the sub-condition.

Discussion

In the current study, we introduced the *Mechanical STopping of Projectiles* (MSTOP) paradigm that simulated the mechanics of the interaction between the object and the hand based on Newton's Second Law. This paradigm replicates the physics of the mechanical interaction between a projectile and the hand. We simulated the interaction such that the "momentum" (mass x velocity) of the object could be stopped by applying an equivalent mechanical impulse (integral area of force-time curve). If the applied impulse exceeded the object momentum, the object bounced back. If it was less than the object momentum, the object continued on its original trajectory. Note that the range of required performance was very strict, ±5% of the target, which is well below the standard Weber fractions for static force, ±10%, and led to many error trials, ~50%. This demanding paradigm was useful since it allows us to precisely control object dynamics. Unlike the real-world, where laws of motion exclusively dictate the mechanical interaction between projectiles and the arm, in augmented-reality we can decouple the physics of that interaction to systematically probe the relationship between object dynamics and limb motor control.

In different conditions, we either varied the speed or the mass of the object to alter its momentum. We hypothesized that visual system processes object momentum (mass x velocity) and feeds that information to the limb motor system to prepare postural responses. The prediction from this hypothesis was that the amplitude of the feedforward motor response would scale with the momentum of the object, regardless of whether the momentum increased due to speed or mass. Our results supported this prediction.

APF and RFD scaled with momentum in both the *Speed* and *Mass* sub-conditions - participants increased the hand force right before contact for objects with higher momentum, regardless of whether the momentum increased due to object speed or mass. This is consistent with the results of a previous study (Lacquaniti & Maioli, 1989b).

We also predicted that the timing of the motor response initiation would be invariant to object motion and momentum. Our prediction was incorrect. We observed that when the object traveled at faster speeds, participants increased hand force closer to the time of contact. The distance of the object from the hand at the time of force increase was similar across all conditions, suggesting that participants may have initiated the force response when the objects were at a fixed distance. Previously, Port and colleagues showed that for objects moving at slow speeds, humans use a time-to-contact threshold to initiate hand movements, whereas for comparatively faster moving objects, they use a distance-to-contact threshold (Port et al., 1997). Our preliminary results support the distance-to-contact threshold in our augmented-reality paradigm. In the four experimental conditions, the mean values of the distance of the target at the point of hand force increase were within 2-3 mm of each other. The human eye can discern spatial distances separated by about 0.016° (1 arc minute). That would correspond to approximately 1.1 mm at a distance of 15 cm from the eye in the KINARM environment (30 cm depth). However, the magnitude of reaching errors made under memory-guided and open-loop (without visual feedback) conditions at that same distance tends to be ~4-10 mm (Heath et al., 2004). This suggests that the proprioceptive system could not have reliably differentiated the 2-3 mm difference that

we saw across conditions. Thus, it seems very likely that participants initiated a force response when the object was at a fixed distance from the hand.

During many activities of daily living, humans interact with objects that are in relative motion with the body. These transient interactions require the limb to produce precise forces to stop the motion between the object and the body. Previously, researchers have used paradigms involving mechanical collisions between the hand and virtual objects (Bowman et al., 2009; Kuling et al., 2019; White et al., 2011) and hand and real projectiles (Lacquaniti & Maioli, 1989b) to probe how the motor system stabilizes posture before and during collisions. In some of these paradigms, collisions have been modeled using Hooke's Law assuming both the hand and the object are non-rigid. This is accomplished by programming a robot to apply position- (stiffness) and velocity-dependent (viscosity) forces on the limb during the collision.

A key feature of these existing paradigms is that collision between the hand and the object is primarily treated as a perturbation to the motor system to quantify pre-collision anticipatory and compensatory stretch-reflex like feedback responses during the collision. However, the mechanical interaction during the collision itself that dictates how force is transferred to projectiles from the hand has not to date been a focus of investigation. During this interaction, the limb produces a reactive force in response to the force generated by the object over the very short collision duration. Quantifying this interaction is important to better understand how humans acquire complex motor skills that require simultaneous force control and posture stabilization.

The present MSTOP paradigm has been designed to probe how humans control this force. We integrate the force applied over a short but modifiable time duration (fixed

at 90 ms in this study) in real-time to calculate the net force impulse that is then transferred to the virtual object to change its momentum (Newton's Second Law). More importantly, this paradigm allows us to manipulate object dynamics to systematically probe how humans learn and form novel sensorimotor maps to interact with moving objects. Future studies with this paradigm are well-positioned to address novel questions about control by manipulating object dynamics across trials and blocks to define how the sensorimotor maps between motion and force control are formed.

Conclusion

In summary, we developed a new augmented-reality based mechanical stopping of projectiles (MSTOP) task which replicates the physics of a stopping task, but not the movement of the hands that are required to stop projectiles in the real-world. Using this paradigm, our study shows that object speed influences both the timing and amplitude of motor responses. We found that faster moving objects delayed the onset of the hand force response closer to the time of contact between the object and the hand. We also found that object momentum scaled the amplitude of the feedforward force response regardless of whether the momentum was increased due to speed or mass. Our results suggest that the timing and amplitude of hand motor responses in this virtual catching task are affected by different features of object motion. Future experiments using this paradigm will help us understand the mechanisms underlying these sensorimotor processes.

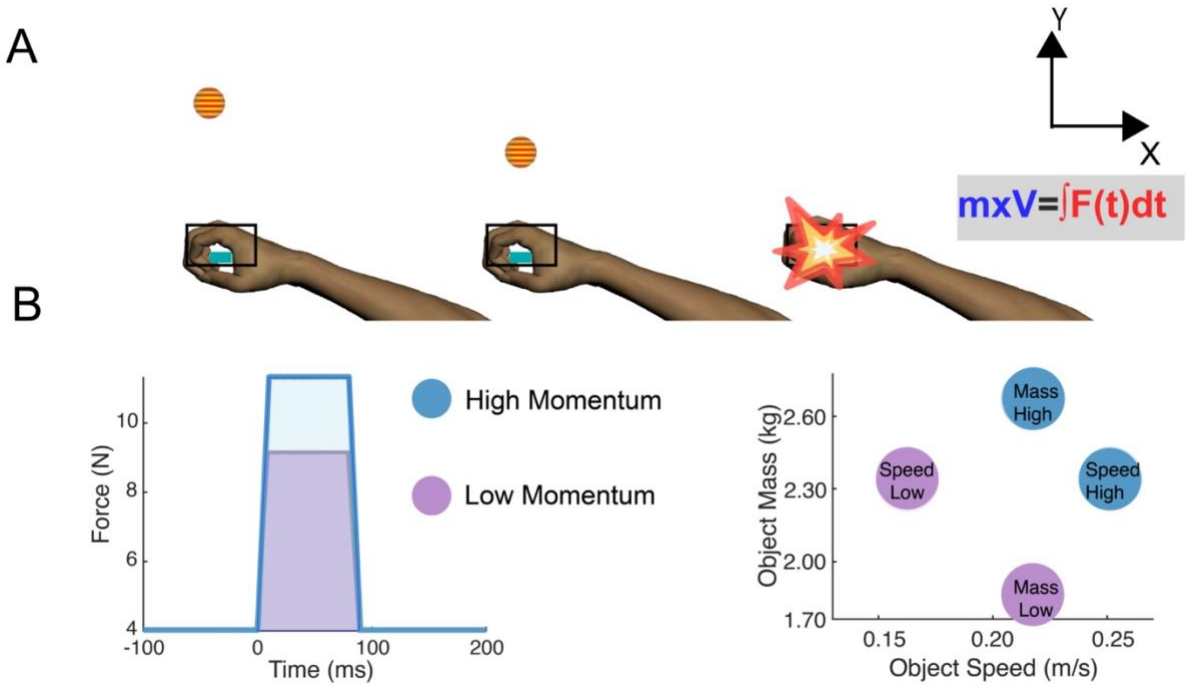

Figure 2.1. Experimental setup. A) Once participants moved their hand into the rectangular box and stabilized their arm against the background load, a fixation cross appeared (not shown). Participants had to fixate on the cross until it disappeared (600 ms). 200 ms after a circular object appeared at the same position and moved towards the participant. Participants were instructed to match the force applied by the robot during the contact. B) Force-time curve for the perturbation applied by the robot. The area under the curve, the impulse, is exactly equal to the momentum carried by the virtual object. The right panel shows the mass and speed values assigned to each sub-condition.

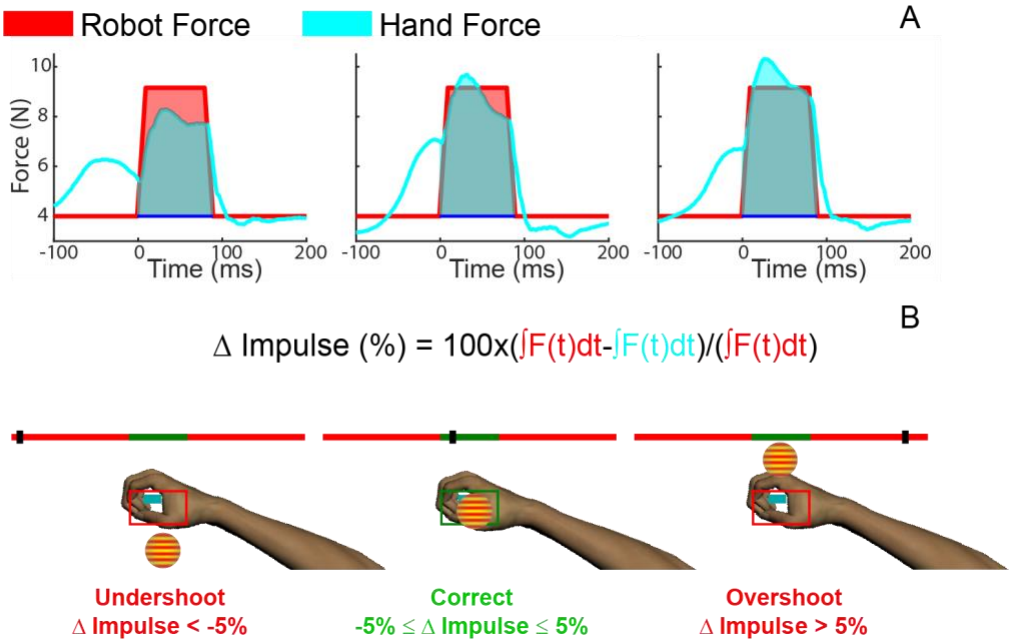

Figure 2.2. Performance feedback. A) Exemplar trials from a participant in three different situations when the participant applied less than 95% of the required impulse (left, undershoot), an impulse within 95-105% of the desired impulse (middle, correct), and more than 105% of the impulse (right, overshoot). The red shaded area is the impulse applied by the robot and the cyan area is the impulse applied by the participant. The red and cyan curves are the force applied by the robot and the hand, respectively. B) The corresponding feedback provided to participants for the three trials in A. The black bar on the horizontal line indicated how far performance for that trial deviated from the ideal impulse (middle of green section of the horizontal line).

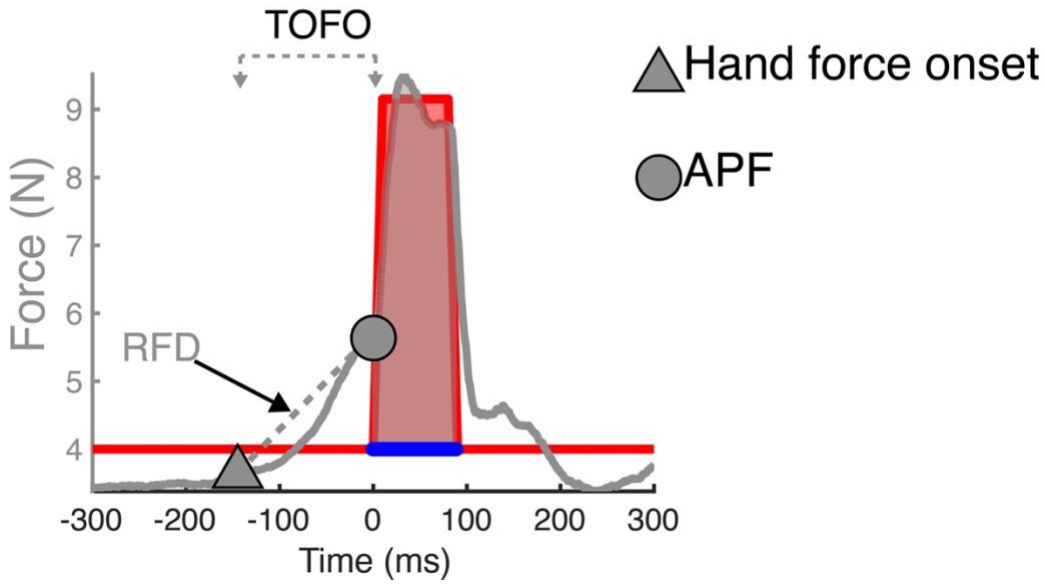

Figure 2.3. Performance variables for subsequent analysis. The y-axis shows the force applied by the participant in the Y direction (grey curve) to counter the impulsive force applied by the robot (red curve) during the contact with the virtual object. The shaded area indicates the impulse applied by the robot (red) and participant (grey). The triangle indicates the hand force onset. The circle indicates the anticipatory peak force (APF). Rate of force development (RFD) is the fitted slope between hand force onset and APF. Time of force onset (TOFO) is defined as the distance between the hand and object at hand force onset, divided by object speed.

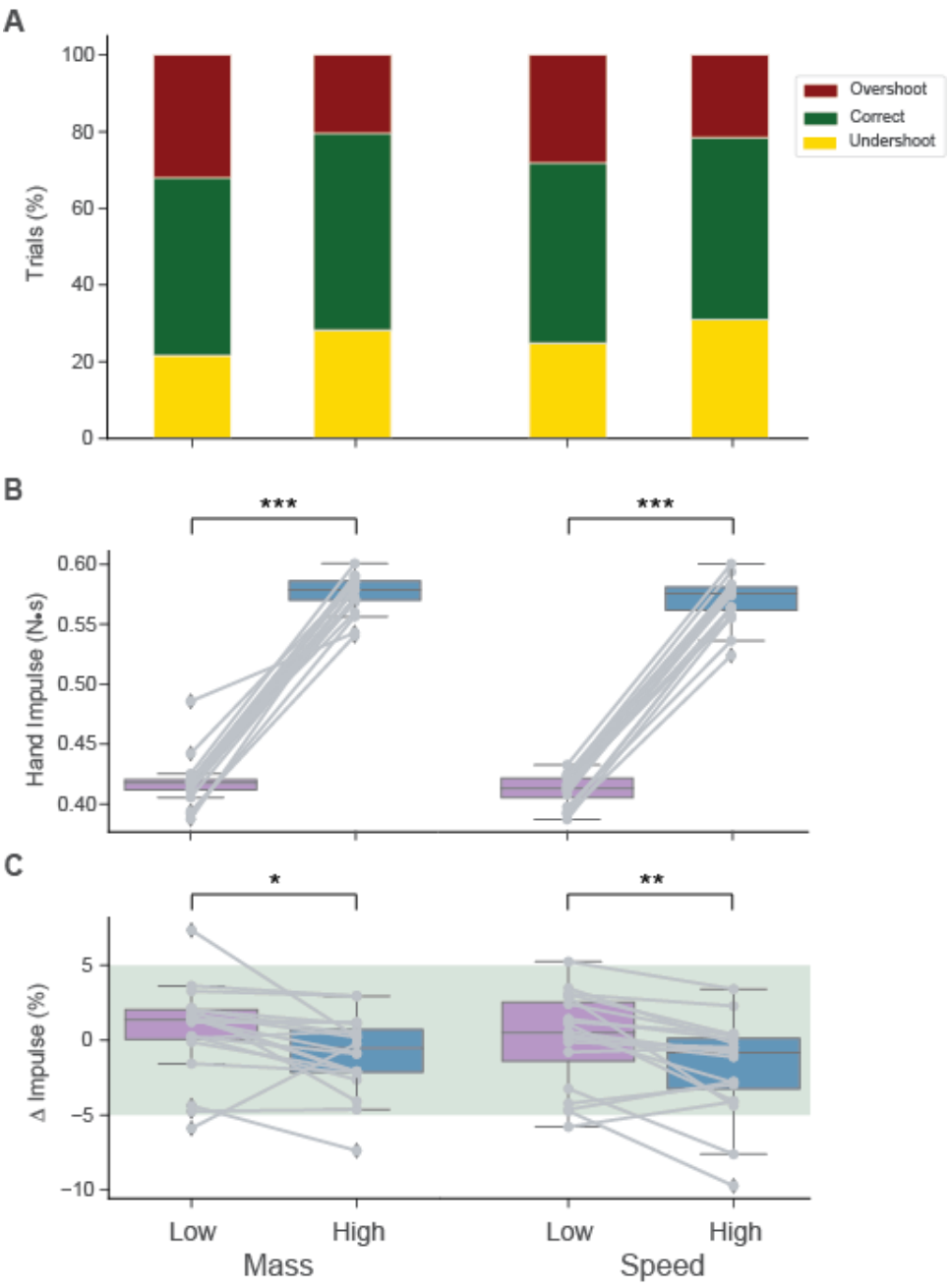

Figure 2.4. Limb force during collision. A) In unsuccessful trials participants tended to overshoot the hand impulse for Low momentum conditions, and to undershoot High momentum conditions. B) On average, participants' hand impulse matched the robot's impulse. C) Percentage difference between the impulse applied by the participant and

the robot. The shaded area indicates the error margin allowable for a trial to be categorized as correct. Post-hoc differences (Bonferroni-adjusted): * indicates $p < 0.05$, ** indicates $p < 0.01$, *** indicates $p < 0.001$.

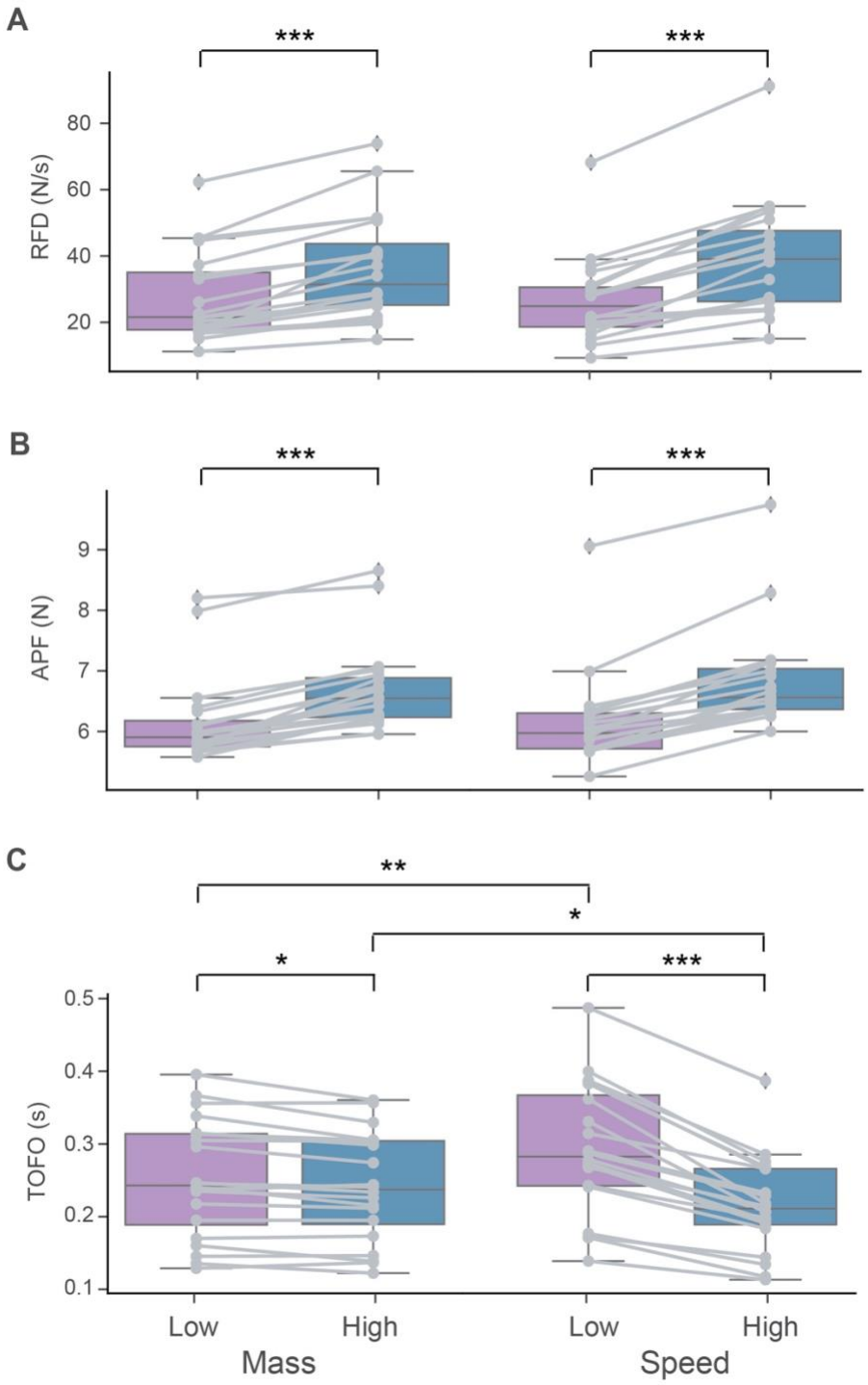

Figure 2.5. Motor response amplitude and timing. A) The rate of force development (RFD) scaled with object momentum. B) APF also scaled with momentum

independently on how the momentum was manipulated. C) Hand force was increased above baseline levels closer to the time of contact in anticipation of higher momentum collisions. Post-hoc differences (Bonferroni-adjusted): * indicates $p < 0.05$, ** indicates $p < 0.01$, *** indicates $p < 0.001$.

CHAPTER 3

EFFECT OF OBJECT MOMENTUM ON MUSCLE ACTIVITY AND SMOOTH PURSUIT EYE MOVEMENTS

Introduction

We interact with moving objects daily, and even though we may not be aware of the laws of physics, we apply them with great success to get moving objects to stop. Examples of this can be seen in many sports, such as lacrosse players catching a ball with their stick or a volleyball player blocking an attack hit. These types of actions require an estimation of the moving object's momentum to prepare impending contact with the object. In both examples, we often move our eyes to gather reliable visual information to know where the ball is and the speed at which it is traveling to estimate the time of contact. And based on the impact that we expect, we need to increase our postural stability to be able to counteract that impact.

Previous studies involving catching a free-falling ball have varied momentum by changing the mass of the ball and/or the height of fall. These studies have shown a positive linear relation between the mean anticipatory electromyography (EMG) activity and the momentum of the object (Lacquaniti & Maioli, 1989b; Shiratori & Latash, 2001). These anticipatory EMG responses during catching have shown a dependency on vision and knowledge of the properties of the object, such as its mass, if these properties are not evident by looking at it (Kazennikov & Lipshits, 2010b; Lacquaniti & Maioli, 1989a). In response to the impact, compensatory EMG activity of both agonist

and antagonist muscles has shown to also scale with momentum during catching (Berg & Hughes, 2017; Lacquaniti & Maioli, 1989b).

When we want continuous and accurate motion perception information of a moving object, we will naturally engage in smooth pursuit eye movements (SPEM), which will provide us with high-acuity vision of the object as well as extraretinal input (Fooken et al., 2021). In a real-world catching study, higher SPEM durations were associated with a higher probability of success (Cesqui et al., 2015). However, eye movements are not always predictors of manual interception accuracy. As reviewed in Fooken et al. (2021), it seems that the predictive role of eye movements is mainly pertinent for tasks with higher object motion uncertainty, for example when the object follows a complex motion trajectory or is occluded.

As introduced in the previous chapter (Chapter 2), we created a virtual *Mechanical STopping Of Projectiles* (MSTOP) task where participants have to "stop" an object moving towards their hand (negative Y direction) by applying a force pulse to bring the object's momentum to 0. The momentum of the object was varied by changing its speed and virtual mass. In Chapter 2 we showed that this new paradigm replicates hand force responses seen in studies involving catching free-falling objects. The aim of the current study is to understand how responses of the effectors either directly (arm muscle activity) or indirectly (eye gaze) involved in the task are affected when systematically varying the momentum of the projectile.

We hypothesized that, as with force, the amplitude of the responses would be scaled by the momentum of the object regardless of how the momentum was modified. This hypothesis predicted that the amplitude of muscle co-contraction before and after

the collision would be higher when the momentum of the object was higher, regardless of the momentum being increased by a higher speed of the object or a higher assigned mass. In relation to the eye-tracking, we hypothesized that participants would have a more difficult time tracking objects moving at higher speeds, resulting in a lower smooth pursuit gain for the higher speeds. We also hypothesized that participants would rely mainly on smooth pursuit eye movements to track the moving object to determine the time of force onset. This hypothesis predicted that there would be a correlation between SPEM duration and time of force onset.

Methods

Participants

The data for this study are a subset of the data used for Chapter 2. Data were collected in 20 participants (20.6 ± 2.04 years: 10 women). Participants were right-handed and had no history of neurological disorders. They had no current injuries or pain of the upper limbs or back and had normal or corrected to normal vision. All participants provided informed consent of their voluntary participation. All procedures were approved by the Institutional Review Board of the University of Georgia.

Apparatus

The task was executed on a robotic manipulandum (KINARM End-Point Lab, KINARM, Kingston, ON, Canada). Participants were seated on a chair and grasped the robotic arm with their right hand while moving in the horizontal plane. To prevent fatigue, a mobile arm support (SaeboMAS, Saebo Inc., Charlotte, NC, USA) was placed on their forearm to support the weight of their arm. EMG activity was collected with bipolar surface electrodes (Bagnoli, Delsys Inc., Boston, MA, USA). Monocular eye

position was recorded with a video-based remote eye-tracking system (Eyelink 1000; SR Research, Ottawa, ON Canada).

Procedure

Detailed procedures are explained in Chapter 2. In brief, participants performed a task called “Stop the ball”, in which they had to apply a force pulse to “virtually stop” an object moving towards them in the negative Y direction. To replicate the mechanics of a projectile interaction in our virtual task, the object was assigned a virtual mass which was multiplied by its speed, providing us with a momentum value. This momentum was applied to the participant’s hand when the object was in contact with the hand during the collision. The hand’s force during the time window of the collision was used to calculate the applied impulse.

At the beginning of each trial, participants moved a rectangular cursor that represented their hand location into a designated box where they experienced a background load (4 N in the -Y direction) until the end of the trial. After a fixed delay of 1700 ms, a fixation cross appeared in the middle of the screen. Participants were asked to maintain fixation on the cross until it disappeared. Then a circular object appeared 200 ms after on the same position and immediately started moving towards the middle of the box. When the moving object reached the Y position of the hand cursor, participants experienced a force during a fixed window of time (90 ms), for which they were told to “match the force applied to the hand so that the object stops”. Importantly, no instruction was given about where to position the eyes after object appearance. This meant that participants were free to decide whether to track the moving object with their eyes (engaging SPEM) or not.

The hand's impulse during the collision was calculated and compared against the object's momentum. If the impulse was matched within a ±5% margin of error the trial was classified as successful. Participants received feedback on their performance after each trial, both by means of the trajectory of the object after the collision (stop, 'bounce back', or continue moving on its original trajectory), and also a visual analog scale representing how far off they were from matching the momentum.

There were different Conditions and sub-conditions of the task (Table 3.1). In the Speed condition the object's momentum was manipulated by varying the object speed (*Low* or *High*) with a constant mass, and in the Mass condition the momentum was manipulated by varying the virtual mass (*Low* or *High*) with a constant speed. In the Mass condition, the different sub-conditions were represented with moving objects of different colors. Participants performed three blocks of each sub-condition, for a total of 12 blocks, with 35 trials in each block. The order of the conditions was counterbalanced across participants, with half of the participants completing all blocks within the Mass condition first and the other half completing the Speed condition first.

Data acquisition and analysis

EMG signals were recorded from 4 muscles: biceps brachii, triceps brachii, anterior deltoid, and posterior deltoid. Before placing the electrodes, the skin surface over each muscle was exfoliated and then cleaned with alcohol. The electrodes were attached to the skin over the muscle belly using double-sided tape, and the ground electrode was placed on the olecranon.

Table 3.1

Object mass, speed, and momentum/robot impulse values for the experimental sub-conditions.

Sub-condition	Mass (kg)	Speed (m/s)	Momentum (kg.m/s) or Impulse (N.s)
Speed Low	2.32	0.18	0.41
Speed High	2.32	0.25	0.58
Mass Low	1.87	0.22	0.41
Mass High	2.65	0.22	0.58

EMG signals were collected at 1,000 Hz, with an amplifier gain of 10^4. The signal was band-pass filtered between 20 and 450 Hz with a 6th order Butterworth filter, with a forward/backward pass to eliminate delays. After filtering, the signal was full-wave rectified and normalized. For each trial, the baseline activity in response to the background load was calculated during a 200 ms window that the fixation cross was on and averaged to subtract it from the raw muscle activity.

The processed EMG signals for each muscle were then ensemble averaged over all trials for each block and then averaged over the three blocks. To calculate the muscle onset activity, we used the same process used for APF (detailed in Chapter 2), but with a 15% cutoff instead of 5% to account for the higher levels of noise in the EMG signals. To quantify shoulder and elbow stabilization before (anticipatory) and during

collision (compensatory), an index of co-contraction was calculated with the mean of the rectified EMG signals; for the shoulder joint, we averaged the anterior and posterior deltoids and for the elbow joint, we averaged the biceps and triceps muscles. A moving average window of 20 ms was used for the EMG data plots.

The hand kinematic variable of time of force onset (TOFO) was used to see its relationship with gaze variables. Details on the data collection, processing and calculation for this variable are included in the previous chapter (Chapter 2).

Gaze position was collected at 500 Hz and low-pass filtered at 15 Hz. Details on gaze data processing and event identification are provided in detail in previous work (Singh et al., 2016). Briefly, the data was processed to remove blinks, one-sample spikes, and screen outliers. Gaze events were identified as saccades, smooth pursuit, and fixations using adaptive velocity and acceleration thresholds (Singh et al., 2016). Since the object started moving towards them as soon as it appeared, the main gaze variables analyzed in this study were related to SPEM. The SPEM gain, a measure of SPEM quality, was calculated as the gaze angular velocity divided by the object angular velocity, and average gain was quantified for the closed-loop phase, which was the period between 100 ms after object onset and TOFO. The SPEM duration was calculated as a percentage of the time between object onset and TOFO in which the participant was pursuing the target. A lower SPEM duration suggests participants spent more time in fixation, had more catch-up saccades during SPEM, or a combination of both. The cut-off to calculate our SPEM variables was TOFO because we were interested in the effect SPEM variables had on the initiation of motor responses. The term SPEM will be used in this study even though the movements that were quantified

were head and eye movements together, due to no head movements being restricted in the apparatus used. Gaze data from one participant was excluded from the processing because of the low quality.

The first three trials in each block were not included in the analysis. All analyses were performed in MATLAB (Mathworks R2021b, Natick, MA).

Statistics

Two-way repeated measures ANOVAs were conducted with sub-condition (Mass or Speed) and object momentum (Low or High) as within-subject factors to compare EMG onset, EMG co-contraction, SPEM gain, and SPEM duration across conditions. Significance level was set at $\alpha = 0.05$, effect sizes are reported using generalized η^2. When appropriate post-hoc comparisons were performed using paired *t*-tests, with adjusted *p* values using the Bonferroni method. Shapiro-Wilk test was used to test normality for each variable. If this test was significant, the data were first normalized using a logarithmic transformation before the analysis. Pearson correlations were conducted between TOFO and SPEM gain; and between TOFO and SPEM duration. All values are reported as mean ± SE. All statistical analyses were performed in R (version 4.0.4).

Results

Object momentum modulated timing of muscle activation and co-contraction before the collision

Participants moved their hand toward the object by executing shoulder flexion, mainly driven by the anterior deltoids, and by extending their elbow, driven by the triceps. The difference in EMG onset prior to the collision was analyzed for each muscle

(Fig. 3.1). The anterior deltoids ($F(1,14) = 22.136$, $p < 0.001$, $\eta^2 = 0.04$) and the triceps ($F(1,16) = 31.154$, $p < 0.001$, $\eta^2 = 0.05$) showed small but significant main effects of object momentum. Post-hoc comparisons showed participants increased their muscle activity above baseline closer to the time of collision for the *High* momentum sub-conditions. In the case of the anterior deltoids this difference was only seen in the Speed sub-conditions ($p = 0.001$), and in the triceps for both Speed ($p = 0.02$) and Mass ($p < 0.001$). Both posterior deltoids and biceps showed no significant interaction or main effects, indicating no differences between the sub-conditions in EMG onset for the antagonist muscles.

The anticipatory co-contraction was measured in the [-100, 0] ms time window before the collision. We observed a significant main effect of object momentum in the anticipatory co-contraction of the proximal muscles (deltoids) ($F(1,17) = 18.363$, $p < 0.001$, $\eta^2 = 0.02$), as well as the distal muscles (biceps and triceps) ($F(1,17) = 20.743$, $p < 0.001$, $\eta^2 = 0.04$) (Fig. 3.2). The post-hoc analysis for the proximal muscles showed an increase in co-contraction for the *High* momentum sub-conditions for both mass (*Mass Low*: 3.93 ± 0.53; *Mass High*: 4.84 ± 0.59, $p = 0.04$) and speed (*Speed Low*: 3.99 ± 0.48; *Speed High*: 4.67 ± 0.65, $p = 0.008$). The same increase was seen in the distal muscles with the increase in momentum for mass (*Mass Low*: 2.03 ± 0.35; *Mass High*: 2.66 ± 0.43, $p = 0.002$) and speed (*Speed Low*: 1.87 ± 0.25; *Speed High*: 2.31 ± 0.31, $p < 0.001$). Together, these results suggest an increase in arm stability in preparation for the stopping the higher momenta objects.

The compensatory co-contraction was measured for a short-latency ([25-50] ms) and a long-latency ([50-100] ms) time window after the beginning of the collision (time =

0) (Fig. 3.2). We observed no significant differences in the compensatory co-contraction for either time windows of the proximal muscles between the sub-conditions. For the distal muscles, we saw a small main effect of momentum in the short-latency window ($F(1,17) = 5.568$, $p = 0.03$, $\eta^2 = 0.04$) with the *Mass High* (2.21 ± 0.42) shower higher co-contraction than the *Mass Low* (1.73 ± 0.35) sub-condition ($p = 0.03$). For the long-latency window of the distal muscles, we also saw a small main effect of momentum ($F(1,17) = 14.779$, $p = 0.001$, $\eta^2 = 0.02$). The post-hoc analysis showed increased activity for the High momentum in both mass (*Mass Low*: 1.40 ± 0.33; *Mass High*: 1.94 ± 0.37, $p = 0.01$) and speed (*Speed Low*: 1.64 ± 0.39; *Speed High*: 1.96 ± 0.46, $p < 0.01$) conditions.

Pursuit gain was higher at lower object speed

SPEM gain showed an interaction effect ($F(1,17) = 40.54$, $p < 0.001$, $\eta^2 = 0.07$) (Fig. 3.3A). Post-hoc analysis revealed a significant difference between *Speed Low* (0.74 ± 0.03) and *Speed High* (0.61 ± 0.03) ($p < 0.001$) which had an object speed of 0.18 m/s and 0.25 m/s respectively; as well as a difference between *Speed Low* (0.74 ± 0.03) and *Mass Low* (0.60 ± 0.03) ($p < 0.001$), which were driven by differences in object speed for these two conditions (0.18 m/s and 0.22 m/s, respectively). This showed that participants were worse at matching higher object speeds with their gaze. There were no differences seen between the momentum sub-conditions for Mass, which is expected since the object in both sub-conditions was moving at the same speed (0.22 m/s).

SPEM duration, representing the percentage of time that participants were tracking the object between object onset and each trial's TOFO, showed no significant differences between the sub-conditions (Fig. 3.3B).

Pursuit duration, not quality, predicts time of force onset

On average, participants pursued the objects for 63.7 ± 1.84% of the time across all conditions. The percentages of SPEM duration ranged from values of 27 to 97% across all conditions, showing very different approaches on which eye movement to rely on in between participants. Closer qualitative examination of the eye movements across trials revealed two general strategies: participants tended to either make multiple saccades between the target and the upcoming contact location (low SPEM duration) or tried to track the target as closely as possible throughout the trial (high SPEM duration). These two strategies are exemplified in Figure 3.4. The first sample trial (left panel Fig. 3.4) is a trial from the Speed High sub-condition. For this trial, the participant had a SPEM duration of 20.74%, with a 0.12 s TOFO, and a 0.71 SPEM gain. The plot shows a large saccade ahead of the position of the object after the object appears, and then a second saccade once the object reaches the gaze position. The second sample trial (right panel Fig. 3.4) shows a trial from a Speed Low sub-condition. In this trial the participant had a SPEM duration of 99.86%, with a 0.52 s TOFO, and a 0.83 SPEM gain. The plot for this trial shows how right after the object starts moving, the participant engages in SPEM all the way leading up to TOFO.

To determine whether these two eye movement strategies affected hand timing, we correlated SPEM duration and TOFO, calculating the mean SPEM duration and TOFO for each participant and condition separately. There was a small but significant

positive correlation between SPEM duration and TOFO ($r = 0.24$, $p = 0.04$) (Fig. 3.5B). This indicates that overall, participants who relied more on SPEM increased their hand force earlier, whereas participants who relied more on saccades and fixations increased their hand force closer to the time of contact. Note that this correlation is not likely to be driven by differences across conditions, we did not find any differences between the sub-conditions for SPEM duration (Fig. 3.3B). Further, this correlation was specific to SPEM duration. There was no significant correlation between SPEM gain and TOFO ($r = -0.04$, $p = 0.73$) (Fig. 3.5A), suggesting that while engaging in pursuit, pursuit quality did not predict time of hand force onset.

Discussion

In this study we used a novel virtual paradigm, MSTOP, that replicates the mechanical interaction between a projectile and the hand. In the current study's protocol, the momentum of the object was modified by changing the object's speed and virtual mass. We aimed to determine if varying the momentum of the projectile affected the muscle activity and SPEM responses, as well as determining if the cause of the change in momentum (speed or virtual mass) influenced these variables.

For the muscle activity, we hypothesized that the amplitude of the responses would scale with the momentum of the object irrespective of the cause of the change in momentum. Our results support this hypothesis, showing an increase in anticipatory co-contraction with momentum, for both proximal and distal arm muscles. The compensatory EMG activity only showed a difference between momentum sub-conditions in the elbow stabilizing muscles. This could indicate that the stiffness of the shoulder from the anticipatory activity was enough to stabilize the arm for the impact,

and the increase in elbow stiffness alone was enough to counteract the force during and after the impact. The anticipatory and compensatory increases in muscle activity seen with higher momentum is in line with previous studies, where both agonist and antagonist muscles showed an increase in EMG when interacting with moving objects (Berg & Hughes, 2017; Eckerle et al., 2012; Lacquaniti & Maioli, 1987, 1989b).

For EMG onset, we only observed differences between the momentum sub-conditions in the agonist muscles (anterior deltoid and triceps), with the EMG onset happening earlier for the *Low* momentum sub-condition. This earlier activation with lower momentum is not in accordance with previous studies that showed the opposite trend of earlier activations corresponding to objects with higher momentum (Lacquaniti & Maioli, 1989b). Even though our results show statistically significant differences, these are very small time differences of no more than 13 ms. This difference can also be caused by the fact that the actual hand movements required for a real-life interaction with a projectile are not replicated with this virtual task.

In relation to the SPEM responses, we hypothesized that participants would rely primarily on SPEM and would have a lower SPEM gain when tracking objects moving at higher speeds. Our results show as expected, that the objects with higher speeds had a lower SPEM gain, replicating previous findings (Cesqui et al., 2015; Lisberger et al., 1981; Schröder et al., 2021). There was no difference in SPEM duration between the sub-conditions, indicating that on average SPEM duration was similar independent of the speed of the object. However, the range of SPEM duration percentages was very wide (27-97%), suggesting the use of different strategies between the participants, with some relying more on SPEM and others on saccades and fixations. The fact that

participants did not always rely on SPEM for this task could be explained by the predictability of the trajectory of the target, which was the same for all the trials, and the consistency of object speeds within one block (Fooken et al., 2021).

Finally, we showed that pursuit duration, but not pursuit gain, predicted the time of force onset. We found that participants with longer SPEM durations also showed earlier force onsets. The time of force onset, as seen in Chapter 2, changes according to the object's speed, but that was not the case for SPEM durations. Future work can further explore whether trial-by-trial SPEM is coupled with hand timing, as is often the case with saccades (Jana et al., 2017). It is also worth exploring if each individual participants utilized the same strategy across the different conditions, or if the strategies depended on the task parameters. The strength of eye-hand coupling often depends on task context, though most of the previous studies investigating this phenomenon have used tasks involving reaching movements to static targets (De Brouwer & Spering, 2022). One previous catching study that analyzed eye movements showed large differences in ocular behaviors across participants observed (Cesqui et al., 2015), suggesting that SPEM behavior may similarly be task-dependent.

Conclusion

In summary, we used the MSTOP paradigm to determine if varying the momentum of the projectile affected the muscle activity and SPEM responses. At the same time, we determined if the cause of the change in momentum influenced these variables. Our study shows anticipatory and compensatory increases in muscle activity with higher momentum. For the agonist muscles only, muscle activity onset showed differences between the momentum sub-conditions, with the muscle activity onset

happening earlier for the *Low* momentum sub-condition. Finally, SPEM gain was affected by object speed, showing lower gains for faster moving objects, and SPEM duration, predicted the time of force onset.

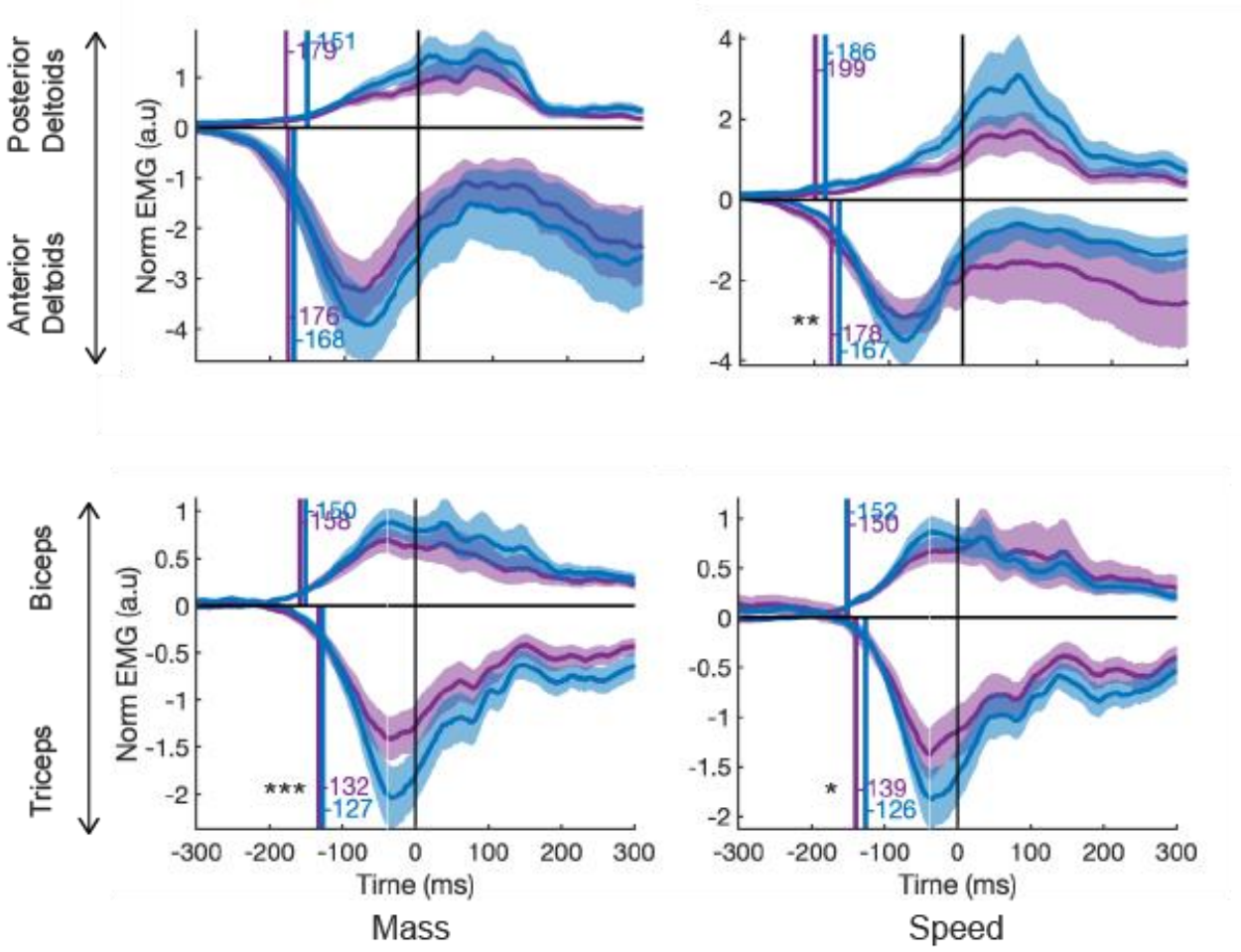

Figure 3.1. Point of EMG increase above baseline value. The upper panel shows the activity for antagonist posterior deltoids (positive) and agonist anterior deltoids (negative). The lower panel shows the activity for the antagonist biceps (positive) and agonist triceps (negative). The blue plots represent the High momentum sub-conditions, and the purple the Low momentum. The black vertical line (time = 0) indicates the time of collision between the hand and the object. The colored vertical lines indicate EMG onset with its corresponding value. Post-hoc differences (Bonferroni-adjusted): * indicates $p < 0.05$, ** indicates $p < 0.01$, *** indicates $p < 0.001$.

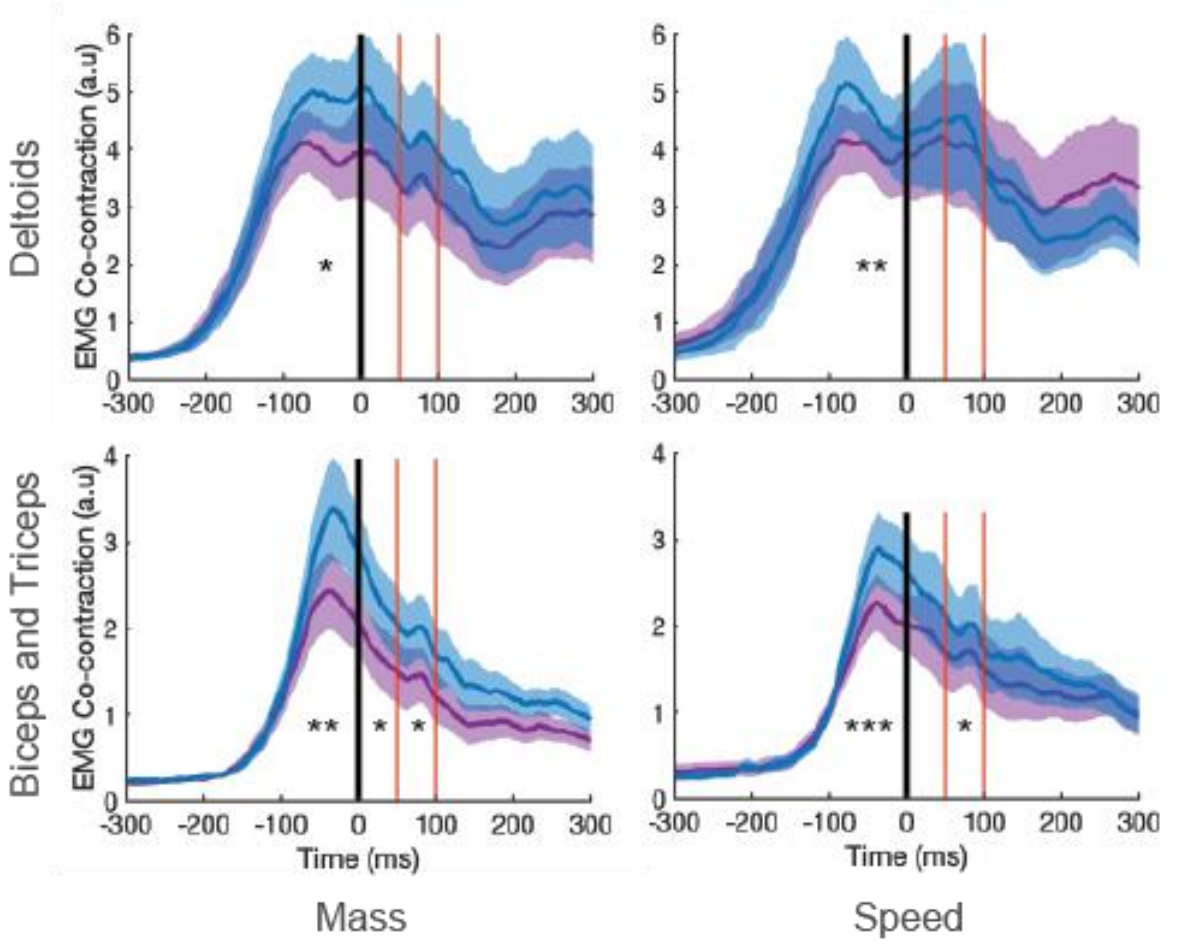

Figure 3.2. EMG co-contraction was higher for higher object momentum. The blue plots represent the High momentum sub-conditions, and the purple the Low momentum. The black vertical line (time = 0) indicates the time of collision between the hand and the object. The red vertical lines indicate short- and long-latency windows. Post-hoc differences (Bonferroni-adjusted): * indicates $p < 0.05$, ** indicates $p < 0.01$, *** indicates $p < 0.001$.

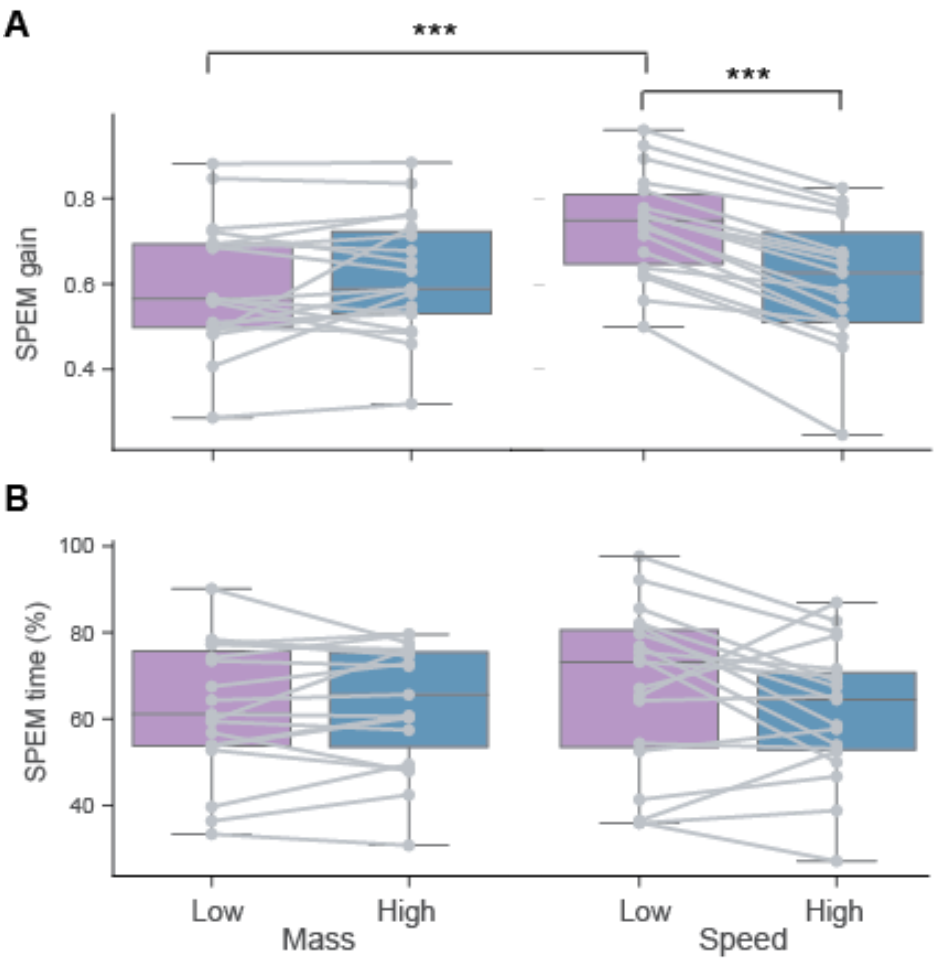

Figure 3.3. Smooth pursuit quality and quantity between conditions. A) SPEM gain was lower for higher speed moving objects. B) The percentage of time spent pursuing the target was on average similar between sub-conditions. Post-hoc differences (Bonferroni-adjusted): *** indicates $p < 0.001$.

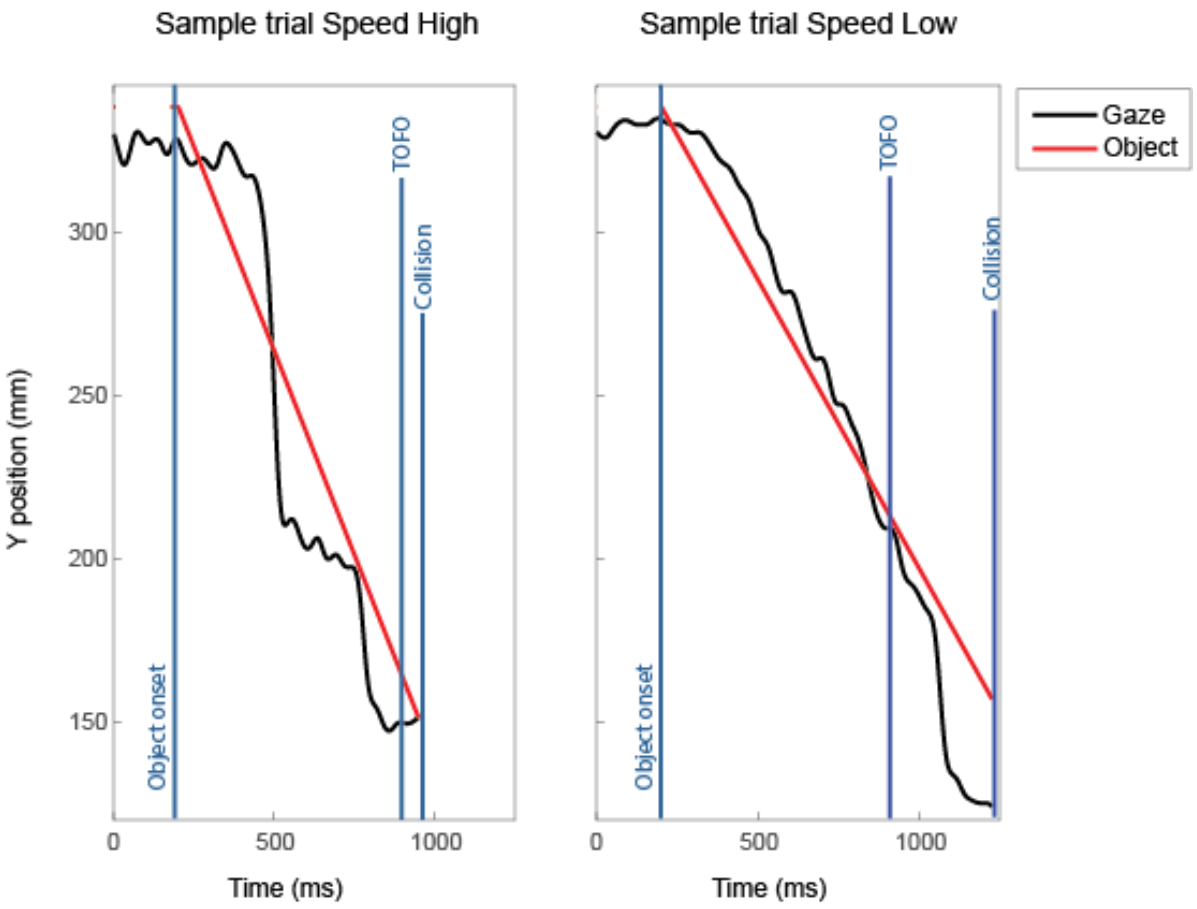

Figure 3.4. Sample trials of gaze and object position. Gaze Y position in relation to the object's Y position from two different participants in two different sub-conditions. The blue vertical lines indicate the time in which the different events occurred.

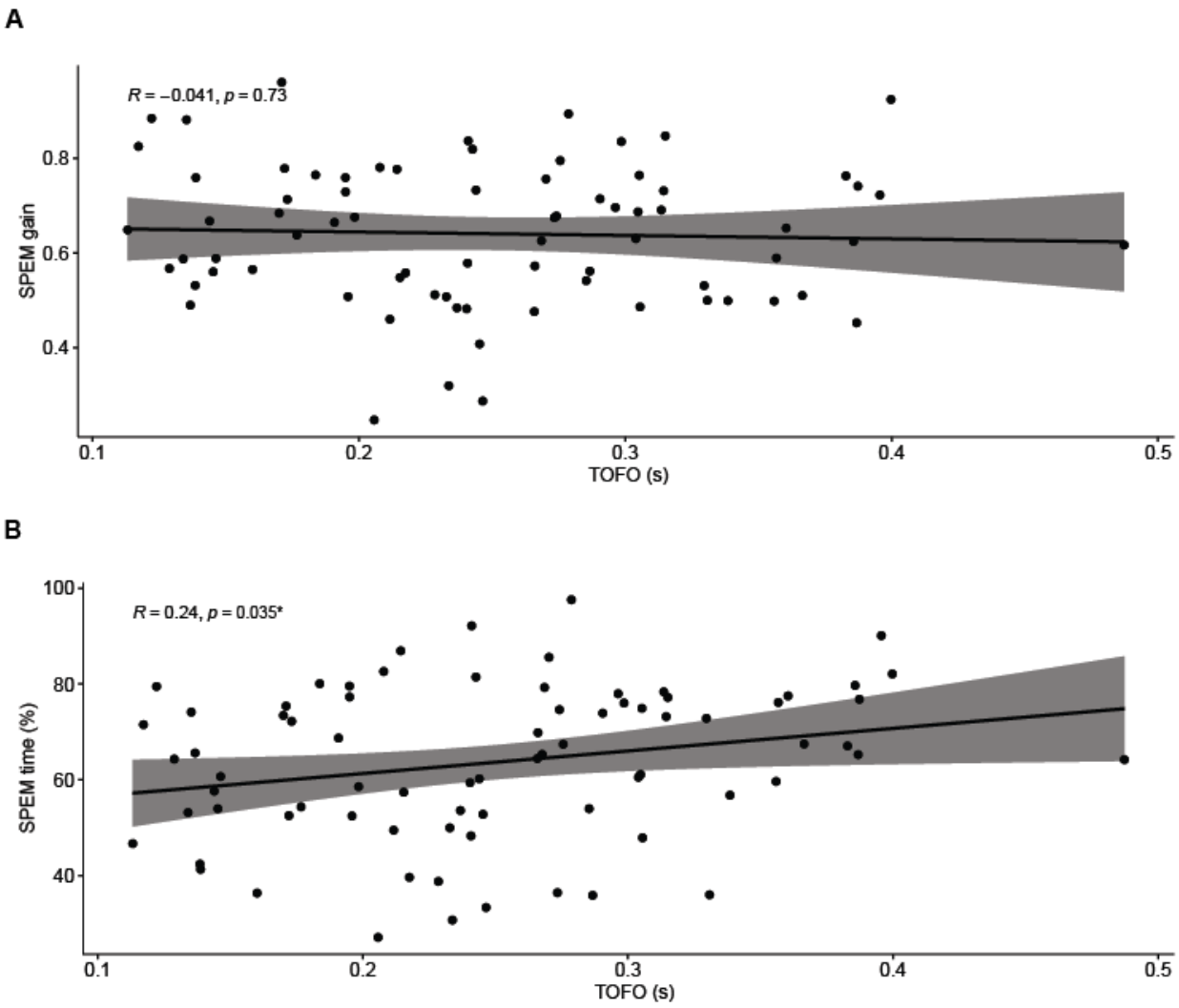

Figure 3.5. Relationships between TOFO, and SPEM gain and duration. A) There is no correlation between SPEM gain and TOFO. B) There is a significant positive correlation between SPEM duration and TOFO. * indicates $p < 0.05$

CHAPTER 4

ACCELERATING AND DECELERATING OBJECTS SHOW A SIMILAR EFFECT ON MOTOR RESPONSES DURING MECHANICAL STOPPING OF PROJECTILES

Introduction

Projectiles in the real world are usually not moving at constant speeds (acceleration = 0 m/s^2). Projectiles will experience changes in acceleration caused by external forces like gravity, air resistance, or friction with surfaces. Even without explicit knowledge of the equations specifying how much an object will speed up or slow down based on these external forces, humans are capable of using internal models based on previous experience to account for these changes. Therefore, the goal of this study is to extend our virtual paradigm to study objects moving at non-constant velocities.

Previous grip force studies have shown that in response to a ball being dropped in a receptacle being held by the participants fingers, both the anticipatory and compensatory force amplitude responses increase with the increase in object momentum caused by an increase of the ball's mass (Johansson & Westling, 1988; Kazennikov & Lipshits, 2010b). In these studies, the ball undergoes a free-fall, starting at 0 m/s and experiencing acceleration due to gravity, ending with a higher speed at the moment of contact. To our knowledge, there are no studies measuring hand force motor responses when interacting with a decelerating physical object.

With the same experimental design, the timing of the anticipatory force response was also measured. The force onset was between 150-200 ms before the impact, and

was constant across momentum conditions when the momentum was varied by changing the mass (Johansson & Westling, 1988; Kazennikov & Lipshits, 2010b). This indicates that timing of the force response under accelerating (gravity) conditions is not modulated by the momentum the participant is about to experience. A previous virtual interception task examining the timing of motor responses showed that the response was triggered earlier when the ball was falling from above, congruent with the acceleration caused by gravity in a free-fall, than when it was rising from below, congruent with the deceleration caused by gravity when throwing an object upwards, independent of the ball's real acceleration (1 gravity, -1 gravity, 0 acceleration) (Senot et al., 2005). This is consistent with an application of gravity-related knowledge (internal model of gravity) that would predict that the interceptive response should occur earlier because of the higher speed of the object.

It has previously been shown that in a prediction motion task, the object acceleration is not taken into account for the prediction of the time to contact (Benguigui & Bennett, 2010). In this task, the object experienced either positive or negative accelerations, and the object was tracked with smooth pursuit eye movements (SPEM). One possibility that acceleration information is not used for prediction is that that our visual system is not very accurate at identifying arbitrary accelerations (Zago & Lacquaniti, 2005b). A second possibility is that we do discriminate between the accelerations, but do not use this information for the estimation of the time to contact and to drive our manual response (Benguigui et al., 2003).

We previously introduced a virtual Mechanical STopping Of Projectiles (MSTOP) task in Chapters 2 and 3, and showed the motor responses linked to stopping a

projectile moving at constant speeds (acceleration = 0 m/s^2). The aim of this study is to examine anticipatory and compensatory motor responses when stopping a projectile with different accelerating conditions. For this we modified the MSTOP paradigm by systematically varying the acceleration of the object across conditions. One group of participants performed the task with moving objects accelerating toward their hand, and the other group with objects decelerating (same magnitude, but opposite sign).

We hypothesized that the motor responses would be affected by the type of acceleration of the moving objects. We predicted that the use of early visual information, as well as the poor accuracy in identifying arbitrary accelerations, would cause participants to underestimate the object's momentum when it was accelerating, and to overestimate the momentum when the object was decelerating. We based this prediction on the fact that if participants use the early visual information of the object's speed, and are not able to correctly estimate the acceleration, participants in the positive acceleration group would base their motor responses on lower speeds compared to the negative acceleration group. This would be seen in the amplitude of the hand force before and after the collision, as well as the timing of the hand force before the collision. We also hypothesized that SPEM responses would be similar for the different acceleration groups because of our visual system's poor ability to identify arbitrary accelerations, showing no effect of acceleration.

Methods

Participants

Data was collected on 22 participants who were divided in 2 groups of 11 participants each: Positive acceleration (mean age 19.3 $\pm$ 1.5 years; 3 males) and

Negative acceleration (mean age 20.9 ± 2.9; 3 males). They were all right-handed with no history of neurological disorders. Participants reported no current injuries or pain of the upper limbs or back and had normal or corrected to normal vision. All participants provided consent for their voluntary participation and received compensation for their time. All procedures were approved by the Institutional Review Board of the University of Georgia.

Apparatus

The task was executed on the KINARM End-Point Lab (KINARM, Kingston, ON, Canada), a robotic manipulandum. Participants were seated on a chair and with their right hand grasped the robotic arm which moved in the horizontal plane. To support the weight of their arm and prevent fatigue, a mobile arm support (SaeboMAS, Saebo Inc., Charlotte, NC, USA) was placed on their forearm. EMG activity was collected with bipolar surface electrodes (Bagnoli, Delsys Inc., Boston, MA, USA). Monocular eye position was recorded with a video-based remote eye-tracking system (Eyelink 1000; SR Research, Ottawa, ON Canada).

Procedure

Detailed procedures are explained in Chapter 2. In this section we will only highlight the changes made to the protocol for this experiment, such as the acceleration value, the color of the object, the aspect of the object for the Mass sub-conditions, the number of momentum sub-conditions, and the number of trials per block. Another difference was the fact that this was a two-day experiment. The two visits were separated by no more than 72 hours from each other. During Day 1 both groups (*Positive* and *Negative* acceleration) performed the same No acceleration conditions,

like in the experiment in Chapter 2 (Table 4.1). This first day was used primarily as a training day for participants to mitigate the effects of learning. Because of this, the data for Day 1 will not be analyzed in this chapter.

For Day 2, there were different Sub-conditions of the task (Table 4.1). The biggest change compared to Day 1 and the experiment in Chapter 2, is that we added an acceleration value (*Positive* or *Negative*) to the object. The *Positive* acceleration values were chosen so that the object would start at a speed of 0 m/s and accelerate to the collision location with a speed equal to the constant speed from the sub-conditions for Day 1. This was done to ensure that momentum values would be the same (as Day 1) at the time of the collision. The *Negative* acceleration magnitude was the same as the *Positive* group but with opposite sign. Based on the acceleration, the initial speed was calculated so that the object would start at a higher speed and decelerate to the point where the speed at the time of collision was the same as Day 1 (and the *Positive* acceleration sub-conditions).

In the Speed condition, the object's momentum was manipulated by varying the object's final speed (*Low*, *Medium*, or *High*) with a constant mass, and in the Mass condition the momentum was manipulated by varying the virtual mass (*Low*, *Medium*, or *High*) with a constant final speed across sub-conditions. In Chapters 2 and 3, there were only two momentum sub-conditions (0.41 kg.m/s – *Low*, and 0.58 kg.m/s – previously identified as *High*, identified as *Medium* in the current chapter). We identified the need for a third sub-condition to be able to identify not only if the modulation of responses depended on the momentum but also to see if there was a linear modulation. This led to a series of piloting test to add a third momentum sub-condition. We decided

to add a higher (*High* in the current chapter) sub-condition where the difference in momentum between *Low* and *Medium* was the same as the difference between *Medium* and *High*.

Unlike in Chapter 2, where the different assigned virtual masses were denoted by changes in color, here the different sub-conditions were represented with moving objects of different sizes. The corresponding radius of the moving objects were *Mass Low* – 0.8 cm, *Mass Medium* – 1.1 cm, *Mass High* – 1.4 cm, all *Speed* sub-conditions – 1 cm. The color of the circular object was uniform (purple) for all conditions, rather than using multiple colors to mimic a Gabor path.

Participants performed three blocks of each sub-condition, for a total of 18 blocks (9 for Mass and 9 for Speed), with 25 trials in each block. The order of the conditions was counterbalanced across participants. On Day 1, half of the participants started with the Mass condition and the other half started with the Speed condition. Participants completed 5 blocks of the first condition, then 9 blocks of the other condition, and finally 4 blocks of the initial condition. For Day 2, the order was flipped.

Table 4.1

Object mass, speed, acceleration, and momentum values for the experimental sub-conditions.

Sub-condition	Mass (kg)	Initial speed (m/s)	Final speed (m/s)	Average speed (m/s)	Acceleration (m/s^2)	Momentum (kg.m/s)
Day 1 - No acceleration						
Speed Low	2.32	0.18	0.18	0.18	0	0.41
Speed Med	2.32	0.25	0.25	0.25	0	0.58
Speed High	2.32	0.32	0.32	0.32	0	0.75
Mass Low	1.87	0.22	0.22	0.22	0	0.41
Mass Med	2.65	0.22	0.22	0.22	0	0.58
Mass High	3.41	0.22	0.22	0.22	0	0.75
Day 2 - Acceleration						
Positive						
Speed Low	2.32	0	0.18	0.09	0.08	0.41
Speed Med	2.32	0	0.25	0.13	0.17	0.58
Speed High	2.32	0	0.32	0.16	0.28	0.75
Mass Low	1.87	0	0.22	0.11	0.13	0.41
Mass Med	2.65	0	0.22	0.11	0.13	0.58
Mass High	3.41	0	0.22	0.11	0.13	0.75
Negative						
Speed Low	2.32	0.25	0.18	0.21	-0.08	0.41
Speed Med	2.32	0.35	0.25	0.30	-0.17	0.58
Speed High	2.32	0.46	0.32	0.39	-0.28	0.75
Mass Low	1.87	0.31	0.22	0.27	-0.13	0.41
Mass Med	2.65	0.31	0.22	0.27	-0.13	0.58
Mass High	3.41	0.31	0.22	0.27	-0.13	0.75

Data acquisition and analysis

Hand kinematics and kinetics were collected at 1,000 Hz and low-pass filtered with a second-order, dual-pass Butterworth filter with a 50 Hz cutoff. Gaze position was collected at 500 Hz and low-pass filtered at 15 Hz. Details on gaze data processing and event identification are provided in detail in previous papers and in Chapter 3 (Singh et al., 2016). EMG signals were collected for 4 muscles: biceps brachii, triceps brachii, anterior deltoid, and posterior deltoid; but were not included in the analysis in this Chapter. The main variables of interest are accuracy, Δ impulse, anticipatory peak force, time of force onset, SPEM gain, and SPEM duration. The data analysis for the hand variables of interest is the same as in Chapter 2, and for the gaze variables the same as in Chapter 3. The first three trials in each block were excluded from the analysis. All analyses were performed in MATLAB (Mathworks R2021b, Natick, MA).

Statistics

Three-way mixed ANOVAs were conducted with sub-condition (*Mass* or *Speed*) and object momentum (*Low*, *Med*, or *High*) as within-subject factors, and acceleration (*Positive* or *Negative*) as between-subject factors to compare collision performance, Δ impulse, anticipatory peak force (APF), time of force onset (TOFO), SPEM gain, and SPEM duration across conditions. Post-hoc comparisons were performed using two-way ANOVAs and paired *t*-tests with adjusted *p* values using the Bonferroni method. Significance level was set at $\alpha = 0.05$, effect sizes are reported using generalized η^2. Values are reported as mean ± SE. All statistical analyses were performed in R (version 4.0.4).

Results

The percentage of overshoot trials decreased with the increase in momentum

On average across all conditions, participants had 52.4 ± 1.42% of correct trials where they were able to match the robot's impulse within 95-105% (Fig. 4.1). For correct trials and for trials that were identified as undershoots, there were small main effects of object momentum (Correct: $F(2,40) = 8.955$, $p < 0.001$, $\eta^2 = 0.04$; Undershoot: $F(2,40) = 19.682$, $p < 0.001$, $\eta^2 = 0.08$). Both of these variables showed no main effect of acceleration (Correct: $F(1,20) = 0.176$, $p = 0.68$, $\eta^2 = 0.01$; Undershoot: $F(1,20) = 1.421$, $p = 0.25$, $\eta^2 = 0.06$). The overshoot trials showed a stronger main effect of object momentum ($F(2,40) = 68.290$, $p < 0.001$, $\eta^2 = 0.43$), where all but two of the pairwise comparisons were significantly different (p's < 0.05). This replicates our previous findings that as the object's momentum increases, the number of overshoots decreases. The main effect of acceleration was also not significant for the overshoot trials ($F(1,20) = 3.072$, $p = 0.10$, $\eta^2 = 0.08$), the generalized effect size is slightly larger than the one for Correct and Undershoot trials. When averaging the overshoot trials across momentum and mass/speed sub-conditions we see a larger percentage of overshoots in the *Negative* group (22.4 ± 1.57%) compared to the *Positive* group (17.1 ± 1.39%). Particularly, the biggest difference is seen between the *Negative Mass Low* (35.4 ± 3.38%) and *Positive Mass Low* (25.3 ± 2.40%) sub-conditions.

There was a significant main effect of object momentum on Δ Impulse ($F(2,40) = 41.316$, $p < 0.001$, $\eta^2 = 0.27$). Post-hoc statistical differences between object momentum sub-conditions are highlighted in Figure 4.2. Overall, the higher the object momentum, the more negative the Δ Impulse values, reflecting the tendency to

overshoot less (and undershoot more) on higher momentum trials. The main effect of acceleration was not significant ($F(1,20) = 2.962$, $p = 0.10$, $\eta^2 = 0.09$), however, when looking at the mean values across momentum and mass/speed sub-conditions for the different groups, the biggest difference is seen when comparing the *Negative Mass Low* (1.98 ± 0.72) and *Positive Mass Low* (-0.03 ± 0.75) sub-conditions. Though although these results did not reach statistical significance, the trend is consistent with the previous result of more overshoots seen in the Negative group.

Limb force amplitude and timing before the collision scale with momentum

Anticipatory peak force (APF) at collision increased with object momentum (main effect of momentum: $F(2,40) = 222.262$, $p < 0.001$, $\eta^2 = 0.43$) (Fig. 4.3). Post-hoc statistical differences between object momentum are highlighted in the corresponding figure. The main effect of acceleration was not significant ($F(1,20) = 0.068$, $p = 0.80$, $\eta^2 = 0.003$). On average across sub-conditions (*Mass* and *Speed*) and acceleration (*Positive* and *Negative*) *Low* momentum had a force of 5.96 ± 0.08 N (compared with the 5.1 N force of the robot), *Medium* momentum 6.57 ± 0.09 N (7.3 N robot force), and *High* momentum a force of 7.25 ± 0.11 N (9.4 N robot force). Thus, though APF scales with object momentum, it does not do so strictly linearly: at lower momentum APF is higher than the robot force, whereas at higher momentum the APF is lower than the robot force.

The timing of the force onset (TOFO) showed a small but significant two-way interaction between object momentum and mass/speed sub-conditions ($F(2,40) = 7.962$, $p = 0.001$, $\eta^2 = 0.005$) (Fig. 4.4). While across groups TOFO decreased as the momentum increased for both mass (*Mass Low*: 0.13 ± 0.01 s; *Mass Medium*: 0.11 ±

0.01 s; *Mass High*: 0.10 ± 0.01 s) and speed (*Speed Low:* 0.14 ± 0.01 s; *Speed Medium:* 0.11 ± 0.01 s; *Speed High:* 0.09 ± 0.01 s), the decrease in the speed sub-conditions had a greater effect size (*Mass*: $\eta^2 = 0.08$; *Speed*: $\eta^2 = 0.15$). The main effect of acceleration was not significant ($F(1,20) = 0.214$, $p = 0.65$, $\eta^2 = 0.01$). This shows that participants increased their hand force above baseline levels closer to the time of contact in anticipation of a higher momentum collision.

Pursuit gain decreased with higher speeds

There was a three-way interaction for SPEM gain ($F(1.39,27.82) = 7.138$, $p = 0.007$, $\eta^2 = 0.03$) (Fig. 4.5). Further two-way analysis revealed a significant interaction between object momentum and acceleration only for the speed sub-condition ($F(1.49,29.8) = 8.18$, $p = 0.003$, $\eta^2 = 0.08$), with main effects of momentum ($F(1.49,29.8) = 39.5$, $p < 0.001$, $\eta^2 = 0.28$) and acceleration ($F(1,20) = 33.0$, $p < 0.001$, $\eta^2 = 0.08$). This pattern of results indicates that SPEM gain decreases with the increase in momentum when that increased momentum is generated by increasing the object's speed. In addition, the overall SPEM gain is lower in the *Negative* acceleration condition, which have higher average speeds compared to the *Positive* acceleration. Post-hoc statistical differences between object momentum can be seen in Figure 4.5.

SPEM duration also showed a small three-way interaction ($F(2,40) = 5.132$, $p = 0.01$, $\eta^2 = 0.02$) (Fig. 4.6). Further analysis revealed that this interaction was driven by the low mean value of the *Negative Speed High* sub-condition. Pairwise comparisons showed a significant difference between *Negative Speed High* (43.8 ± 3.95%) and *Negative Mass High* (59.7 ± 5.59%) ($p = 0.002$), as well as a difference between *Negative Speed High* and *Positive Speed High* (63.7 ± 6.38%) ($p = 0.046$). Despite the

three-way interaction, the mean values for the sub-conditions were similar. As in Chapter 3, there was considerable variability in mean SPEM durations across all conditions, ranging from 15-94%.

Discussion

In the current study, we used the MSTOP paradigm to examine anticipatory and compensatory motor responses while systematically changing the object's acceleration. One group of participants experienced objects moving with positive acceleration, and another group experienced objects moving with negative acceleration. The initial speed values were selected so that the object speed at the time of the collision was the same for both groups, i.e., participants in each group experienced the same range of momentum values at collision (and the same momentum at collision as their constant speed training blocks), but with different object kinematics leading up to the collision. Hand force and SPEM were analyzed to see the effect of the accelerations.

Our hypothesis for both compensatory and anticipatory force amplitude was that participants would underestimate the object's momentum in the *Positive* acceleration group, and overestimate the momentum in the *Negative* acceleration group, causing them to have overall lower force values for *Positive* acceleration and higher force values for *Negative* acceleration. We also expected to see an effect of object momentum with higher force values for higher momentum objects.

The compensatory phase results from our accuracy variables (undershoot, correct, overshoot) and Δ Impulse show only a significant main effect of object momentum, with no main effect of acceleration. However, we do see some non-significant partial support for our acceleration hypothesis with an overestimation of

momentum in the *Negative* acceleration group. This is exemplified in the *Mass Low* sub-conditions, where there were more overshoots and the highest Δ Impulse value in the Negative group. This trend that we see should be further examined with a larger sample size per acceleration group, to determine if the absence of the main effect of acceleration is due to an underpowered analysis.

For the amplitude of anticipatory hand force response, our results partially support our predictions, showing higher APF values for higher momentum conditions, but no acceleration effect. However, the object momentum modulation shown is not strictly linear, showing higher APF compared to the robot force for the *Low* momentum, in contrast to lower APF compared to the robot force at higher momentum sub-conditions. Overall, the main effect of object momentum is consistent with our finding for no acceleration conditions (Chapter 2), as well as previous catching literature (Lacquaniti & Maioli, 1989b).

In relation to the timing of the hand force response, we hypothesized that there would be an effect of acceleration, where the Positive acceleration group would show results that more closely resemble real-world catching results, where the timing of the hand force is invariant to object motion characteristics (Lacquaniti & Maioli, 1989b). In contrast we do not see an effect of acceleration between the groups. In both acceleration condition groups, participants increased their hand force above baseline levels closer to the time of contact in anticipation of a higher momentum collision, and that this effect was stronger when the increase in momentum was caused by a higher acceleration value (Speed sub-condition). These results replicate our previous finding (Chapter 2) seen with objects moving at constant speeds, where the timing of the force

onset is modulated by momentum. In that case, it seemed that participants were using a distance-to-contact threshold (Port et al., 1997) since the mean values of the distance between the hand and the target at the time of force onset for the different sub-conditions only varied within 2-3 mm of each other. In the current study however, the mean distances across conditions ranged from 45-59 mm, clearly indicating that the force response was not fixed to a distance between the object and the hand.

Finally, we hypothesized that the SPEM responses for the different acceleration groups would be similar because of our visual system's poor ability to identify arbitrary accelerations and therefore poorer ability to use this information to guide motor responses. Our results show a decrease in SPEM gain with the increase in momentum in the *Speed* sub-condition, which has higher object speeds compared to the *Mass* sub-condition. SPEM gain values were also lower in the *Negative* acceleration group compared to the *Positive*, which is also mainly driven by the object speeds being higher in the *Negative* acceleration group. This is a consistent finding where higher speeds show a lower SPEM gain (Cesqui et al., 2015; Lisberger et al., 1981; Schröder et al., 2021). Despite much poorer quality SPEM in the *Negative* acceleration group, there were no differences between groups in the hand motor responses. Suggesting that specifically for this task, SPEM quality does not play a role on the hand motor responses. In relation to the SPEM duration, other than a low mean value seen in the Negative Speed High sub-condition, overall, the mean SPEM duration was not affected by acceleration or momentum. As in Chapter 3, there was large range of SPEM duration percentages (15-94%), which suggests that there are different gaze strategies among

participants, and that this does not necessarily have an effect in accuracy or motor behavior for the current task.

Conclusion

In summary, we examined anticipatory and compensatory motor responses when stopping a projectile with different accelerating conditions, utilizing the MSTOP paradigm. Our anticipatory and compensatory hand motor responses did not support our main hypothesis of an effect of acceleration (*Positive* vs *Negative*). However, a slight trend is seen in support of the hypothesis, for which we recommend increasing the number of participants per group, in case the non-significance is due to an underpower in the analysis. Finally, our SPEM quality and quantity variables suggest that for this task SPEM is not important.

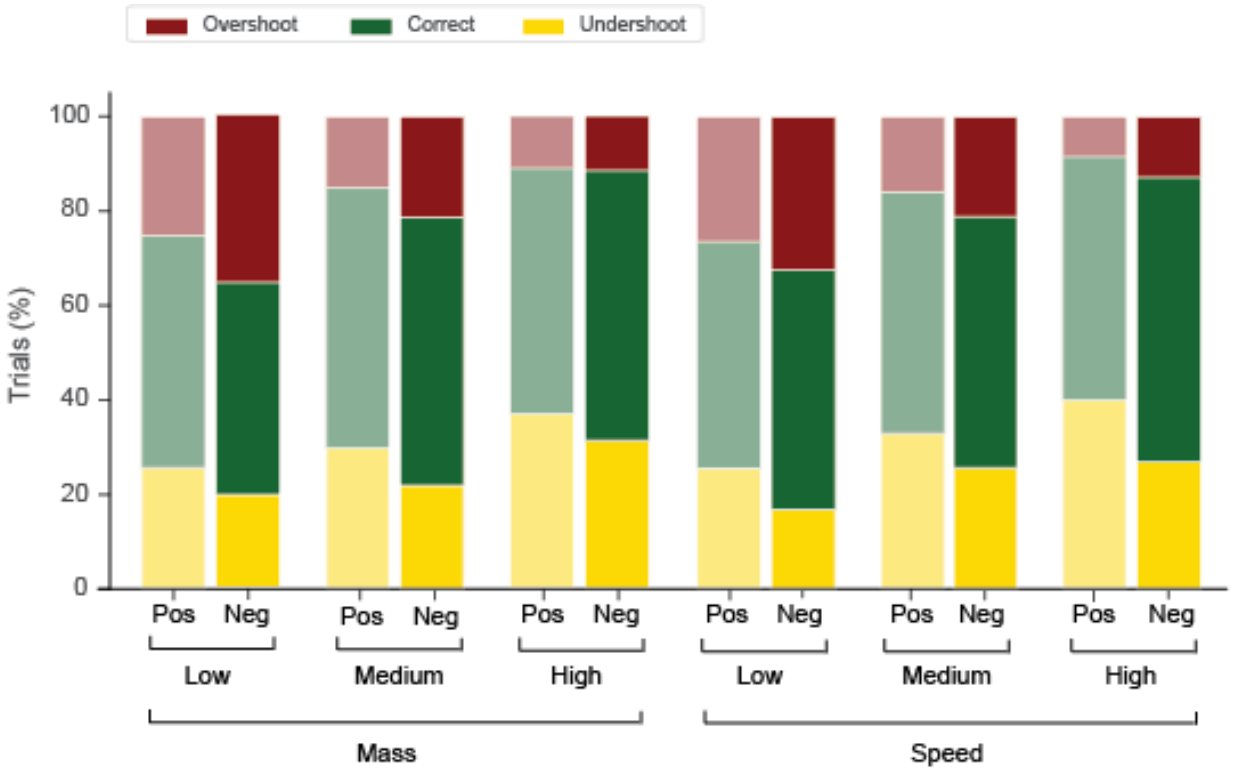

Figure 4.1. Accuracy for both Positive and Negative acceleration groups in the different sub-conditions. Overshoots: hand impulse greater than 95% of the robot's impulse. Correct: hand impulse between 95-105% of the robot's impulse. Undershoots: hand impulse lower than 95% of the robot's impulse.

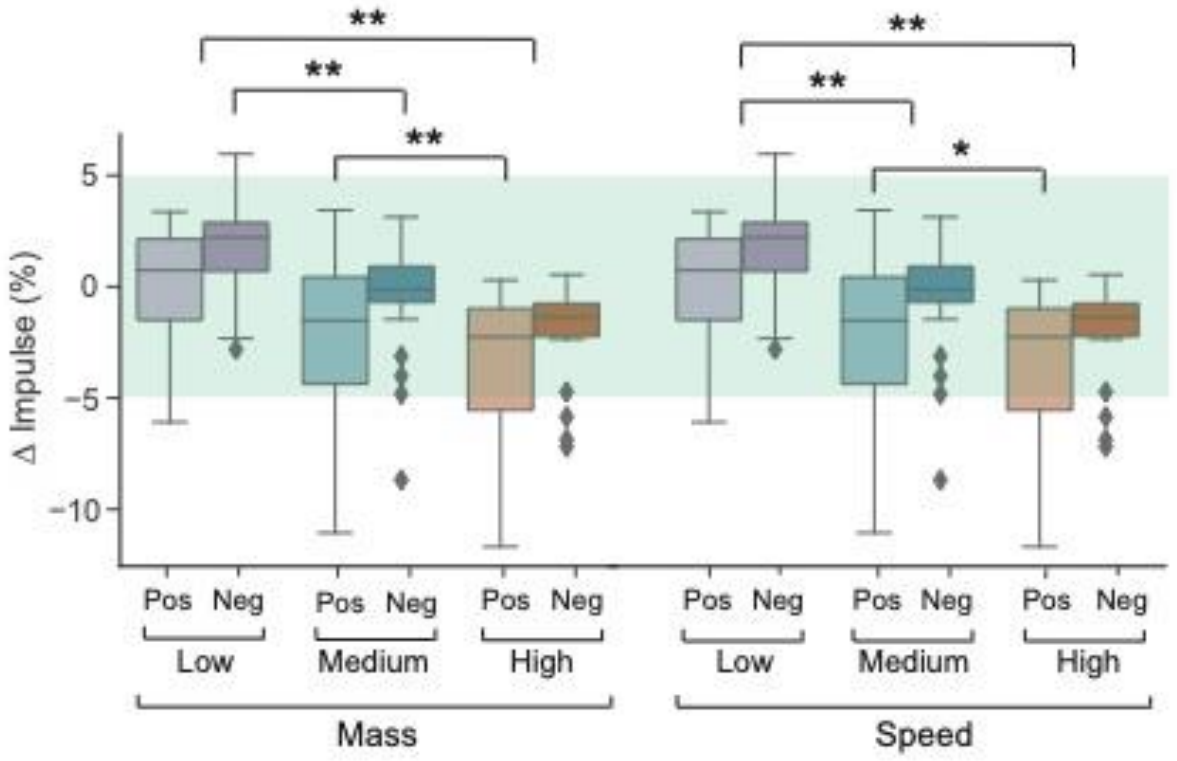

Figure 4.2. Limb force during collision. The shaded area indicates the error margin allowable for a trial to be categorized as correct. The upper panel shows the data for the Positive acceleration group, and the lower panel for the Negative acceleration group. Post-hoc differences (Bonferroni-adjusted): * indicates $p < 0.05$, ** indicates $p < 0.01$, *** indicates $p < 0.001$. Brackets placed between the Positive and Negative group in a momentum sub-condition, indicate differences for both Positive and Negative acceleration groups.

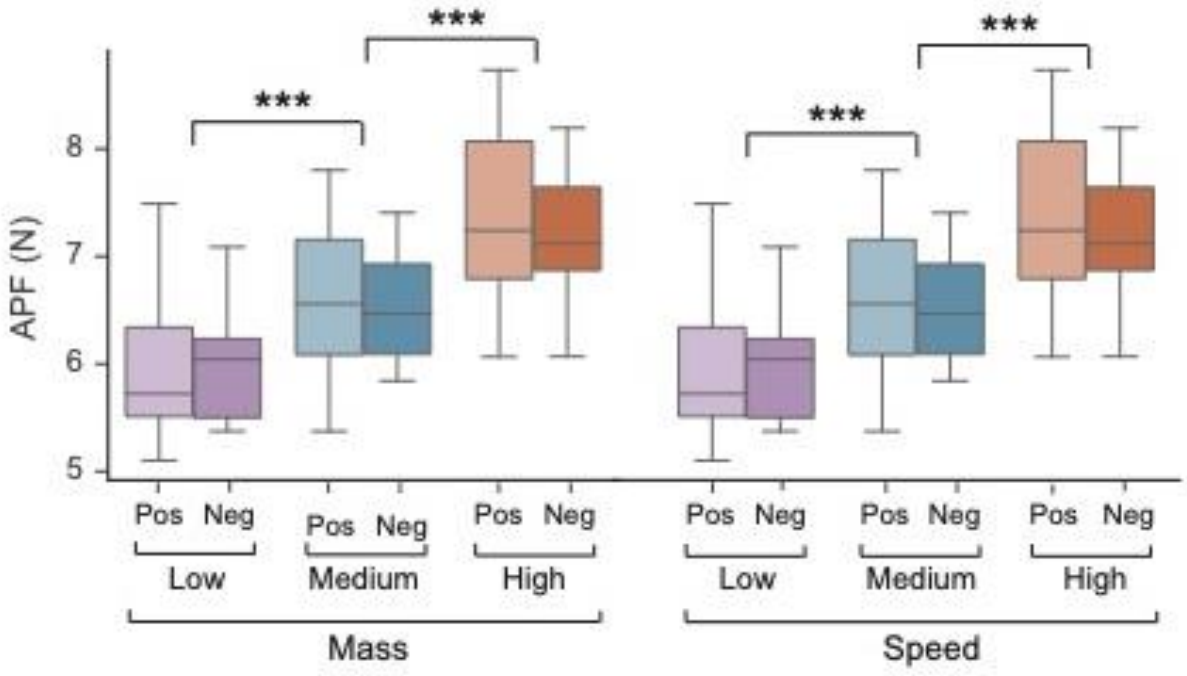

Figure 4.3. Limb force amplitude before the collision. APF scaled with object momentum. The upper panel shows the data for the Positive acceleration group, and the lower panel for the Negative acceleration group. Post-hoc differences (Bonferroni-adjusted): *** indicates $p < 0.001$. Brackets placed between the Positive and Negative group in a momentum sub-condition, indicate differences for both Positive and Negative acceleration groups.

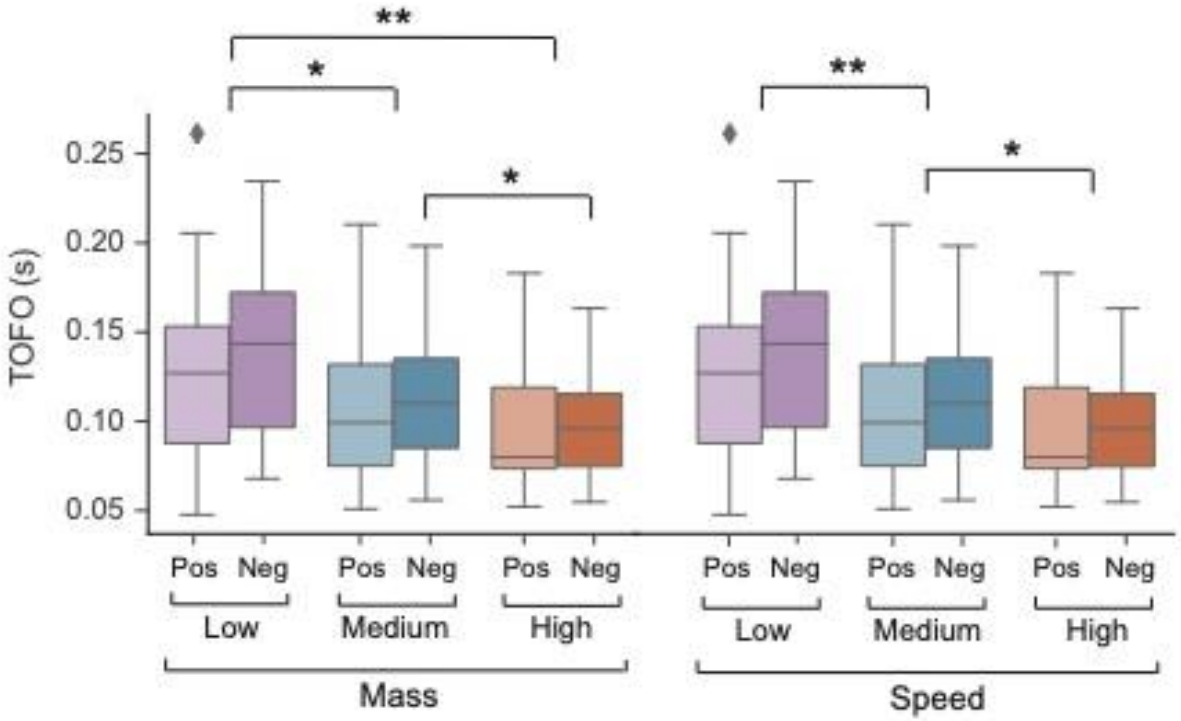

Figure 4.4. Timing of motor response before the collision. Hand force was increased above baseline levels closer to the time of contact for higher momentum trials. The upper panel shows the data for the Positive acceleration group, and the lower panel for the Negative acceleration group. Post-hoc differences (Bonferroni-adjusted): * indicates $p < 0.05$, ** indicates $p < 0.01$, *** indicates $p < 0.001$. Brackets placed between the Positive and Negative group in a momentum sub-condition, indicate differences for both Positive and Negative acceleration groups.

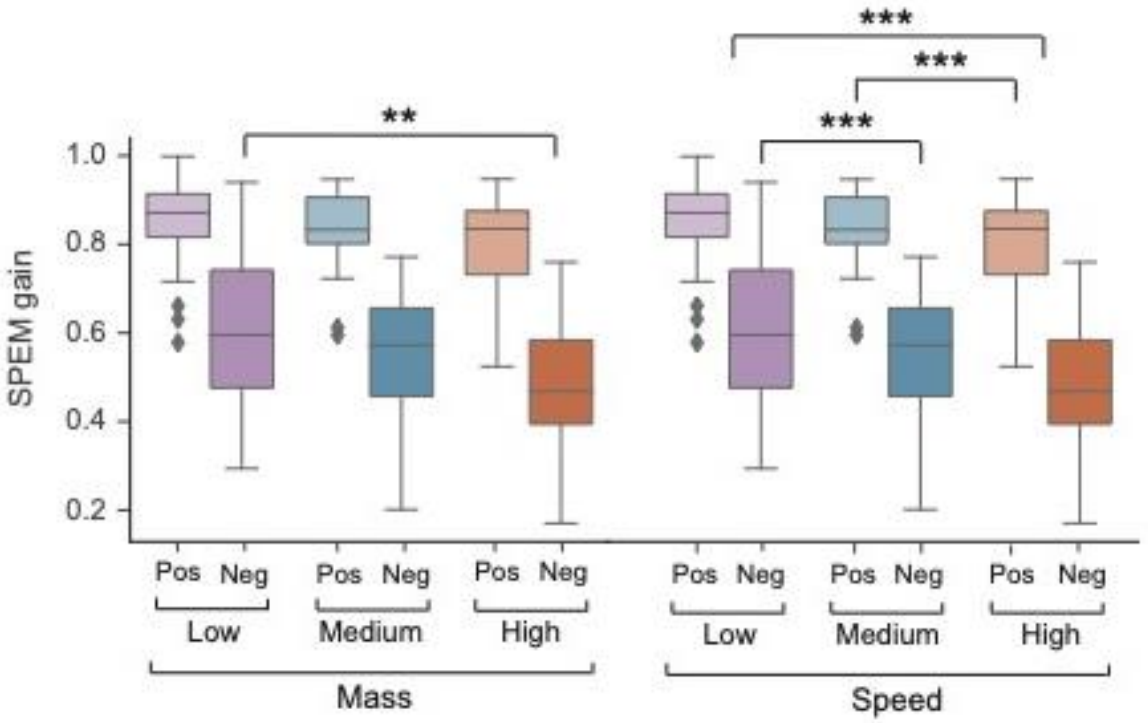

Figure 4.5. Smooth pursuit quality. SPEM gain decreased with higher object speeds. The upper panel shows the data for the Positive acceleration group, and the lower panel for the Negative acceleration group. Post-hoc differences (Bonferroni-adjusted): ** indicates $p < 0.01$, *** indicates $p < 0.001$. Brackets placed between the Positive and Negative group in a momentum sub-condition, indicate differences for both Positive and Negative acceleration groups.

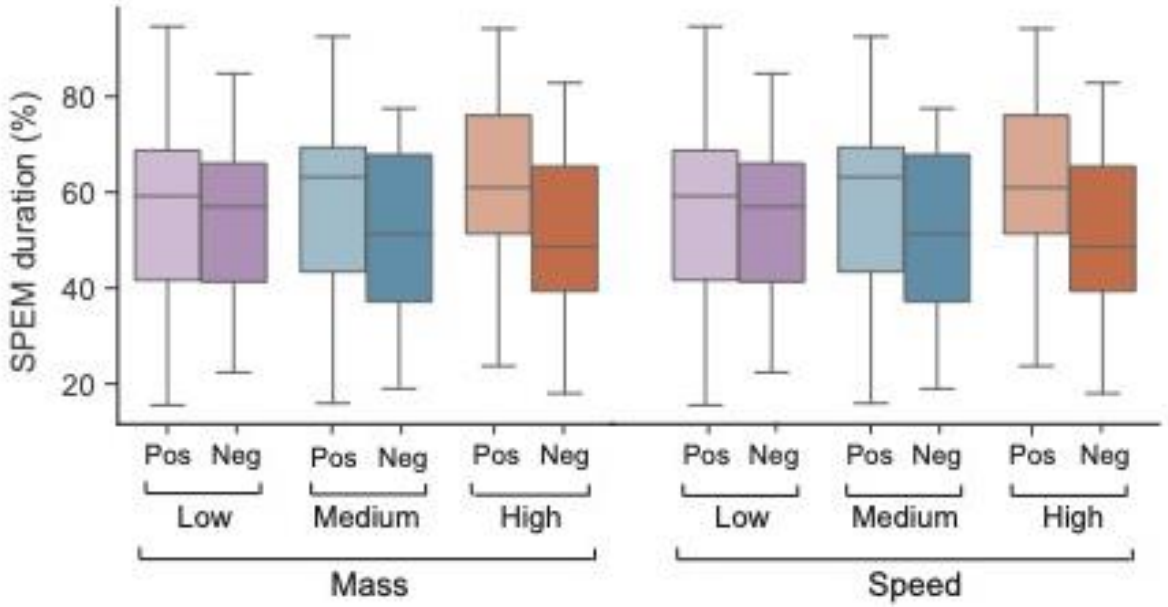

Figure 4.6. Percentage of time spent pursuing the moving object. SPEM duration was similar across conditions. The upper panel shows the data for the Positive acceleration group, and the lower panel for the Negative acceleration group.

CHAPTER 5

GENERAL DISCUSSION

The purpose of this dissertation was to develop a virtual paradigm, Mechanical STopping Of Projectiles (MSTOP) to simulate the physics of mechanical interactions with projectiles, allowing us to address novel questions about how varying the momentum of the projectile by changing its speed, acceleration, and virtual mass affect anticipatory and compensatory motor responses. For the anticipatory phase, we focused our analyses on hand force, arm muscles activation, and eye movements between stimulus motion onset and the collision. For the compensatory phase, we analyzed hand force and arm muscles activation in response to the collision.

The goal of developing the MSTOP task is to bridge the gap between current virtual tasks and real-world projectile interaction tasks, by allowing us to isolate a particular component of visuomotor control that is necessary for successful interactions with projectiles. The majority of the virtual tasks that study timing of motor responses when interacting with moving targets are based on interception of massless targets (Benguigui & Bennett, 2010; Bosco et al., 2012; Fink et al., 2009; Le Runigo et al., 2005; Senot et al., 2005; Witt & Sugovic, 2013). A limitation of this prior work is that the paradigms do not consider how the motor responses are shaped by the expected momentum (mass x velocity) of the object, and not only the kinematic characteristics. On the other hand, real-world projectile interaction tasks present the advantage of giving us information on motor responses based on the impact between the hand and a

real object (Berg & Hughes, 2017; Bockemühl et al., 2010; Cesqui et al., 2012; D'Andola et al., 2013; d'Avella et al., 2011; Eckerle et al., 2012; Kazennikov, 2011). However, in this case, the motor responses will always be shaped to objects experiencing gravity-specific acceleration.

Being able to decouple object motion properties with our novel virtual task has the potential of helping us identify specific visuomotor deficits in clinical populations, such as after brain injury or in neurodegenerative disease. The task framework allows for a fuller understanding of how we shape our responses as a consequence of different object characteristics, which could further guide the development of both behavioral-based diagnosis tools and rehabilitation strategies. As a diagnosis tool, it would aid in the identification of which motor responses are being affected (e.g., eye movements, muscle activity timing, force amplitude), and if the deficit is specific to anticipatory or compensatory control. After the identification of the specific deficit, the task can also be used and modified to target that specific aspect with different degrees of complexity, to aid with the rehabilitation of the cortical or musculoskeletal deficits, or to help the patient develop compensatory strategies to overcome those deficits.

Anticipatory Phase

This phase involves the motor responses that occur in *anticipation* to what we think the impact between the object and the hand will be like. In all experimental manipulations across both experiments (Chapters 2 and 4), we found that the amplitude of the hand force scaled with object momentum. We observed that participants applied a higher hand force right before contact for objects with higher momentum, regardless of whether the momentum increase was due to object speed, acceleration, or mass.

This finding is consistent with results from previous studies of free-falling catching, where the momentum of the object determined the amplitude of the force response, regardless of what caused the change in momentum (Johansson & Westling, 1988; Kazennikov & Lipshits, 2010b; Lacquaniti & Maioli, 1989b). In these studies, the change in momentum was caused by changes in the object's mass and the height of the drop—since they were all under free-fall conditions, the objects were experiencing gravity's constant acceleration. Our results with the MSTOP task not only replicate momentum-dependent force responses in a virtual environment, but also generalize this finding to show that it occurs for objects moving at constant speeds (no acceleration), objects accelerating at rates different than that of gravity, and decelerating objects.

In both experiments, our results showed that participants increased their hand force above baseline levels *closer* to the time of contact between the hand and the object in anticipation of higher momentum collisions. This was seen for objects moving at a constant speed as well as accelerating ones, and the effect was also seen if the increase in momentum was due to an increase in (virtual) mass. In the first experiment, where the objects were moving at constant speeds (no acceleration), the distance between the hand and the object at the time of force onset was very similar (no statistical difference) for all sub-conditions. For the second experiment, where objects were experiencing some type of acceleration, the distance at the time of force onset was not the same between the sub-conditions. These findings are contrary to what has been seen on previous studies, where the timing of the force onset is invariant to object motion and momentum (Kazennikov & Lipshits, 2010b; Lacquaniti & Maioli, 1989b). This difference can be due to the fact that our task is a virtual paradigm and participants

are well aware that the movement of the object is not being affected by natural gravity laws, so the responses differ from those of real-life tasks. One possible reason for this discrepancy is the force timing, but not amplitude, is dependent on a second-order internal model of gravity to estimate the time of contact between the hand and the ball (McIntyre et al., 2001). Our results suggest that in conditions in which object motion does not conform to the laws of gravity, humans base their responses on different internal models.

Our anticipatory muscle activity results mirrored the results for hand force. There was an increase in co-contraction of the task-relevant muscles with an increase in momentum, for both the proximal and distal arm. This is in line with previous studies, where both agonist and antagonist muscles show an increase in EMG when interacting with higher momentum objects (Berg & Hughes, 2017; Eckerle et al., 2012). For the onset of the EMG signals we saw differences in the agonist muscles (anterior deltoid and triceps), such that the onset occurred earlier for the lower momentum sub-conditions. Our results differ from free-fall catching studies that show an earlier muscle activation for balls dropped at higher heights (Lacquaniti & Maioli, 1989b; Shiratori & Latash, 2001). Considering that in free-falling the objects are accelerating, objects dropped at higher heights will be traveling at faster speeds at the time of contact, which explains the need to initiate the response earlier to account for the object's speed. In our virtual task, the objects were moving at constant speeds, which might account for the discrepancy seen with catching studies. The differences might also be explained by the fact that our task does not simulate the hand movement required for real-life catching, which could be modifying the muscle activation patterns.

The final anticipatory phase variables examined concerned smooth pursuit eye movements (SPEM). SPEM gain, the variable measuring how well participants' eye velocity matches the object's velocity, was lower for objects moving at higher speeds, both for objects moving at constant speeds and with acceleration. This result is in accordance with previous findings when tracking both real and virtual objects (Cesqui et al., 2015; Lisberger et al., 1981; Schröder et al., 2021). SPEM duration showed no differences between the sub-conditions of both experiments. The mean values were similar across sub-conditions, however, the range of the values in both experiments was very wide, suggesting the use of different strategies between the participants. A previous catching study showed a large variability in ocular behaviors across participants (Cesqui et al., 2015), and this seems to be the case also for our study. However, they did show a relationship between SPEM duration and catching performance, where even if SPEM deteriorated with higher speeds, in these faster conditions SPEM duration became crucial for ball motion prediction. In our task, the non-significant differences in SPEM duration despite our different speed and acceleration conditions, and the high variability between participants, might suggest a non-necessity to rely on SPEM, which could be explained by the low complexity of the task in relation to object trajectory and consistency of speeds across trials in a block (Fooken et al., 2021).

Overall, in the anticipatory phase we see variables such as APF and EMG amplitude that seem to be driven by a general principle: regardless of the presence or absence of gravity – or any arbitrary acceleration – we modulate our responses in a similar way. The timing of these responses however, seem to be context-dependent,

where as shown in real-life studies, responses are most likely driven by internal gravity related model, but this is not the case for our virtual experiments.

Compensatory Phase

This phase involves the motor responses that occur in response to the impact between the object and the hand. The compensatory response, as measured by forces after contact showed an increase with the increase in object momentum, regardless of the cause for the increase in momentum. This finding is similar to previous studies on catching falling objects with different masses (Kazennikov & Lipshits, 2010b).

For the EMG amplitude, we examined co-contraction responses in short- ([25-50] ms) and long-latency ([50-100] ms) windows. For the distal arm muscles (biceps and triceps), we saw an effect of momentum in both short- and long-latency windows, with an increase in activity seen with higher momentum. This increase in EMG seen in response to higher momentum is similar to previous catching studies (Berg & Hughes, 2017; Lacquaniti & Maioli, 1987). Together, this suggests that even in virtual environments, participants are primed for fast feedback control to mechanical perturbations in a momentum-dependent manner.

The compensatory responses for both force and EMG amplitude follow the same pattern seen in the anticipatory responses for these variables. Before the collision, both force and EMG amplitude were already higher for higher momentum conditions. This indicates that the anticipatory information influenced the compensatory phase. To isolate feedback responses specific to the compensatory phase, the visual information immediately before the collision can be occluded to minimize the effect of the anticipatory responses. An alternative strategy is to design a task environment in which

the visual information during the anticipatory phase is incongruent with the actual momentum of the object to cause perturbations of the visuomotor system and record compensatory responses based on the proprioceptive and sensory feedback from the collision.

Limitations

There were methodological limitations in the current experiments. Because of our interest in gaze variables and the limited area in the display in which we can get reliable eye-tracking quality, we were limited in the maximum distance between the start of the moving object and the collision box, which in our case was 20 cm. This maximum distance also influenced the speed and acceleration conditions that we could include in the protocols, since we could not have the objects moving so fast that the participants would not be able to modulate their motor responses appropriately. These differs from real-world catching studies, in which balls are typically dropped from heights exceeding 30 cm.

Another limitation of our paradigm is that even though we replicate the physics of a stopping task, the movement of the hands that are required to stop projectiles in the real-world is not the same. In our augmented-reality set-up, participants use a tool (a handle) to receive the impact and counteract the force. Even though we have been using mainly real-world catching studies to compare our results, we are aware that our paradigm is certainly not a ‘catching’ task. Therefore, we recognize that this might limit the interpretation of our results, specifically the compensatory phase, as the response needed is in a sense completely different. However, compared to other virtual tasks, our paradigm mimics the forces we experience when interacting with a real object, and not

only the kinematics as seen in interception tasks. It gives us the advantage to be able to isolate a particular component of visuomotor control that is necessary for successful catching, and at the same time there is an advantage over real-life tasks, because of the possibility of manipulating kinetic and kinematic variables without environmental constraints.

Future Directions

We introduced the MSTOP paradigm and showed that it replicates the physics of stopping projectiles in the real-world. An advantage of MSTOP paradigm is that task parameters can be easily manipulated to better understand different aspects of how we interact with projectiles. The design that we used for the current set of experiments was a blocked design for the different sub-conditions, which allowed participants to use information from previous trials to tune their motor responses. This could also have influenced the fact that some participants did not rely much on pursuit eye movements because the target was moving at the same speed across trials in a block. Randomizing trials from different sub-conditions in a block would give insight into the dependence on eye movements to estimate the time-to-contact based on the different speeds and accelerations of the moving object.

Another change that could be implemented is the specific instructions to the participants. In the current studies, the only requirement for the participants was to fixate on a cross before the moving object appeared. After the cross disappeared, participants were not instructed on what to do with their gaze, which resulted in large variability across participants, with some mostly tracking the object, and others relying mostly on saccades and fixations. In future studies, instructions on what to do when the

moving object appears would help standardize our eye movement measurements and give important information on gaze-dependent responses across task contexts. For example, the participants could be instructed to fixate on the cross for the entirety of the trial, making them use their peripheral vision to estimate the speed of the objects, or in a similar way, they could be instructed to pursue the object from the beginning to end.

There are two main variables of interest about the collision itself that can be modified. The first is the size of the area in which the collision has to happen. This area specifies the amount of hand movement allowed before the collision. In the current tasks, the collision area has the dimensions of a 5 x 10 cm rectangle. These dimensions allowed for a maximum of about 3 cm of movement before the collision. This area can be modified so to further restricts the movement of the hand before the collision, or to allow a greater movement or a free range in the case that participants are told to wait outside the box but to intercept the target in a specific collision area. Collision duration is a second aspect that may affect the pattern of observed results. Currently, participants experience a collision of 90 ms between the hand and the object. This value can be modified to change the feel of the collision, for example to mimic collisions with different types of materials.

Aspects about object motion distance, direction, and trajectory can also be modified. In the current task, the object moves in the negative Y direction following a linear path, and it starts at the same distance from the hand in every trial. Changing these factors could influence the object motion perception as well as the muscles needed to counteract the collision.

Lastly, this novel paradigm can be used as a diagnosis and/or rehabilitation tool for patients with visuomotor deficits. Once the characteristic behavior is identified in healthy population for different conditions in the new paradigm, deviations from this behavior can be identified in patient populations. With this, task conditions can be adjusted specifically for that patient to target specific deficits, and be used as a rehabilitation tool through repeated task practice. An example of this would be patients with cerebellar ataxia. These patients have trouble adapting their anticipatory responses when catching balls of different weights (Lang & Bastian, 1999) even when they receive prior information about the weight of the ball. Some patients show no adaptation at all, whereas others show a slower adaptation rate compared to controls. Depending on the extent of the damage of the cerebellum, the MSTOP task could be used in some patients as a rehabilitation tool. For example, with this task, multiple object kinematics can be presented to the patient, starting with easier conditions (blocked trials), and advancing to more complex protocols with randomized trials. Patients could then receive trial-by-trial performance feedback aimed at modulating anticipatory responses. Being exposed to this type of task-specific training could help foster strategies for improving anticipatory control, which could then generalize to improved motor performance in real-world tasks.

Conclusion

In conclusion, we developed a new augmented-reality based task which replicates the physics of a stopping a projectile task, but not the movement of the hand that is required for the interaction with projectiles in the real-world. With this task, we showed that the amplitude of force and EMG responses, both before and after the

collision, are similar to what we see in real-life catching studies. The timing of these motor responses in the anticipatory phase, however, are different to what we see in objects in the real-world experiencing acceleration because of gravity. Finally, pursuit eye movements did not seem to play a role modulating the hand motor responses under the conditions of our experiments. Together, our experiments present a viable framework for using virtual paradigms to mimic the physics of mechanical interactions needed for stopping a projectile, opening new possibilities for understanding how we prepare and update our visuomotor responses in dynamic environments.

REFERENCES

Alexander, G. E., & Crutcher, M. D. (1990a). Functional architecture of basal ganglia circuits: neural substrates of parallel processing. *Trends in neurosciences*, *13*(7), 266-271.

Alexander, G. E., & Crutcher, M. D. (1990b). Neural representations of the target (goal) of visually guided arm movements in three motor areas of the monkey. *Journal of neurophysiology*, *64*(1), 164-178.

Alexander, G. E., DeLong, M. R., & Strick, P. L. (1986). Parallel organization of functionally segregated circuits linking basal ganglia and cortex. *Annual review of neuroscience*, *9*(1), 357-381.

Archambault, P. S., Ferrari-Toniolo, S., & Battaglia-Mayer, A. (2011). Online control of hand trajectory and evolution of motor intention in the parietofrontal system. *Journal of Neuroscience*, *31*(2), 742-752.

Barany, D. A., Gómez-Granados, A., Schrayer, M., Cutts, S. A., & Singh, T. (2020). Perceptual decisions about object shape bias visuomotor coordination during rapid interception movements. *Journal of Neurophysiology*.

Bassi, C. J., & Lehmkuhle, S. (1990). Clinical implications of parallel visual pathways. *J Am Optom Assoc*, *61*(2), 98-110.

Basso, M. A., Krauzlis, R. J., & Wurtz, R. H. (2000). Activation and inactivation of rostral superior colliculus neurons during smooth-pursuit eye movements in monkeys. *Journal of Neurophysiology*, *84*(2), 892-908.

Basso, M. A., Pokorny, J. J., & Liu, P. (2005). Activity of substantia nigra pars reticulata neurons during smooth pursuit eye movements in monkeys. *European Journal of Neuroscience*, *22*(2), 448-464.

Bastian, A. J. (2006). Learning to predict the future: the cerebellum adapts feedforward movement control. *Current Opinion in Neurobiology*, *16*(6), 645-649. https://doi.org/https://doi.org/10.1016/j.conb.2006.08.016

Benguigui, N., & Bennett, S. J. (2010). Ocular pursuit and the estimation of time-to-contact with accelerating objects in prediction motion are controlled independently based on first-order estimates. *Experimental brain research*, *202*(2), 327-339.

Benguigui, N., Ripoll, H., & Broderick, M. P. (2003). Time-to-contact estimation of accelerated stimuli is based on first-order information. *Journal of experimental Psychology: Human perception and performance*, *29*(6), 1083.

Bennett, S. J., Baures, R., Hecht, H., & Benguigui, N. (2010). Eye movements influence estimation of time-to-contact in prediction motion. *Experimental brain research*, *206*(4), 399-407.

Berg, W. P., & Hughes, M. R. (2017). The effect of load uncertainty and foreperiod regularity on anticipatory and compensatory neuromotor control in catching. *Motor control*, *21*(1), 1-25.

Berg, W. P., & Hughes, M. R. (2019). The effect of load uncertainty on neuromotor control in catching: gender differences and short foreperiods. *Journal of motor behavior*.

Beurze, S. M., De Lange, F. P., Toni, I., & Medendorp, W. P. (2007). Integration of target and effector information in the human brain during reach planning. *Journal of neurophysiology*, *97*(1), 188-199.

Bockemühl, T., Troje, N. F., & Dürr, V. (2010). Inter-joint coupling and joint angle synergies of human catching movements. *Human Movement Science*, *29*(1), 73-93.

Bosco, G., Delle Monache, S., & Lacquaniti, F. (2012). Catching what we can't see: manual interception of occluded fly-ball trajectories. *PLoS One*, *7*(11), e49381.

Bowman, M. C., Johannson, R. S., & Flanagan, J. R. (2009). Eye–hand coordination in a sequential target contact task. *Experimental brain research*, *195*(2), 273-283.

Brenner, E., & Smeets, J. B. (2011). Continuous visual control of interception. *Human movement science*, *30*(3), 475-494.

Bridgeman, B., Hendry, D., & Stark, L. (1975). Failure to detect displacement of the visual world during saccadic eye movements. *Vision research*, *15*(6), 719-722.

Brown, P., Chen, C. C., Wang, S., Kühn, A. A., Doyle, L., Yarrow, K., . . . Aziz, T. (2006). Involvement of human basal ganglia in offline feedback control of voluntary movement. *Current biology*, *16*(21), 2129-2134.

Brunia, C. (1999). Neural aspects of anticipatory behavior. *Acta psychologica*, *101*(2-3), 213-242.

Burdet, E., Franklin, D. W., & Milner, T. E. (2013). *Human robotics: neuromechanics and motor control*. MIT press.

Burkholder, T. J. (2016). Model-based approaches to understanding musculoskeletal filtering of neural signals. In *Neuromechanical Modeling of Posture and Locomotion* (pp. 103-120). Springer.

Cannon, S. C., & Robinson, D. A. (1987). Loss of the neural integrator of the oculomotor system from brain stem lesions in monkey. *Journal of neurophysiology*, *57*(5), 1383-1409.

Cesqui, B., d'Avella, A., Portone, A., & Lacquaniti, F. (2012). Catching a ball at the right time and place: individual factors matter. *PLoS one*, *7*(2), e31770.

Cesqui, B., Mezzetti, M., Lacquaniti, F., & d'Avella, A. (2015). Gaze behavior in one-handed catching and its relation with interceptive performance: What the eyes can't tell. *PLoS One*, *10*(3), e0119445.

Cluff, T., & Scott, S. H. (2013). Rapid feedback responses correlate with reach adaptation and properties of novel upper limb loads. *Journal of Neuroscience*, *33*(40), 15903-15914.

Collewijn, H., & Tamminga, E. P. (1984). Human smooth and saccadic eye movements during voluntary pursuit of different target motions on different backgrounds. *The Journal of physiology*, *351*(1), 217-250.

Coull, J. T., & Nobre, A. C. (1998). Where and when to pay attention: the neural systems for directing attention to spatial locations and to time intervals as revealed by both PET and fMRI. *Journal of Neuroscience*, *18*(18), 7426-7435.

Cui, D.-M., Yan, Y.-J., & Lynch, J. C. (2003). Pursuit subregion of the frontal eye field projects to the caudate nucleus in monkeys. *Journal of neurophysiology*, *89*(5), 2678-2684.

Cullen, K. E., Chen-Huang, C., & McCREA, R. A. (1993). Firing behavior of brain stem neurons during voluntary cancellation of the horizontal vestibuloocular reflex. II. Eye movement related neurons. *Journal of neurophysiology*, *70*(2), 844-856.

D'Andola, M., Cesqui, B., Portone, A., Fernandes, L., Lacquaniti, F., & d'Avella, A. (2013). Spatiotemporal characteristics of muscle patterns for ball catching. *Frontiers in computational neuroscience*, *7*, 107.

de Azevedo Neto, R. M., & Bartels, A. (2021). Disrupting short-term memory maintenance in premotor cortex affects serial dependence in visuomotor integration. *Journal of Neuroscience*, *41*(45), 9392-9402.

De Brouwer, A. J., & Spering, M. (2022). Eye-hand coordination during online reach corrections is task dependent. *Journal of Neurophysiology*, *127*(4), 885-895.

Debats, N. B., Kingma, I., Beek, P. J., & Smeets, J. B. (2012). Moving the weber fraction: the perceptual precision for moment of inertia increases with exploration force.

Desmurget, M., Epstein, C., Turner, R., Prablanc, C., Alexander, G., & Grafton, S. (1999). Role of the posterior parietal cortex in updating reaching movements to a visual target. *Nature neuroscience*, *2*(6), 563-567.

Desmurget, M., & Grafton, S. (2000). Forward modeling allows feedback control for fast reaching movements. *Trends in cognitive sciences*, *4*(11), 423-431.

Dum, R. P., & Strick, P. L. (2005). Frontal lobe inputs to the digit representations of the motor areas on the lateral surface of the hemisphere. *Journal of Neuroscience*, *25*(6), 1375-1386.

d'Avella, A., Cesqui, B., Portone, A., & Lacquaniti, F. (2011). A new ball launching system with controlled flight parameters for catching experiments. *Journal of neuroscience methods*, *196*(2), 264-275.

Ebner, T. J., & Pasalar, S. (2008). Cerebellum predicts the future motor state. *The Cerebellum*, *7*(4), 583-588.

Eckerle, J. J., Berg, W. P., & Ward, R. M. (2012). The effect of load uncertainty on anticipatory muscle activity in catching. *Experimental brain research*, *220*(3), 311-318.

Ehrsson, H. H., Fagergren, A., Johansson, R. S., & Forssberg, H. (2003). Evidence for the involvement of the posterior parietal cortex in coordination of fingertip forces for grasp stability in manipulation. *Journal of neurophysiology*, *90*(5), 2978-2986.

Faisal, A. A., & Wolpert, D. M. (2009). Near optimal combination of sensory and motor uncertainty in time during a naturalistic perception-action task. *Journal of neurophysiology*, *101*(4), 1901-1912.

Fautrelle, L., Pichat, C., Ricolfi, F., Peyrin, C., & Bonnetblanc, F. (2011). Catching falling objects: the role of the cerebellum in processing sensory–motor errors that may influence updating of feedforward commands. An fMRI study. *Neuroscience*, *190*, 135-144.

Filimon, F. (2010). Human cortical control of hand movements: parietofrontal networks for reaching, grasping, and pointing. *The Neuroscientist*, *16*(4), 388-407.

Fink, P. W., Foo, P. S., & Warren, W. H. (2009). Catching fly balls in virtual reality: A critical test of the outfielder problem. *Journal of vision*, *9*(13), 14-14.

Fisher, B., Boyd, L., & Winstein, C. (2006). Contralateral cerebellar damage impairs imperative planning but not updating of aimed arm movements in humans. *Experimental brain research*, *174*(3), 453-466.

Fooken, J., Kreyenmeier, P., & Spering, M. (2021). The role of eye movements in manual interception: A mini-review. *Vision Research*, *183*, 81-90.

Fukushima, K., Yamanobe, T., Shinmei, Y., & Fukushima, J. (2002). Predictive responses of periarcuate pursuit neurons to visual target motion. *Experimental brain research*, *145*(1), 104-120.

Fukushima, K., Yamanobe, T., Shinmei, Y., Fukushima, J., Kurkin, S., & Peterson, B. W. (2002). Coding of smooth eye movements in three-dimensional space by frontal cortex. *Nature*, *419*(6903), 157-162.

Gallivan, J. P., & Culham, J. C. (2015). Neural coding within human brain areas involved in actions. *Current opinion in neurobiology*, *33*, 141-149.

Gamlin, P. D., & Yoon, K. (2000). An area for vergence eye movement in primate frontal cortex. *Nature*, *407*(6807), 1003-1007.

Gibson, J. J., Smith, O. W., Steinschneider, A., & Johnson, C. W. (1957). The relative accuracy of visual perception of motion during fixation and pursuit. *The American Journal of Psychology*, *70*(1), 64-68.

Glickstein, M., Gerrits, N., Kralj-Hans, I., Mercier, B., Stein, J., & Voogd, J. (1994). Visual pontocerebellar projections in the macaque. *Journal of Comparative Neurology*, *349*(1), 51-72.

Gottlieb, J. P., MAcAVOY, M. G., & Bruce, C. J. (1994). Neural responses related to smooth-pursuit eye movements and their correspondence with electrically elicited

smooth eye movements in the primate frontal eye field. *Journal of Neurophysiology*, *72*(4), 1634-1653.

Haber, S. N. (2010). Integrative networks across basal ganglia circuits. *Handbook Of Behavioral Neuroscience*, *20*, 409-427.

Hafed, Z. M., & Krauzlis, R. J. (2006). Ongoing eye movements constrain visual perception. *Nature Neuroscience*, *9*(11), 1449-1457.

Heath, M., Westwood, D. A., & Binsted, G. (2004). The control of memory-guided reaching movements in peripersonal space. *Motor control*, *8*(1), 76-106.

Hoshi, E., & Tanji, J. (2007). Distinctions between dorsal and ventral premotor areas: anatomical connectivity and functional properties. *Current opinion in neurobiology*, *17*(2), 234-242.

Ilg, U. J. (1997). Slow eye movements. *Progress in neurobiology*, *53*(3), 293-329.

Ilg, U. J. (2008). The role of areas MT and MST in coding of visual motion underlying the execution of smooth pursuit. *Vision Research*, *48*(20), 2062-2069. https://doi.org/https://doi.org/10.1016/j.visres.2008.04.015

Ilg, U. J., Schumann, S., & Thier, P. (2004). Posterior parietal cortex neurons encode target motion in world-centered coordinates. *Neuron*, *43*(1), 145-151.

Ilg, U. J., & Thier, P. (2003). Visual tracking neurons in primate area MST are activated by smooth-pursuit eye movements of an “imaginary” target. *Journal of neurophysiology*, *90*(3), 1489-1502.

Jana, S., Gopal, A., & Murthy, A. (2017). A computational framework for understanding eye–hand coordination. *Journal of the Indian Institute of Science*, *97*(4), 543-554.

Johansson, R., & Westling, G. (1988). Programmed and triggered actions to rapid load changes during precision grip. *Experimental brain research*, *71*(1), 72-86.

Jones, L. A. (1986). Perception of force and weight: theory and research. *Psychological bulletin*, *100*(1), 29.

Kakei, S., Lee, J., Mitoma, H., Tanaka, H., Manto, M., & Hampe, C. S. (2019). Contribution of the cerebellum to predictive motor control and its evaluation in ataxic patients. *Frontiers in Human Neuroscience*, *13*, 216.

Kawato, M. (1999). Internal models for motor control and trajectory planning. *Current opinion in neurobiology*, *9*(6), 718-727.

Kazennikov, O. (2011). Dependence of anticipatory changes in the hand muscle activity and the grip force on the height of the fall when catching a falling object. *Human Physiology*, *37*(3), 304-311.

Kazennikov, O., & Lipshits, M. (2010a). Dependence of the anticipatory change in the grip force in the catching task on the result of the preceding trial. *Human physiology*, *36*(3), 370-371.

Kazennikov, O., & Lipshits, M. (2010b). Influence of preliminary information about the mass on anticipatory muscle activity during the catching of a falling object. *Human physiology*, *36*(2), 198-202.

Keller, E., & Heinen, S. (1991). Generation of smooth-pursuit eye movements: neuronal mechanisms and pathways. *Neuroscience research*, *11*(2), 79-107.

Kempf, F., Brücke, C., Kühn, A. A., Schneider, G.-H., Kupsch, A., Chen, C. C., . . . Nuttin, B. (2007). Modulation by dopamine of human basal ganglia involvement in feedback control of movement. *Current biology*, *17*(15), R587-R589.

Krauzlis, R. J. (2001). Extraretinal inputs to neurons in the rostral superior colliculus of the monkey during smooth-pursuit eye movements. *Journal of Neurophysiology*, *86*(5), 2629-2633.

Krauzlis, R. J. (2003). Neuronal activity in the rostral superior colliculus related to the initiation of pursuit and saccadic eye movements. *Journal of Neuroscience*, *23*(10), 4333-4344.

Krauzlis, R. J. (2005). The control of voluntary eye movements: new perspectives. *The Neuroscientist*, *11*(2), 124-137.

Krukowski, A. E., Pirog, K. A., Beutter, B. R., Brooks, K. R., & Stone, L. S. (2003). Human discrimination of visual direction of motion with and without smooth pursuit eye movements. *Journal of Vision*, *3*(11), 16-16.

Kuling, I. A., Salmen, F., & Lefèvre, P. (2019). Grip force preparation for collisions. *Experimental Brain Research*, *237*(10), 2585-2594.

Kurtzer, I. L. (2015). Long-latency reflexes account for limb biomechanics through several supraspinal pathways. *Frontiers in integrative neuroscience*, *8*, 99.

Lacquaniti, F., Borghese, N., & Carrozzo, M. (1991). Transient reversal of the stretch reflex in human arm muscles. *Journal of Neurophysiology*, *66*(3), 939-954.

Lacquaniti, F., Borghese, N., & Carrozzo, M. (1992). Internal models of limb geometry in the control of hand compliance. *Journal of Neuroscience*, *12*(5), 1750-1762.

Lacquaniti, F., Carrozzo, M., & Borghese, N. (1993). Time-varying mechanical behavior of multijointed arm in man. *Journal of neurophysiology*, *69*(5), 1443-1464.

Lacquaniti, F., & Maioli, C. (1987). Anticipatory and reflex coactivation of antagonist muscles in catching. *Brain research*, *406*(1-2), 373-378.

Lacquaniti, F., & Maioli, C. (1989a). Adaptation to suppression of visual information during catching. *The Journal of Neuroscience*, *9*(1), 149-159. https://doi.org/10.1523/jneurosci.09-01-00149.1989

Lacquaniti, F., & Maioli, C. (1989b). The role of preparation in tuning anticipatory and reflex responses during catching. *Journal of Neuroscience*, *9*(1), 134-148.

Lang, C. E., & Bastian, A. J. (1999). Cerebellar subjects show impaired adaptation of anticipatory EMG during catching. *Journal of neurophysiology*, *82*(5), 2108-2119.

Lang, C. E., & Bastian, A. J. (2001). Additional somatosensory information does not improve cerebellar adaptation during catching. *Clinical Neurophysiology*, *112*(5), 895-907. https://doi.org/https://doi.org/10.1016/S1388-2457(01)00518-1

Le Runigo, C., Benguigui, N., & Bardy, B. G. (2005). Perception–action coupling and expertise in interceptive actions. *Human Movement Science*, *24*(3), 429-445. https://doi.org/https://doi.org/10.1016/j.humov.2005.06.008

Lee, D. N. (1976). A theory of visual control of braking based on information about time-to-collision. *Perception*, *5*(4), 437-459.

Lee, D. N. (1998). Guiding movement by coupling taus. *Ecological psychology*, *10*(3-4), 221-250.

Lisberger, S., Evinger, C., Johanson, G., & Fuchs, A. (1981). Relationship between eye acceleration and retinal image velocity during foveal smooth pursuit in man and monkey. *Journal of Neurophysiology*, *46*(2), 229-249.

Lisberger, S., Pavelko, T., & Broussard, D. (1994). Responses during eye movements of brain stem neurons that receive monosynaptic inhibition from the flocculus and ventral paraflocculus in monkeys. *Journal of Neurophysiology*, *72*(2), 909-927.

Lisberger, S. G. (2010). Visual guidance of smooth-pursuit eye movements: sensation, action, and what happens in between. *Neuron*, *66*(4), 477-491.

Lynd-Balta, E., & Haber, S. (1994). Primate striatonigral projections: a comparison of the sensorimotor-related striatum and the ventral striatum. *Journal of Comparative Neurology*, *345*(4), 562-578.

Machado, S., Cunha, M., Portella, C. E., Silva, J. G., Velasques, B., Bastos, V. H., . . . Cagy, M. (2008). Integration of cortical areas during performance of a catching ball task. *Neuroscience letters*, *446*(1), 7-10.

Malla, C. d. l., Smeets, J. B., & Brenner, E. (2017). Potential systematic interception errors are avoided when tracking the target with one's eyes. *Scientific reports*, *7*(1), 1-12.

Maschke, M., Gomez, C. M., Ebner, T. J., & Konczak, J. (2004). Hereditary cerebellar ataxia progressively impairs force adaptation during goal-directed arm movements. *Journal of neurophysiology*, *91*(1), 230-238.

Maunsell, J. H., & Van Essen, D. C. (1983). Functional properties of neurons in middle temporal visual area of the macaque monkey. I. Selectivity for stimulus direction, speed, and orientation. *Journal of neurophysiology*, *49*(5), 1127-1147.

May, J., Keller, E. L., & Suzuki, D. A. (1988). Smooth-pursuit eye movement deficits with chemical lesions in the dorsolateral pontine nucleus of the monkey. *Journal of Neurophysiology*, *59*(3), 952-977.

McFarland, N. R., & Haber, S. N. (2002). Thalamic relay nuclei of the basal ganglia form both reciprocal and nonreciprocal cortical connections, linking multiple frontal cortical areas. *Journal of Neuroscience*, *22*(18), 8117-8132.

McIntyre, J., Zago, M., Berthoz, A., & Lacquaniti, F. (2001). Does the brain model Newton's laws? *Nature neuroscience*, *4*(7), 693-694.

Merigan, W. H., & Maunsell, J. H. (1993). How parallel are the primate visual pathways? *Annual review of neuroscience*, *16*(1), 369-402.

Miall, R., & Jenkinson, E. (2005). Functional imaging of changes in cerebellar activity related to learning during a novel eye–hand tracking task. *Experimental Brain Research*, *166*(2), 170-183.

Miall, R. C., Weir, D. J., Wolpert, D. M., & Stein, J. (1993). Is the cerebellum a smith predictor? *Journal of motor behavior*, *25*(3), 203-216.

Miles, F. (1974). Single unit firing patterns in the vestibular nuclei related to voluntary eye movements and passive body rotation in conscious monkeys. *Brain research*, *71*(2-3), 215-224.

Missal, M., & Heinen, S. J. (2004). Supplementary eye fields stimulation facilitates anticipatory pursuit. *Journal of Neurophysiology*, *92*(2), 1257-1262.

Monzée, J., & Smith, A. M. (2004). Responses of cerebellar interpositus neurons to predictable perturbations applied to an object held in a precision grip. *Journal of neurophysiology*, *91*(3), 1230-1239.

Mrotek, L. A., & Soechting, J. F. (2007). Target interception: hand–eye coordination and strategies. *Journal of Neuroscience*, *27*(27), 7297-7309.

Mulliken, G. H., Musallam, S., & Andersen, R. A. (2008). Forward estimation of movement state in posterior parietal cortex. *Proceedings of the National Academy of Sciences*, *105*(24), 8170-8177.

Mustari, M. J., Fuchs, A. F., & Wallman, J. (1988). Response properties of dorsolateral pontine units during smooth pursuit in the rhesus macaque. *Journal of Neurophysiology*, *60*(2), 664-686.

Newsome, W. T., Wurtz, R. H., & Komatsu, H. (1988). Relation of cortical areas MT and MST to pursuit eye movements. II. Differentiation of retinal from extraretinal inputs. *Journal of neurophysiology*, *60*(2), 604-620.

Nowak, D. A., & Hermsdörfer, J. (2004). Predictability influences finger force control when catching a free-falling object. *Experimental brain research*, *154*(4), 411-416.

Ohyama, T., Nores, W. L., Murphy, M., & Mauk, M. D. (2003). What the cerebellum computes. *Trends in neurosciences*, *26*(4), 222-227.

Omrani, M., Murnaghan, C. D., Pruszynski, J. A., & Scott, S. H. (2016). Distributed task-specific processing of somatosensory feedback for voluntary motor control. *Elife*, *5*.

Ono, S. (2015). The neuronal basis of on-line visual control in smooth pursuit eye movements. *Vision research*, *110*, 257-264.

Ono, S., & Mustari, M. J. (2007). Horizontal smooth pursuit adaptation in macaques after muscimol inactivation of the dorsolateral pontine nucleus (DLPN). *Journal of neurophysiology*, *98*(5), 2918-2932.

Ono, S., & Mustari, M. J. (2011). Role of MSTd Extraretinal Signals in Smooth Pursuit Adaptation. *Cerebral Cortex*, *22*(5), 1139-1147. https://doi.org/10.1093/cercor/bhr188

Orban de Xivry, J. J., & Lefevre, P. (2007). Saccades and pursuit: two outcomes of a single sensorimotor process. *The Journal of physiology*, *584*(1), 11-23.

Padberg, J., Cerkevich, C., Engle, J., Rajan, A. T., Recanzone, G., Kaas, J., & Krubitzer, L. (2009). Thalamocortical connections of parietal somatosensory cortical fields in macaque monkeys are highly divergent and convergent. *Cerebral cortex*, *19*(9), 2038-2064.

Panchuk, D., Davids, K., Sakadjian, A., MacMahon, C., & Parrington, L. (2013). Did you see that? Dissociating advanced visual information and ball flight constrains perception and action processes during one-handed catching. *Acta Psychologica*, *142*(3), 394-401. https://doi.org/https://doi.org/10.1016/j.actpsy.2013.01.014

Paradiso, G., Cunic, D., Saint-Cyr, J. A., Hoque, T., Lozano, A. M., Lang, A. E., & Chen, R. (2004). Involvement of human thalamus in the preparation of self-paced movement. *Brain*, *127*(12), 2717-2731.

Pisotta, I., & Molinari, M. (2014). Cerebellar contribution to feedforward control of locomotion [Review]. *Frontiers in Human Neuroscience*, *8*(475). https://doi.org/10.3389/fnhum.2014.00475

Port, N. L., Lee, D., Dassonville, P., & Georgopoulos, A. P. (1997). Manual interception of moving targets I. Performance and movement initiation. *Experimental Brain Research*, *116*(3), 406-420.

Pruszynski, J. A., Kurtzer, I., Nashed, J. Y., Omrani, M., Brouwer, B., & Scott, S. H. (2011). Primary motor cortex underlies multi-joint integration for fast feedback control. *Nature*, *478*(7369), 387-390.

Pruszynski, J. A., Kurtzer, I., & Scott, S. H. (2008). Rapid motor responses are appropriately tuned to the metrics of a visuospatial task. *Journal of neurophysiology*, *100*(1), 224-238.

Ramnani, N., Toni, I., Passingham, R. E., & Haggard, P. (2001). The cerebellum and parietal cortex play a specific role in coordination: a PET study. *Neuroimage*, *14*(4), 899-911.

Roy, J. E., & Cullen, K. E. (2003). Brain stem pursuit pathways: dissociating visual, vestibular, and proprioceptive inputs during combined eye-head gaze tracking. *Journal of neurophysiology*, *90*(1), 271-290.

Schell, G. R., & Strick, P. L. (1984). The origin of thalamic inputs to the arcuate premotor and supplementary motor areas. *Journal of Neuroscience*, *4*(2), 539-560.

Schröder, R., Baumert, P. M., & Ettinger, U. (2021). Replicability and reliability of the background and target velocity effects in smooth pursuit eye movements. *Acta psychologica*, *219*, 103364.

Scott, S. H. (2012). The computational and neural basis of voluntary motor control and planning. *Trends in cognitive sciences*, *16*(11), 541-549.

Scott, S. H., Cluff, T., Lowrey, C. R., & Takei, T. (2015). Feedback control during voluntary motor actions. *Current opinion in neurobiology*, *33*, 85-94.

Scott, S. H., & Kalaska, J. F. (1997). Reaching movements with similar hand paths but different arm orientations. I. Activity of individual cells in motor cortex. *Journal of neurophysiology*, *77*(2), 826-852.

Seidler, R. D., Noll, D. C., & Thiers, G. (2004). Feedforward and feedback processes in motor control. *NeuroImage*, *22*(4), 1775-1783. https://doi.org/https://doi.org/10.1016/j.neuroimage.2004.05.003

Senot, P., Zago, M., Lacquaniti, F., & McIntyre, J. (2005). Anticipating the effects of gravity when intercepting moving objects: differentiating up and down based on nonvisual cues. *Journal of neurophysiology*, *94*(6), 4471-4480.

Shinmei, Y., Yamanobe, T., Fukushima, J., & Fukushima, K. (2002). Purkinje cells of the cerebellar dorsal vermis: simple-spike activity during pursuit and passive whole-body rotation. *Journal of neurophysiology*, *87*(4), 1836-1849.

Shiratori, T., & Latash, M. L. (2001). Anticipatory postural adjustments during load catching by standing subjects. *Clinical neurophysiology*, *112*(7), 1250-1265.

Shook, B., Schlag-Rey, M., & Schlag, J. (1990). Primate supplementary eye field: I. Comparative aspects of mesencephalic and pontine connections. *Journal of Comparative Neurology*, *301*(4), 618-642.

Singh, T., Fridriksson, J., Perry, C. M., Tryon, S. C., Ross, A., Fritz, S., & Herter, T. M. (2017). A novel computational model to probe visual search deficits during motor performance. *Journal of neurophysiology*, *117*(1), 79-92.

Singh, T., Perry, C. M., & Herter, T. M. (2016). A geometric method for computing ocular kinematics and classifying gaze events using monocular remote eye tracking in a robotic environment. *Journal of neuroengineering and rehabilitation*, *13*(1), 1-17.

Smith, M. A., & Shadmehr, R. (2005). Intact ability to learn internal models of arm dynamics in Huntington's disease but not cerebellar degeneration. *Journal of neurophysiology*, *93*(5), 2809-2821.

Souto, D., & Kerzel, D. (2021). Visual selective attention and the control of tracking eye movements: A critical review. *Journal of Neurophysiology*, *125*(5), 1552-1576.

Spencer, H. J. (1976). Antagonism of cortical excitation of striatal neurons by glutamic acid diethyl ester: evidence for glutamic acid as an excitatory transmitter in the rat striatum. *Brain research*, *102*(1), 91-101.

Spering, M., & Montagnini, A. (2011). Do we track what we see? Common versus independent processing for motion perception and smooth pursuit eye movements: A review. *Vision research*, *51*(8), 836-852.

Spering, M., Schütz, A. C., Braun, D. I., & Gegenfurtner, K. R. (2011). Keep your eyes on the ball: smooth pursuit eye movements enhance prediction of visual motion. *Journal of Neurophysiology*, *105*(4), 1756-1767.

Stone, L., & Lisberger, S. (1990). Visual responses of Purkinje cells in the cerebellar flocculus during smooth-pursuit eye movements in monkeys. I. Simple spikes. *Journal of neurophysiology*, *63*(5), 1241-1261.

Strick, P. L. (1976). Anatomical analysis of ventrolateral thalamic input to primate motor cortex. *Journal of neurophysiology*, *39*(5), 1020-1031.

Suzuki, D. A., Yamada, T., Hoedema, R., & Yee, R. D. (1999). Smooth-pursuit eye-movement deficits with chemical lesions in macaque nucleus reticularis tegmenti pontis. *Journal of neurophysiology*, *82*(3), 1178-1186.

Szurhaj, W., Derambure, P., Labyt, E., Cassim, F., Bourriez, J.-L., Isnard, J., . . . Mauguière, F. (2003). Basic mechanisms of central rhythms reactivity to preparation and execution of a voluntary movement: a stereoelectroencephalographic study. *Clinical neurophysiology*, *114*(1), 107-119.

Takagi, M., Zee, D. S., & Tamargo, R. J. (2000). Effects of lesions of the oculomotor cerebellar vermis on eye movements in primate: smooth pursuit. *Journal of Neurophysiology*, *83*(4), 2047-2062.

Takei, T., Crevecoeur, F., Herter, T. M., Cross, K. P., & Scott, S. H. (2018). Correlations between primary motor cortex activity with recent past and future limb motion during unperturbed reaching. *Journal of Neuroscience*, *38*(36), 7787-7799.

Takei, T., Lomber, S. G., Cook, D. J., & Scott, S. H. (2021). Transient deactivation of dorsal premotor cortex or parietal area 5 impairs feedback control of the limb in macaques. *Current Biology*, *31*(7), 1476-1487. e1475.

Tanaka, H., Ishikawa, T., Lee, J., & Kakei, S. (2020). The cerebro-cerebellum as a locus of forward model: a review. *Frontiers in systems neuroscience*, *14*, 19.

Tanaka, M., & Lisberger, S. G. (2002a). Enhancement of multiple components of pursuit eye movement by microstimulation in the arcuate frontal pursuit area in monkeys. *Journal of neurophysiology*, *87*(2), 802-818.

Tanaka, M., & Lisberger, S. G. (2002b). Role of arcuate frontal cortex of monkeys in smooth pursuit eye movements. I. Basic response properties to retinal image motion and position. *Journal of Neurophysiology*, *87*(6), 2684-2699.

Therrien, A. S., & Bastian, A. J. (2019). The cerebellum as a movement sensor. *Neuroscience letters*, *688*, 37-40.

Thielert, C. D., & Thier, P. (1993). Patterns of projections from the pontine nuclei and the nucleus reticularis tegmenti pontis to the posterior vermis in the rhesus monkey: a study using retrograde tracers. *Journal of Comparative Neurology*, *337*(1), 113-126.

Thier, P., & Erickson, R. (1992). Responses of visual-tracking neurons from cortical area MST-I to visual, eye and head motion. *European Journal of Neuroscience*, *4*(6), 539-553.

Thier, P., & Ilg, U. J. (2005). The neural basis of smooth-pursuit eye movements. *Current opinion in neurobiology*, *15*(6), 645-652.

Tombini, M., Zappasodi, F., Zollo, L., Pellegrino, G., Cavallo, G., Tecchio, F., . . . Rossini, P. M. (2009). Brain activity preceding a 2D manual catching task. *Neuroimage*, *47*(4), 1735-1746.

Tresilian, J. R. (1991). Empirical and theoretical issues in the perception of time to contact. *Journal of Experimental Psychology: Human Perception and Performance*, *17*(3), 865.

Tresilian, J. R. (1999). Visually timed action: time-out for 'tau'? *Trends in cognitive sciences*, *3*(8), 301-310.

Tresilian, J. R. (2005). Hitting a moving target: perception and action in the timing of rapid interceptions. *Perception & Psychophysics*, *67*(1), 129-149.

Turano, K. A., & Heidenreich, S. M. (1999). Eye movements affect the perceived speed of visual motion. *Vision Research*, *39*(6), 1177-1187.

Wheaton, L. A., Shibasaki, H., & Hallett, M. (2005). Temporal activation pattern of parietal and premotor areas related to praxis movements. *Clinical neurophysiology*, *116*(5), 1201-1212.

White, O., Thonnard, J.-L., Wing, A., Bracewell, R., Diedrichsen, J., & Lefèvre, P. (2011). Grip force regulates hand impedance to optimize object stability in high impact loads. *Neuroscience*, *189*, 269-276.

Williams, J. G. (1992). Catching Action: Visuomotor Adaptations in Children. *Perceptual and Motor Skills*, *75*(1), 211-219. https://doi.org/10.2466/pms.1992.75.1.211

Witt, J. K., & Sugovic, M. (2013). Catching ease influences perceived speed: Evidence for action-specific effects from action-based measures. *Psychonomic Bulletin & Review*, *20*(6), 1364-1370.

Wolpert, D. M., Miall, R. C., & Kawato, M. (1998). Internal models in the cerebellum. *Trends in cognitive sciences*, *2*(9), 338-347.

Zago, M., & Lacquaniti, F. (2005a). Cognitive, perceptual and action-oriented representations of falling objects. *Neuropsychologia*, *43*(2), 178-188.

Zago, M., & Lacquaniti, F. (2005b). Visual perception and interception of falling objects: a review of evidence for an internal model of gravity. *Journal of Neural Engineering*, *2*(3), S198.

Zang, Y., Jia, F., Weng, X., Li, E., Cui, S., Wang, Y., . . . Ivry, R. (2003). Functional organization of the primary motor cortex characterized by event-related fMRI during movement preparation and execution. *Neuroscience Letters*, *337*(2), 69-72.